

CHARACTERIZATION AND PROMOTER IDENTIFICATION OF
METASTASIS ASSOCIATED PROTEIN 1 IN HUMAN COLORECTAL
CARCINOMA CELL LINES

A THESIS SUBMITTED TO
THE GRADUATE SCHOOL OF NATURAL AND APPLIED SCIENCES
OF
MIDDLE EAST TECHNICAL UNIVERSITY

BY

SEDA TUNÇAY ÇAĞATAY

IN PARTIAL FULFILLMENT OF THE REQUIREMENTS
FOR
THE DEGREE OF DOCTOR OF PHILOSOPHY
IN
BIOLOGY

JANUARY 2014

Approval of the thesis:

**CHARACTERIZATION AND PROMOTER IDENTIFICATION OF
METASTASIS ASSOCIATED PROTEIN 1 IN HUMAN COLORECTAL
CARCINOMA CELL LINES**

submitted by **SEDA TUNÇAY ÇAĞATAY** in partial fulfillment of the requirements for the degree of **Doctor of Philosophy in Biology Department, Middle East Technical University** by,

Prof. Dr. Canan Özgen
Dean, Graduate School of **Natural and Applied Sciences**

Prof. Dr. Gülay Özcengiz
Head of Department, **Biology**

Assoc. Prof. Dr. Sreeparna Banerjee
Supervisor, **Biology Dept., METU**

Examining Committee Members:

Assoc. Prof. Dr. Mesut Muyan
Biology Dept., METU

Assoc. Prof. Dr. Sreeparna Banerjee
Biology Dept., METU

Assoc. Prof. Dr. A. Elif Erson Bensan
Biology Dept., METU

Assoc. Prof. Dr. Özlen Konu
Molecular Biology and Genetics Dept.,
Bilkent University

Assoc. Prof. Dr. Tülin Yanık
Biology Dept., METU

Date:17.01.2014

I hereby declare that all information in this document has been obtained and presented in accordance with academic rules and ethical conduct. I also declare that, as required by these rules and conduct, I have fully cited and referenced all material and results that are not original to this work.

Name, Last name: Seda Tunçay Çağatay

Signature :

ABSTRACT

CHARACTERIZATION AND PROMOTER IDENTIFICATION OF METASTASIS ASSOCIATED PROTEIN 1 IN HUMAN COLORECTAL CARCINOMA CELL LINES

Tunçay Çağatay, Seda

Ph.D., Department of Biology

Supervisor: Assoc. Prof. Dr. Sreeparna Banerjee

January 2014, 174 pages

Metastasis associated protein 1 (MTA1) is a member of the nuclear remodeling and histone deacetylase (NuRD) complex, which is known to repress the expression of several tumor suppressor genes and has been widely linked to tumor metastasis. 15-lipoxygenase-1 (15-LOX-1) is a lipid metabolizing enzyme that has tumor suppressive properties and is silenced by the NuRD complex in colorectal cancer (CRC). We have previously shown that reexpression of 15-LOX-1 inhibited metastasis in CRC, inhibited the inflammatory transcription factor nuclear factor kappa B (NF- κ B) and resulted in reduced expression of MTA1 indicating the presence of a cross talk. In this study, we have first investigated the role of MTA1 in CRC. For this, the gene was silenced and overexpressed in the CRC cell line HCT-116. MTA1 overexpression enhanced metastasis and epithelial mesenchymal transition (EMT) like characteristics of the cells while silencing of MTA1 resulted in reversal of these features.

Reexpression of 15-LOX-1 in CRC cell lines HT-29 and LoVo resulted in decreased expression of MTA1. This was due to a decrease in the nuclear levels and the recruitment of p53 to its binding motifs on the MTA1 promoter as well as inhibition of transcriptional activity of NF- κ B.

As a conclusion, this study not only shows the protumorigenic properties of MTA1 in CRC but also identifies a novel regulatory mechanism by 15-LOX-1 thereby providing a rationale for the development of anti-metastatic intervention strategies targeting MTA1 or 15-LOX-1 expressions.

Key words: MTA1, 15-LOX-1, NF- κ B, colorectal carcinoma, metastasis, EMT.

ÖZ

METASTASIS ASSOCIATED PROTEIN 1' İN KOLOREKTAL KANSER HÜCRE HATLARINDA KARAKTERİZASYONU VE PROMOTOR BELİRLENMESİ

Tunçay Çağatay, Seda

Doktora, Biyoloji Bölümü

Tez Yöneticisi: Doç.Dr. Sreeparna Banerjee

Ocak 2014, 174 sayfa

Metastasis associated protein 1 (MTA1), pek çok tümör baskılayıcı geni (tümör süpresör gen) inhibe eden baskılayıcı nükleozom yeniden modelleme ve histon deasetilaz (NuRD) kompleksinin bir üyesidir ve büyük ölçüde kanserle ilişkilendirilmiştir. 15-Lipoksijenaz (15-LOX-1) lipid metabolizmasında görevli anti-tümörjenik özellikleri olan bir enzimdir ve NuRD kompleksi tarafından baskılandığı gösterilmiştir. Daha önce 15-LOX-1'in kolorektal kanserde metastazı azalttığını, enflamatuar transkripsiyon faktörü NF- κ B'nin aktivitesini inhibe ettiğini ve MTA1 ifadesini azalttığını göstermiş, dolayısıyla karşılıklı bir etkileşimin varlığına işaret etmiş bulunmaktayız. Bu çalışmada ilk olarak MTA1'in kolorektal kanserdeki rolünü incelemiş bulunmaktayız. Bu amaçla, MTA1 geni HCT-116 kolorektal kanser hücre hattında susturulmuş ve aşırı ifade ettirilmiştir. MTA1 aşırı ifadesi hücrelerin metastatik ve epitelyal-mezenkimal geçiş (EMT) ile ilgili özelliklerini artırırken; genin susturulması ise bu özelliklerin tersine dönmesine sebep olmuştur.

15-LOX-1 geninin HT-29 and LoVo kolorektal kanser hücre hatlarında ektopik olarak ifade ettirilmesi MTA1 ifadesinde azalışa sebep olmuştur. Bunun sebebi p65'in nükleer seviyelerindeki azalış ile MTA1 promotorundaki MTA1 bağlanma

motiflerine baęlanışının azalmasına ve NF-κB'nin transkripsiyonel aktivitesinin inhibe edilmesine baęlıdır.

Sonuç olarak, bu çalışma kolorektal kanserde MTA1'in t moriyenik yapısını g stermesinin yanı sıra, 15-LOX-1'in MTA1'i d zenlemesiyle ilgili yeni bir mekanizma ortaya koyuyor ve b ylece MTA1 ve ya 15-LOX-1'i hedef alan anti-metastatik m dahale stratejilerinin geliřtirilmesi konusunda yeni fikirler saęlamaktadır.

Anahtar kelimeler: MTA1, 15-LOX-1, NF-κB, kolorektal kanser, metastaz, EMT

To My Family

ACKNOWLEDGEMENTS

Firstly, I would like to express my gratitude to my supervisor Assoc.Prof.Dr. Sreeparna Banerjee for her guidance, encouragement, support and comments throughout my study. I feel lucky to carry out my graduate studies under her supervision.

My special thanks go to Assoc.Prof.Dr. Özlen Konu, Assoc.Prof.Dr. Ayşe Elif Erson-Bensan, Assoc.Prof.Dr. Mesut Muyan and Assoc.Prof.Dr Tülin Yanık for their great advices and support.

I would like to extend my thanks to Assoc.Prof.Dr. Ali Güre and Murat İşbilen for their help with microarray data analysis and the use of Real Time PCR facility; Assoc. Prof.Dr. Mayda Gürsel METU, Assoc. Prof.Dr. İhsan Gürsel and Dr. Tamer Kahraman for the use of the flow cytometry facility.

I would like to thank my dear friends and lab mates and I would particularly like to thank Aslı Sade Memişoğlu and M. Şeyma Ceyhan for their support, motivation and companionship.

I am deeply grateful to my parents Zehra and Hüseyin Tunçay, my brother Ali Tunçay and my sister Saniye Tunçay for their encouragement, endless help, confidence, understanding and supporting me spiritually throughout my life.

Finally, I would like to express my deepest gratitude and love to my dear husband Kartal Çağatay for his efforts, patience, extreme encouragements and trust.

TABLE OF CONTENTS

ABSTRACT.....	v
ÖZ	vii
ACKNOWLEDGEMENTS	x
TABLE OF CONTENTS.....	xi
LIST OF TABLES.....	xvi
LIST OF FIGURES.....	xvii
CHAPTERS	
1 INTRODUCTION.....	1
1.1 Cancer.....	1
1.2 Hallmarks of cancer.....	1
1.2.1 Sustaining Proliferative Signaling	1
1.2.2 Evading Growth Suppressors.....	2
1.2.3 Resisting apoptosis	2
1.2.4 Replicative immortality	3
1.2.5 Stimulation of angiogenesis.....	3
1.2.6 Activating metastasis and epithelial mesenchymal transition (EMT)	4
1.3 Colorectal Cancer	5
1.4 MTA family.....	7
1.4.1 Members of MTA family.....	7
1.4.2 Domain structures of MTA family proteins	8
1.4.3 Expression of the MTA genes	8
1.4.4 Subcellular localization of MTA proteins	9
1.5 Metastasis Associated Protein 1	10

1.5.1	The expression of MTA1 in various cancers and its clinicopathological and biological relevance	10
1.5.2	Molecular mechanisms of the MTA1 in cancer	13
1.6	Lipoxygenase function and metabolism.....	14
1.7	15-Lipoxygenase-1 expression.....	15
1.7.1	15-Lipoxygenase-1 in cancer.....	16
1.8	Nuclear factor kappa B (NF- κ B).....	17
1.9	Scope of the study	17
2	MATERIALS AND METHODS	21
2.1	Cell culture	21
2.2	Cell culture	21
2.3	Transfection of cell lines	22
2.3.1	Cloning MTA1 silencing oligo (shRNA) into pSuper plasmid.....	22
2.3.2	Generation of pcDNA3.1/V5-His-TOPO (empty vector) from MTA1-pcDNA3.1/ V5-His-TOPO plasmid	23
2.3.3	Geneticin (G-418) kill curve for HCT-116 cells	24
2.3.4	Stable Transfections	24
2.3.5	Transient Transfections	25
2.4	Protein expression analysis	26
2.4.1	Total Protein isolation and quantification	26
2.4.2	Nuclear /cytoplasmic protein isolation and quantification	26
2.4.3	Western blotting	27
2.5	mRNA expression analysis	28
2.5.1	RNA isolation	28
2.5.2	DNase-1 Treatment.....	28
2.5.3	cDNA synthesis	29
2.5.4	Reverse transcriptase PCR.....	29

2.5.5	Quantitative (Real Time PCR).....	29
2.6	Cell viability assay	30
2.6.1	MTT assay	30
2.7	Cell proliferation assay.....	31
2.7.1	BrdU assay:.....	31
2.8	Cellular motility	32
2.8.1	<i>In vitro</i> scratch wound healing assay.....	32
2.9	Apoptosis assay	32
2.9.1	Annexin V Staining	32
2.10	Anchorage independent growth.....	33
2.10.1	Soft Agar Assay	33
2.11	Cell Adhesion Assay	33
2.12	Boyden chamber Cell Migration Assay	34
2.13	Boyden chamber Cell Invasion Assay.....	35
2.14	VEGF ELISA Assay	37
2.15	<i>In vitro</i> angiogenesis assay:.....	37
2.16	Determination of NF- κ B binding sites on the MTA1 promoter region	38
2.17	Chromatin Immunoprecipitation (ChIP) Assay:	38
2.18	Reporter gene assays	40
2.18.1	Construction of reporter plasmids.....	40
2.18.2	Luciferase/renilla dual system assays	41
2.19	Electrophoretic mobility shift assay (EMSA)	42
2.20	Microarray data analysis	45
2.21	TissueScan Aray.....	45
2.22	Statistical analysis	46

3	RESULTS	47
3.1	MTA1 expression in CRC cell lines	47
3.2	MTA1 expression in transfected HCT-116 cells.....	48
3.3	Cell viability assay	49
3.3.1	MTT.....	49
3.4	Cell proliferation assay.....	51
3.4.1	BrdU assay.....	51
3.5	Anchorage Independent Cell Growth.....	53
3.5.1	Soft Agar colony formation assay	53
3.6	Cell adhesion assay	55
3.7	Wound healing	56
3.8	Boyden chamber migration and invasion assays.....	59
3.9	MTA1 induces survival signals in CRC cell lines	63
3.9.1	Apoptosis assay	63
3.9.2	Angiogenesis assays	68
3.10	MTA1 expression induces Epithelial Mesenchymal Transition (EMT) in CRC cell lines.....	75
3.11	MTA1 expression levels in 15-LOX-1 transfected cells.....	79
3.12	Nuclear translocation of NF- κ B in the cells expressing 15-LOX-1	81
3.13	Detection of NF- κ B binding regions on the MTA1 promoter region	82
3.14	NF- κ B recruitment onto the MTA1 promoter in the presence of 15-LOX-1 expression.....	83
3.15	Transcriptional activity in region RI and RII in the presence of 15-LOX-1 expression.....	87
3.16	Electrophoretic mobility shift assay (EMSA) for NF- κ B binding on the MTA1 promoter	89

3.17	Correlation analysis of 15-LOX-1 and MTA1 expressions in CRC patients	94
3.18	Tissue scan array	97
4	DISCUSSION	101
5	CONCLUSION	113
	REFERENCES.....	115
	APPENDIX	
	Appendix A: Vector Maps.....	135
	Appendix B: Generation of vectors.....	139
	Appendix C: Isolation of electrophoretically separated DNA fragments.....	152
	Appendix D: High Pure PCR Product Purification.....	153
	Appendix E: Competent E.coli Preparation.....	154
	Appendix F: Transformation Protocol.....	155
	Appendix G: Plasmid isolation protocol.....	156
	Appendix H: Protein isolation Protocol with M-PER.....	157
	Appendix I: RNA isolation protocol with Qiagen Rneasy Kit.....	158
	Appendix J: First strand cDNA synthesis with Revert Aid First strand cDNA Synthesis kit.....	159
	Appendix K: Coomassie Protein Assay Standard Test Tube Protocol.....	160
	Appendix L: VEGF ELISA Assay Standard Preparation protocol	161
	Appendix M: Kill curve assay.....	162
	Appendix N: ChIP PCR.....	163
	Appendix O: Reporter gene assay transfection optimizations.....	164
	Appendix P: BUFFERS.....	165
	Appendix R: SDS-PAGE and polyacrylamide gels.....	167
	Appendix S: RT-PCR thermal cycling conditions.....	168
	Appendix T: Appendix Quantitative PCR Standards.....	169
	CURRICULUM VITAE.....	172

LIST OF TABLES

TABLES

Table 1 Clinicopathological implications of high MTA1 expression in different.....	12
Table 2 Primers used for ChIP assays.....	39
Table 3 Oligo and primer sequences used for generation of reporter vectors	40
Table 4. EMSA oligo sequences	44
Table 5. RT-PCR primers used in TissueScan array	46
Table A. 1 Checking for the positive clones.....	141
Table A. 2 Region II PCR amplification conditions.....	148
Table A. 3. Table ChIP PCR conditions for both Region I and II.....	163
Table A. 4 10% SDS-PAGE Gel	167
Table A. 5 8% polyacrylamide gel	167
Table A. 6 15-LOX-1 RT-PCR thermal cycling conditions	168
Table A. 7 MTA1 RT-PCR thermal cycling conditions	168
Table A. 8 β -actin RT-PCR thermal cycling conditions.....	168

LIST OF FIGURES

FIGURES

Figure 1. 1 Estimated age-standardized incidence and mortality rates for CRC (Ferlay et al., 2010).	6
Figure 1. 2 Crosstalk between 15-LOX-1, NF-κB and MTA1 proteins.	18
Figure 3. 1 Western blot of MTA1 protein expression in five different CRC cell lines including HT-29, LoVo, HCT-116, SW620 and Caco-2.	47
Figure 3. 2 Western blot analysis of MTA1 overexpressing (MTA1 oex polyclone I and II), MTA1 silenced (shMTA1b1 and shMTA1d1) and corresponding empty vector carrying control HCT-116 cells EV(pcDNA3.1) and EV(pSUPER).....	49
Figure 3. 3 MTT cell viability assay showing a significant increase (** $p < 0,001$ and ** $p < 0,01$) in proliferation in MTA1 overexpressing cells.....	50
Figure 3. 4 MTT cell viability assay showing significant decrease (** $p < 0,001$) in proliferation in MTA1 silenced HCT-116 cells	51
Figure 3. 5 BrdU incorporation assay (chemiluminescent) showing a significant increase with MTA1 overexpressing (MTA1 oex polyclone I), and a significant decrease in MTA1 silenced HCT-116 (shMTA1d1 and shMTA1b1) cells.....	52
Figure 3. 6 Representative images (10X objective) of colonies formed in soft agar, showing the anchorage independent growth potential of MTA1 overexpressing, MTA1 silenced and the control cells. Scale bars: 100 μm.....	54
Figure 3. 7 Quantitative analysis of colonies formed in soft agar, showing significantly increased and decreased anchorage independent growth potential of MTA1 overexpressing (MTA1 oex polyclone I) and MTA1 silenced (shMTA1d1) cells respectively, compared to the the control cells.....	55
Figure 3. 8 Adhesion assay graph showing increased and decreased cell adhesion to fibronectin in MTA1 overexpressing and MTA1 silenced cells, respectively, compared to the control cells	56

Figure 3. 9 Wound closure representative pictures showing increased wound closure area in MTA1 overexpressing (MTA1 oex polyclone I), and decreased wound closure area in silenced (shMTA1d1) cells compared to control cells. 57

Figure 3. 10 Quantification of motility in MTA1 overexpressing (MTA1 oex polyclone I), MTA1 silenced (shMTA1d1) and the control cells..... 58

Figure 3. 11 Migration assay representative membrane images (20X objective) showing higher number of migrated MTA1 overexpressing cells (MTA1 oex polyclone I) and lower number of migrated MTA1 silenced (shMTA1d1) and the control HCT-116 cells..... 60

Figure 3. 12 Quantitative analysis of cell migration through the Transwells. Data are presented as mean \pm SD of three independent experiments. Statistical significance was determined with Mann–Whitney U-test ($*p < 0.05$ and $** p < 0.01$). 61

Figure 3. 13 Invasion assay representative membrane images. 62

Figure 3. 14 Quantitative analysis of number of cells that invade through Transwells and Matrigel. 63

Figure 3. 15 MTA1 expression has an effect on apoptotic properties of HCT-116 cells 64

Figure 3. 16 Quantitative analysis of early, late and total apoptotic cells percentages showing reduced number of apoptotic cells in MTA1 overexpressing (MTA1 oex polyclone I) cell population compared to empty vector transfected (EV(pcDNA3.1)) cell population..... 65

Figure 3. 17 Quantitative analysis of early, late and total apoptotic cells percentages showing increased number of apoptotic cells in MTA1 silenced (shMTA1d1) cell population compared to empty vector transfected EV(pSUPER) cell population..... 66

Figure 3. 18 Western blot analysis showing increased Bcl-x1 protein expression in MTA1 overexpressing cells and decreased Bcl-x1 protein expression in MTA1 silenced HCT-116 cells..... 67

Figure 3. 19 Western blot analysis of XIAP protein showing reduced amounts of protein in MTA1 silenced monoclonal cells compared to corresponding empty vector transfected cells..... 68

Figure 3. 20 VEGF concentrations (pg/ml) shown determined by VEGF immunoassay showing higher levels of secreted VEGF in MTA1 overexpressing (MTA1 oex polyclone I) cells conditioned media and lower levels of MTA1 silenced (shMTA1d1) conditioned media compared to corresponding empty vector transfected cells.....	69
Figure 3. 21 Endothelial Tube Formation assay 10X objective representative images in MTA1 overexpressing, MTA1 silenced and control cells.	71
Figure 3. 22 Endothelial Tube Formation assay 4X objective representative images (evaluated by S.Co Lifesciences) in MTA1 overexpressing, MTA1 silenced and control cells.	72
Figure 3. 23 Endothelial Tube Formation assay showing higher amount of a) Total Length of skeleton, b) Number of nodal structures, c) Number of branching points, (d) Number of tubes in MTA1 overexpressing cells compared to control cells.....	73
Figure 3. 24 Endothelial Tube Formation assay showing lower a) Total Length of skeleton, b) Number of nodal structures, c) Number of branching points, (d) Number of tubes in MTA1 silenced cells compared to control cells.	74
Figure 3. 25 MTA1 expression affects the expression levels of EMT markers EMT regulator transcription factors..	76
Figure 3. 26 Western blot analysis of E-cadherin, ZO-1, SNAI1, SLUG, vimentin and β -catenin proteins in MTA1 silenced LoVo (LoVo-1F7 and 1F2) and the control cells. β -actin was used as a loading control.	77
Figure 3. 27 ChIP assay showed a reduction in recruitment of SNAI1 and SLUG proteins onto the E-cadherin promoter E-box elements in MTA1 silenced shMTA1d1 cells compared to empty vector transfected EV(pSUPER) control cells	78
Figure 3. 28 Western blot analysis of 15-LOX-1 (75 kDa) and MTA-1 proteins (80 kDa) in different cell lines.....	80
Figure 3. 29 Western blot analysis of nuclear and cytoplasmic extracts isolated from 15-LOX-1 expressing HT-29 and LoVo cells.....	82
Figure 3. 30 Schematic diagram of NF- κ B binding sites in the region between chr14: 105884100-105886185 on the MTA1 promoter, detected by AliBaba 2.1 Program.	83

Figure 3. 31 15-LOX-1 expression decreases p65 recruitment onto the MTA1 promoter (Region I (chr14:105884312-105884461); and Region II (chr 14: 105884853-105885464)) as shown by ChIP assay in HT-29 cells.....	85
Figure 3. 32 15-LOX-1 expression decreases p65 recruitment onto the MTA1 promoter (Region I (chr14:105884312-105884461); and Region II (chr 14: 105884853-105885464)) as shown by ChIP assay in LoVo cells	86
Figure 3. 33 15-LOX-1 expression does not change p65 recruitment onto the MTA1 promoter (Region I (chr14:105884312-105884461); and Region II (chr 14: 105884853-105885464)) as shown by ChIP assay in SW620 cells.	87
Figure 3. 34 MTA1 promoter activity in Region I and II is decreased in 15-LOX-1 expressing HT-29 cells. The data are nomalized to pLuc-MCS-EV (empty vector) /pHRLTK ratios.	88
Figure 3. 35 MTA1 promoter activity is decreased in Region I and II in 15-LOX-1 expressing LoVo cells.....	89
Figure 3. 36 EMSA using oligo 1, 2 and 3 in HT-29 cells	91
Figure 3. 37 EMSA using oligo 4, 5 and 6 in HT-29 cells	92
Figure 3. 38 EMSA using oligo 1&6 in HT-29 cells.....	93
Figure 3. 39 EMSA using oligo 1 & 6 in LoVo cells	94
Figure 3. 40 Correlation analysis of 15-LOX-1 and MTA1 expressions in normal colon tissues obtained from publicly available microarray data set (GSE41258).	95
Figure 3. 41 Correlation analysis of 15-LOX-1 and MTA1 expressions in Stage I and Stage II CRC patients obtained from publicly available microarray data set (GSE41258)	96
Figure 3. 42 Correlation analysis of 15-LOX-1 and MTA1 expressions in Stage III and IV CRC patients obtained from publicly available microarray data set (GSE41258)	96
Figure 3. 43 Correlation analysis of 15-LOX-1 and MTA1 expressions in normal tissue with the data obtained from TissueScan array (Pearson r = -0.02317).....	98
Figure 3. 44 Correlation analysis of 15-LOX-1 and MTA1 expressions in Stage I and II-IIA CRC patients with the data obtained from TissueScan array.....	98

Figure 3. 45 Correlation analysis of 15-LOX-1 and MTA1 expressions in Stage III CRC patients with the data obtained from TissueScan array (Pearson $r = 0.1019$)..	99
Figure 3. 46 Correlation analysis of 15-LOX-1 and MTA1 expressions in Stage IIIA-B-C and Stage IV CRC patients with the data obtained from TissueScan array.	100
Figure 4. 1 Summary of the study.....	111
Figure A. 1 pSUPERIOR.retro.neo+gfp vector map (8368 bp).....	135
Figure A. 2 pcDNA3.1/V5-His-TOPO vector map (5523 bp).....	136
Figure A. 3 pcDNA3.1/ZEO (+) vector map (5015 bp).....	137
Figure A. 4 pLuc-MCS vector map (5.7 kb).....	138
Figure A. 5 Figure EcoRI & HindIII double digested MTA1-shRNA-pSUPER and pSUPER plasmids.	142
Figure A. 6 Alignment results of MTA1-shRNA-pSUPER sequence to shRNA-MTA1 sequence in MAFFT.....	143
Figure A. 7 Agarose gel images of MTA-1-pcDNA3.1/V5-His-TOPO and pcDNA3.1/V5-His-TOPO vectors after restriction digestion with A. XbaI restriction enzyme B. HindIII ve XhoI restriction enzymes.	145
Figure A. 8 RT-PCR analysis of the MTA-1 transcript from MTA-1-pcDNA3.1/V5-His-TOPO and pcDNA3.1/V5-His-TOPO (product size: 244 bp).	146
Figure A. 9 Region II PCR products (~600 bp).....	149
Figure A. 10 Double digested pLuc-MCS plasmid DNA.....	150
Figure A. 11 pLuc-MCS-RI sequencing results on NCBI Blast.....	151
Figure A. 12 pLuc-MCS-RII sequencing results on NCBI blast.....	151
Figure A. 13 Protein standard curve.	160
Figure A. 14 VEGF standard curve.....	161
Figure A. 15 Geneticin (G-418) kill curve in HCT-116 cells.....	162
Figure A. 16 Transfection vs luciferase/renilla signal ratios in LoVo cells.....	164
Figure A. 17 MTA1 RT-PCR Melt curve analysis.....	169
Figure A. 18 15-lox-1 RT-PCR Melt curve analysis.....	170
Figure A. 19 β -actin RT-PCR Melt curve analysis.....	171

CHAPTER 1

INTRODUCTION

1.1 Cancer

Cancer is a leading cause of morbidity and mortality worldwide. According to WHO reports, the number of global cancer deaths is estimated to increase by 45% from 2007 (7.9 million deaths) to 2030 (11.5 million deaths), in part due to increasing and aging global population. New cancer cases are expected to increase to 15.5 million from 11.3 million in the same period (<http://www.who.int/features/qa/15/en/index.html>).

1.2 Hallmarks of cancer

1.2.1 Sustaining Proliferative Signaling

Normal cells and tissues control the production and release of growth promoting signals that drive cell cycle, thereby maintaining normal tissue structure and function. Cancer cells, on the other hand, have an unrestrictive potential of proliferation by deregulating growth signals or gaining ability to proliferate in the absence of growth signals. Cancer cells can gain capability to maintain proliferative signaling in various ways; such as production of growth factor ligands themselves

resulting in autocrine proliferative stimulation, or through induction of normal cells within stroma which can supply cancer cells with growth factors (Bhowmick et al., 2004; Cheng et al., 2008; Hanahan and Weinberg, 2011). Another way can be the deregulation of receptors displayed on the cell surface resulting in hyperresponsiveness of those cells or constitutive activation of component of signaling pathways downstream of these receptors eliminating the necessity for ligand mediated receptor activation (Hanahan and Weinberg, 2011).

1.2.2 Evading Growth Suppressors

Cancer cells inhibit mechanisms that regulate cell proliferation which are mainly driven tumor suppressor genes. RB and TP53 proteins are two critical tumor suppressor genes, as RB collect signals from intracellular and extracellular environment and decide whether or not the cell will proceed through cell cycle (Burkhart and Sage, 2008; Deshpande et al., 2005; Sherr and McCormick, 2002); while TP53 acquires inputs from stress and abnormality sensors and is capable of stopping cell cycle progression or drive the cell to apoptosis (Hanahan and Weinberg, 2011). Contact inhibition, which denotes the suppression of cell proliferation due to cell to cell contacts in confluent monolayers, is abolished in various types of cancers.

1.2.3 Resisting apoptosis

Apoptosis (programmed cell death) acts as a natural barrier against cancer development (Adams and Cory, 2007; Evan and Littlewood, 1998; Lowe et al., 2004). Apoptosis can be divided as extrinsic or intrinsic apoptotic program both activating latent protease (caspases 8 and 9, respectively), which in turn initiate a series of proteolysis events involving effector caspases which carry out the

execution phase of apoptosis. The intrinsic apoptotic program is more widely implicated as a barrier to cancer pathogenesis. Cancer cells use several different mechanisms to inhibit apoptosis such as eliminating important damage sensor and tumor suppressor TP53 function which normally induces apoptosis. Moreover, tumor cells may downregulate antiapoptotic proteins such as Bcl-2 and Bcl-XL or upregulate proapoptotic proteins including Bax, Bim and PUMA (Hanahan and Weinberg, 2011).

1.2.4 Replicative immortality

Normal cells are able to go through a finite number of cell growth and division cycles, which is either because of cell senescence or crisis. The cells that can overcome crisis are the ones that gained unlimited replicative potential and became immortalized. Telomeres provide protection of the end of chromosomes and non-immortalized cells lose their telomere sequences progressively in each cell division cycle. Telomerase, a polymerase enzyme that adds hexanucleotide repeats to the end of telomeric DNA is almost never expressed in nonimmortalized cells while it is expressed at significant levels in the majority (90%) of immortalized cells, including human cancer cells (Blasco, 2005; Hanahan and Weinberg, 2011; Shay and Wright, 2000).

1.2.5 Stimulation of angiogenesis

Angiogenesis, the formation of new blood vessels, is required for invasive tumor growth, metastasis and cancer progression (Folkman, 2002). Tumor angiogenesis is induced by factors such as vascular endothelial growth factor (VEGF), basic fibroblast growth factor (bFGF) and transforming growth factor (TGF), while VEGF and its receptors constitute the main regulators of angiogenesis as well as

tumor growth (Ferrara and Davis-Smyth, 1997; Plate et al., 1992). VEGF expression can be induced both by hypoxia and oncogene signalling (Carmeliet, 2005; Ferrara, 2009; Mac Gabhann and Popel, 2008). For example, Hypoxia-inducible factor-1 (HIF-1) induces the transcription of VEGF through binding to the hypoxia response element (HRE) in the VEGF promoter region (Forsythe et al., 1996; Semenza, 2000) HIF-1 levels in cell are found to be correlated with tumorigenicity and angiogenesis (Maxwell et al., 1997). Moreover, extracellular matrix degrading proteases can release and activate VEGF ligands sequestered in the extracellular matrix (Kessenbrock et al., 2010). Angiogenesis is shown to be induced in early stages of the development of invasive cancers both in animal models and humans (Hanahan and Folkman, 1996; Raica et al., 2009).

1.2.6 Activating metastasis and epithelial mesenchymal transition (EMT)

Metastasis is governed by many gene products that are involved in the detachment of neoplastic cells from the primary tumor, passage into the blood and lymphatics, dissemination at distant sites and finally growth at metastatic sites (Liotta et al., 1991; Nicolson, 1988).

Epithelial-mesenchymal transition (EMT) has been implicated in recent years in cancer progression and metastasis as a way for transformed cells to acquire the abilities to invade, resist apoptosis and disseminate (Barrallo-Gimeno and Nieto, 2005; Iwatsuki et al., 2010; Klymkowsky and Savagner, 2009; Lehenbre et al., 2008; Polyak and Weinberg, 2009; Thiery, 2002; Thiery et al., 2009; Yilmaz and Christofori, 2009). The biology of EMT has been understood in tumor samples through use of EMT associated markers including epithelial markers (e.i. E-cadherin, cytokeratin) (Dorudi et al., 1993; Kowalski et al., 2003), mesenchymal

markers (i.e. vimentin and fibronectin) (Ngan et al., 2007; Raymond and Leong, 1989) and transcriptional regulators (i.e. SNAIL and SLUG) (Peinado et al., 2007). The most significant event in EMT is the loss of cell-cell adhesion with suppressed expression of a calcium-dependent transmembrane glycoprotein E-cadherin, which is expressed in most epithelial tissues, constructs tight junctions and maintains the quiescence of cells (Iwatsuki et al., 2010). The suppression or complete loss of E-cadherin results in tumor progression, metastasis as well as poorer prognosis in various human carcinomas (Chan et al., 2003; Dorudi et al., 1993; Gould Rothberg and Bracken, 2006; Kowalski et al., 2003). During EMT, while epithelial markers such as E-cadherin are downregulated; mesenchymal markers such as vimentin, fibronectin are upregulated (Mani et al., 2008).

In the course of EMT various transcription factors such as SNAIL, SLUG, Twist, and Zeb1/2, are expressed in several combinations in a variety of malignant tumor types (Micalizzi et al., 2010; Schmalhofer et al., 2009; Taube et al., 2010; Yang and Weinberg, 2008).

1.3 Colorectal Cancer

Over 600,000 people worldwide die of colorectal cancer (CRC) annually (<http://globocan.iarc.fr/>). CRC is the third most common cancer in men with 663,000 cases and second in women with 570,000 cases; while it is the fourth most common cause of cancer related death worldwide (Ferlay et al., 2010).

Incidence rates of CRC change 10-fold in both sexes worldwide having highest rates in Australia/New Zealand and Western Europe and lowest in Africa (except Southern Africa), South-Central Asia; while incidence and mortality rates are lower in women than in men worldwide except the Caribbean (Ferlay et al., 2010).

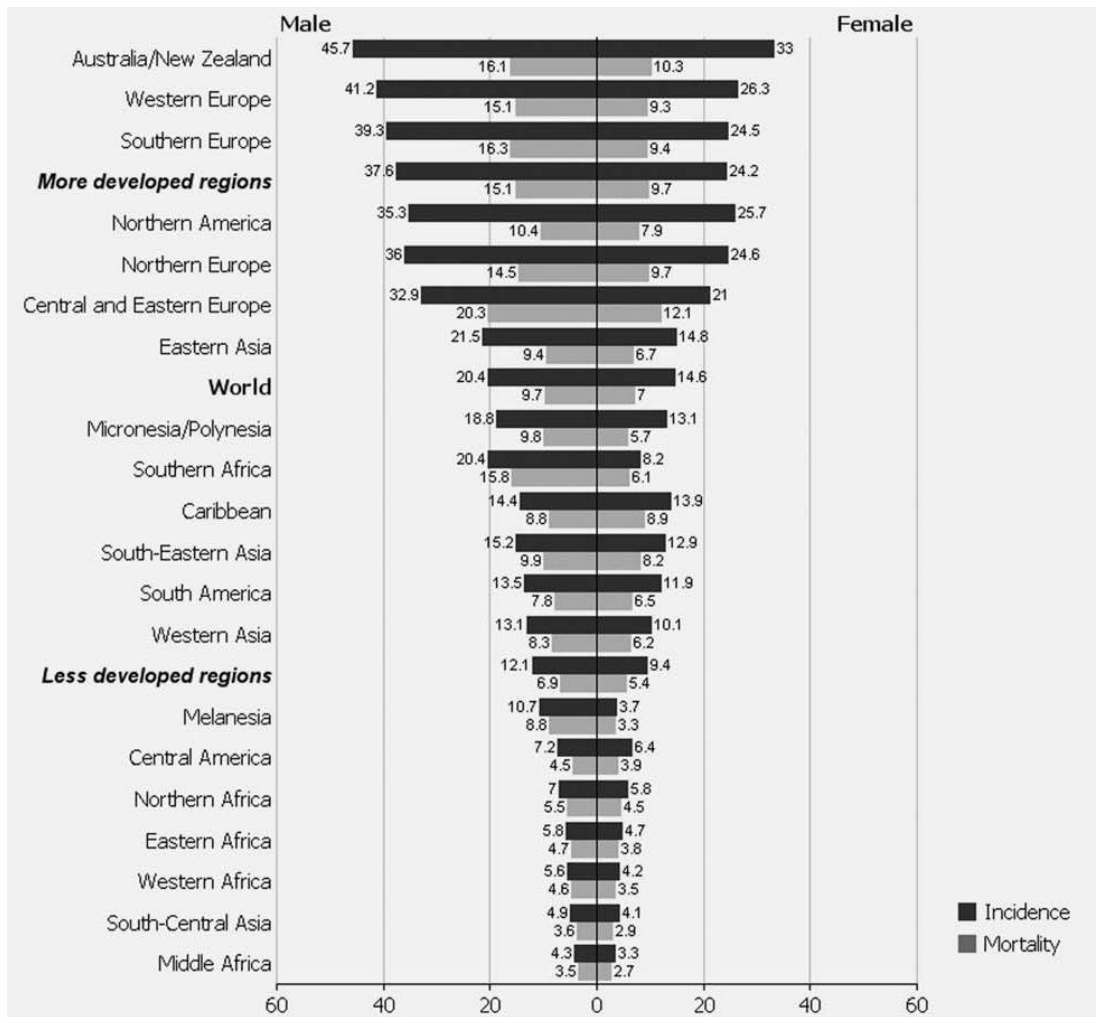


Figure 1. 1 Estimated age-standardized incidence and mortality rates for CRC (Ferlay et al., 2010).

CRC development is a multi-step and multigene process, involving inactivation and downregulation of tumor suppressor genes and activation and overexpression of oncogenes, which cause changes in CRC tumorigenesis, including cell proliferation,

apoptosis, invasion, and metastasis. Understanding its genetic mechanisms is a key for improving risk prediction, prognosis and treatment.

In CRC, metastasis is negatively correlated with patient survival. Therefore, detection of new molecular biomarkers for early identification of tumors with high metastatic potential is of vital importance. For identification of genes that have a potential role in breast cancer Toh et al. used differential screening method on cDNA library obtained from metastatic and nonmetastatic adenocarcinoma cell lines from rat mammary glands and cloned a novel gene named metastasis-associated tumor gene (*mta1*) (Toh et al., 1994). The homologous gene was found to be expressed in human cancer cell lines (Toh et al., 1994) and its human cDNA counterpart, MTA1 was cloned by Nawa et al. (Nawa et al., 2000). Subsequently, several other genes related to MTA1 have been found indicating MTA1 is a part of a gene family, called “MTA family”(Toh and Nicolson, 2009).

1.4 MTA family

1.4.1 Members of MTA family

MTA1 belongs to a family of proteins with the main members MTA1 (80 kDa), MTA2 (70 kDa), and MTA3 (65 kDa), that are associated with nucleosome remodeling and histone deacetylation (NuRD) complex (Toh and Nicolson, 2009) which couples histone deacetylation and ATP dependent chromatin remodelling in the same complex and provide chromatin compaction and transcriptional repression (Kumar et al., 2010). There are also six reported isoforms MTA1, MTA1s, MTA1-ZG29p, MTA2, MTA3 and MTA3L that have been reported so far.

1.4.2 Domain structures of MTA family proteins

The MTA family of proteins possess several common domain structures except for ZG-29p, such as bromo-adjacent homology (BAH) domain which has a role in protein-protein interactions or SWI, ADA2, N-CoR, TFIIB-B (SANT) domain that is possibly involved in DNA binding (Manavathi and Kumar, 2007). Another common domain is egl-27 and MTA1 homology (ELM) domain with an unknown function (Solari et al., 1999). Moreover, members of the family carry a highly conserved GATA type zinc finger motif indicating a direct interaction with DNA (Nawa et al., 2000).

Besides, MTA1 has shown to have two src-homology (SH)-binding motifs at its C-terminal region, which implies that it may have roles in signal transduction (Singh and Kumar, 2007; Toh et al., 1994).

1.4.3 Expression of the MTA genes

MTA genes are encoded at three separate loci; MTA1 at 14q; MTA2 at 11q; and MTA3 at 2q. MTA1 and MTA2 are ubiquitously expressed proteins while MTA3 is known to be expressed predominantly in breast cancer cells and B-lymphocytes (Manavathi et al., 2007).

MTA1 expression has been shown to be induced by heregulin through HER3 and HER4 receptor in breast cancer cells (Mazumdar et al., 2001). Moreover, c-Myc has been shown to target MTA1 promoter in normal diploid human fibroblast. MTA1 was found to be expressed under hypoxic conditions (Yoo et al., 2006). MTA1 has recently shown to be transcriptionally upregulated by the inflammatory anti-

apoptotic transcription factor nuclear factor kappa B (NF- κ B) in a murine model (Pakala et al., 2010a).

On the other hand, MTA3 expression was found to be regulated by estrogen in breast cancer cells (Fujita et al., 2003; Mishra et al., 2004), while MTA2 transcription is upregulated by both ETS-1 and SP-1 transcription factors (Xia and Zhang, 2001).

1.4.4 Subcellular localization of MTA proteins

Studies in several mouse tissues have shown that MTA1 protein is expressed in multiple organ systems such as lung, liver, kidney, heart, and testes at varying but detectable levels (Mazumdar et al., 2001).

MTA proteins have basic nuclear localization signals (Singh and Kumar, 2007; Toh et al., 1994) and various MTA1 immunohistochemical studies have showed that MTA1 predominantly localizes to nucleus in various cancerous tissues, including ovarian, lung, gastric, and colorectal cancers (Manavathi and Kumar, 2007; Toh et al., 1997; Tuncay Cagatay et al., 2013). However, studies in human B-cell lymphomas and human hepatocarcinoma (HCC) cells have showed both nuclear and cytoplasmic localization of MTA1 (Balasenthil et al., 2006; Moon et al., 2004).

On the other hand, MTA3 has been shown to localize to both cytoplasmic and nuclear compartments, although there is no apparent nuclear localization signal (Fujita et al., 2003); while MTA1s, a short splice-variant of MTA1 is localized in cytoplasm due to lack of nuclear localization signal (Kumar et al., 2002).

1.5 Metastasis Associated Protein 1

Chromosomal loci for *MTA1* gene in humans is 14q32.3; with the exact genome position of chr14:105,886,186-105937066 (50,908 bp) on the plus strand. *MTA1* is transcribed to 2.7 kb mRNA consisting 21 coding exon which in turn transcribed to 715 aminoacid, 80 kDa protein.

MTA1 protein acts as an important co-regulator where it associates either directly with transcription factors such as c-Myc, or modulates histones which can in turn affect transcription factor accessibility (Li et al., 2011). Several lines of evidence suggest that MTA1, whether as a part of the NuRD complex, or independently, is a key regulator of tumor progression in several different cancer types.

1.5.1 The expression of MTA1 in various cancers and its clinicopathological and biological relevance

The expression of MTA1 has been associated with cancer metastasis in a number cell based and mouse-model studies (Manavathi and Kumar, 2007). In the case of colorectal cancer, RT-PCR of mRNA isolated from primary tumors indicated that the gene is expressed more in tumors than in matched normal cells (Giannini and Cavallini, 2005) and that expression of the gene was correlated to increased lymph node metastasis and deeper invasion (Toh et al., 1997). Toh et al. also reported that increased mRNA expression of MTA1 was associated with more advanced Dukes' staging of the cancer although the correlation did not reach statistical significance (Toh et al., 1997). In our studies including immunohistochemistry of normal mucosa, Grade II and Grade III adenocarcinomas; we have documented that the normal mucosa showed little or no nuclear MTA1 staining, while Grade II

carcinomas showed more intense nuclear MTA1 staining and Grade III carcinomas showed the most intense nuclear MTA1 staining (Tuncay Cagatay et al., 2013).

Table 1 Clinicopathological implications of high MTA1 expression in different human cancer tissues.

<i>Method</i>	<i>Clinicopathological implications</i>	<i>References</i>
<i>Breast cancer</i>		
MCF7 cell line IHC	Increased metastatic behavior Lymph node metastasis Earlier recurrence and correlation with tumor grade	(Mazumdar et al., 2001) (Martin et al., 2001; Martin et al., 2006) (Jang et al., 2006)
<i>Colorectal cancer</i>		
RT-PCR IHC	Increased expression in tumor cells Deeper invasion, increased lymph node metastasis and increased expression in later stages of CRC	(Giannini and Cavallini, 2005) (Toh et al., 1997) (Tuncay Cagatay et al., 2013)
<i>Gastrointestinal cancer</i>		
RT-PCR	Deeper invasion and increased lymph node metastasis	(Toh et al., 1997)
<i>Esophageal cancer</i>		
RT-PCR	Higher lymph node metastasis	(Toh et al., 1999)
<i>Pancreatic cancer</i>		
PANC-1 cell line IHC	Increased metastatic behavior Poorer prognosis	(Hofer et al., 2004b) (Miyake et al., 2008)
<i>Hepatocellular cancer</i>		
IHC	Large tumor size, more vascular invasion	Ryu et al., 2008)
<i>NSCLC</i>		
RT-PCR	Large tumor size, more lymph node invasion	(Sasaki et al., 2002)
<i>Skin cancer</i>		
Immortalized keratinocytes	Increased metastatic behavior	(Mahoney et al., 2002)
<i>Ovarian cancer</i>		
RT-PCR IHC	Higher lymph node metastasis More advanced stage Higher FIGO staining	(Dannenmann et al., 2008; Yi et al., 2003)
<i>Prostate cancer</i>		
IHC	Metastatic prostate cancer	(Hofer et al., 2004a)
<i>Lymphoma</i>		
Microarray	Highest expression in diffuse B-cell lymphoma	(Hofer et al., 2006)
<i>HNSCC</i>		
Microarray IHC	Higher lymph node metastasis Higher lymph node metastasis More advanced stage Deeper wall invasion	(Roepman et al., 2006)

IHC: Immunohistochemistry, NSCLC: Non-small cell lung carcinoma, HNSCC: head and neck squamous cell carcinoma.

1.5.2 Molecular mechanisms of the MTA1 in cancer

1. MTA1 has recently shown to be transcriptionally upregulated by the inflammatory anti-apoptotic transcription factor nuclear factor kappa B (NF- κ B). Interestingly, MTA1 could also positively regulate the expression of NF- κ B target genes such as IL-1 β , TNF α and MIP2 that function as inflammatory cytokines (Pakala et al., 2010a).
2. p53 protein has been shown to be deacetylated by MTA1/HDAC1 complex which inhibited p53 induced apoptosis in human non-small cell lung carcinoma and hepatoma cells (Moon et al., 2007).
3. MTA1 was found to be expressed under hypoxic conditions and could stabilize the angiogenesis regulator hypoxia inducible factor alpha (HIF α) by deacetylation (Moon et al., 2006).
4. The NuRD complex, of which MTA1 is a component, has shown to hypoacetylate and repress the transcriptional activity of estrogen receptor alpha (ER α). This converted breast cancer cells to a more aggressive phenotype (Mazumdar et al., 2001).
5. Down-regulation of MTA1 by RNAi approach has been reported to provide re-expression of ER alpha in ER-negative breast cancer cell lines MDA-MB-231, and to reduce protein levels of MMP-9 and CyclinD1 (Jiang et al., 2011).
6. Expression profiling studies have shown that MTA1 protein is a target of the c-MYC in primary human cancer cells and it has been also shown that c-MYC binds to the genomic locus of MTA1 and recruits transcriptional coactivators (Zhang et al., 2005)

7. Silencing of MTA1 has been shown to decrease VEGF levels in the conditioned media of PC3 cells (Kai et al., 2011).

8 siRNA mediated silencing of MTA1 resulted in significant upregulation of p53 and E-cadherin protein expression, while β -catenin levels were significantly reduced in cervical cancer cells (Rao et al., 2011)

9. 15-lipoxygenase-1, which has tumor suppressive properties in colorectal cancer, has also shown to be repressed by the NuRD complex (Zuo et al., 2009b).

10. Hyaluronic-mediated Motility Receptor (HMMR), a cell surface oncogenic protein which is widely upregulated in human cancers and correlates well with the cell motility and invasion, has recently shown to be transcriptionally stimulated by MTA1 (Sankaran et al., 2012).

1.6 Lipoxygenase function and metabolism

Polyunsaturated fatty acids (PUFAs) like arachidonic and linoleic acids (PUFAs with n-6 function) are pro-carcinogenic unlike fish oils or PUFAs with n-3 function, which may be protective (Gong et al., 2007) (Hamberg and Samuelsson, 1974; Shureiqi and Lippman, 2001). Products of oxidative metabolism of arachidonic and linoleic acids by the lipoxygenase (LOX) and cyclooxygenase (COX) enzymes contribute to the pathogenesis and progression of various cancers, particularly colorectal cancer (Gong et al., 2007).

Lipoxygenases (LOXs) are cytosolic di-oxygenases, composed of a 75-80 kDa single polypeptide chain react with PUFAs to produce the corresponding hydroperoxy derivatives. They have two domains consisting of the smaller N-terminal - barrel domain and the larger C-terminal catalytic domain. A single non-heme iron is liganded to the latter domain by four histidines and the C-terminal

isoleucine. In the active state of this enzyme, the iron is in ferric form and reduced to the ferrous form in the inactive state.

There are 6 functional *LOX* genes in humans including 5-LOX, 12/15-LOX (15-LOX-1), platelet-type 12-LOX, 12R-LOX, epidermis-type 15-LOX (15-LOX-2) and epidermis-Alox3. Except Alox3 all these genes express a catalytically active enzyme. In mice, in addition to the human orthologs, mice also express the additional epidermis-type *12S-LOX* gene, which is present in humans as a non-functional pseudogene (Brash, 1999; Heidt et al., 2000; Kuhn and Thiele, 1999).

After enzymatic hydrolyzation from membrane phospholipids by phospholipase A₂, arachidonic acid is metabolized by both LOXs and COXs in the inflammatory eicosanoid pathway (Ara and Teicher, 1996; Tavolari et al., 2008). On the other hand, linoleic acid is only metabolised by LOX. Both 15-LOX-1 and -2 metabolize arachidonic and linoleic acids. Arachidonic acid is converted to 15-S-hydroxyeicosatetraenoic acid (15-S-HETE) by both enzymes. On the other hand, linoleic acid is converted to 13-S-HODE solely by 15-LOX-1 since 15-LOX-2 reacts poorly with linoleic acid (Baer et al., 1991; Brash et al., 1997; Daret et al., 1989).

1.7 15-Lipoxygenase-1 expression

The human 15-LOX-1 protein is mainly expressed in the colon, skin, epithelium of the tracheobronchial tree, eosinophils and reticulocytes (Funk, 1996; Kamitani et al., 1998).

15-LOX-1 is expressed in the cytoplasm of epithelial cells within the tumour and surrounding normal tissue, and also in stromal fibroblasts, but not in Peyer's patches in human colon (Bhattacharya et al., 2009; Ikawa et al., 1999).

1.7.1 15-Lipoxygenase-1 in cancer

15-lipoxygenase-1 (15-LOX-1) is an inducible and highly regulated enzyme in normal human cells, which metabolizes linoleic acid to 13-hydroxyoctadecadienoic acid (13-HODE) (Il Lee et al., 2011). 15-LOX-1 expression is downregulated in several human cancers including colon cancer (Cimen et al., 2009a; Heslin et al., 2005; Nixon et al., 2004; Shureiqi et al., 1999), esophageal cancer (Shureiqi et al., 2001), breast cancer (Jiang et al., 2006), and pancreatic cancer (Hennig et al., 2007), urinary bladder cancer (Philips et al., 2008) and lung cancer (Yuan et al., 2010).

Multiple lines of evidence collected from various experimental models in different human cancers suggest that 15-LOX-1 plays an anti-tumorigenic role by promoting several anti-tumorigenic events such as cell differentiation, apoptosis, and inhibiting chronic inflammation, angiogenesis and metastasis while, re-expression of 15-LOX-1 in various cancer cell lines inhibits tumorigenesis (Cimen et al., 2009a; Hennig et al., 2007; Jostarndt et al., 2002; Kim et al., 2006; Shureiqi et al., 1999; Shureiqi et al., 2001; Wu et al., 2003).

Importantly, we have also reported that expression of 15-LOX-1 reduced the metastatic potential of colon cancer cell lines, at least in part by reducing the expression of MTA1 (Cimen et al., 2009a), indicating the presence of a feedback loop.

Transcriptional repression of 15-LOX-1 involves several mechanisms such as promoter methylation, (Liu et al., 2004) through binding of the nucleosome remodeling and histone deacetylase repression complex (Zuo et al., 2009a), or by the overexpression of the transcription factor GATA- 6 (Shureiqi et al., 2007).

The reduced degradation of inhibitor of kappa B ($I\kappa B\alpha$), as well as decrease in nuclear translocation of p65 and p50, DNA binding and transcriptional activity of Nuclear factor kappa B (NF- κ B) have been observed in the presence of ectopic 15-LOX-1 expression in HCT-116 and HT-29 CRC cell lines (Cimen et al., 2011).

1.8 Nuclear factor kappa B (NF- κ B)

NF- κ B represents a family of transcription factors made of hetero- or homo-dimers mostly including one subunit of p65 (relA) and another subunit such as p50, c-rel or relB (Baeuerle and Baltimore, 1996; Cortes Sempere et al., 2008), which are retained in the cytoplasm in an inactive form by binding to the $I\kappa B$ inhibitory proteins (Cortes Sempere et al., 2008). After phosphorylation and degradation of $I\kappa B$ alpha, NF- κ B is free to translocate into the nucleus and control transcription of variety of genes. NF- κ B plays important roles in promoting chronic inflammation and tumorigenesis, especially in colon cancer (Karin, 2006).

1.9 Scope of the study

Based on the numerous biological effects of MTA1 expression and clinicopathological implications of the increased MTA1 expression in various human cancer tissues, it is likely that MTA1 has a very important role in the metastatic potential of colorectal cancer. In order to determine these effects we

proposed to characterize MTA1 gene in human colorectal cancer cell line HCT-116 through particularly metastasis and closely related EMT contexts.

15-LOX-1 is a lipid metabolizing enzyme that has tumor suppressive properties in CRC and is silenced by the NuRD complex of which MTA1 is a component. We have previously shown that reexpression of 15-LOX-1 inhibited metastasis in CRC, inhibited the inflammatory transcription factor nuclear factor kappa B (NF- κ B) through PPAR γ activation and resulted in reduced expression of MTA1 indicating the presence of a cross talk (Figure 1. 2). To this effect, we proposed to examine the effect of the ectopic expression of 15-LOX-1 on the expression of MTA1 in a panel of colon cancer cell lines; and then to further investigate the transcriptional regulation of MTA1 by NF- κ B. Furthermore, we also aimed to understand whether there is a negative correlation between 15-LOX-1 and MTA1 expression patterns in colorectal cancer patients.

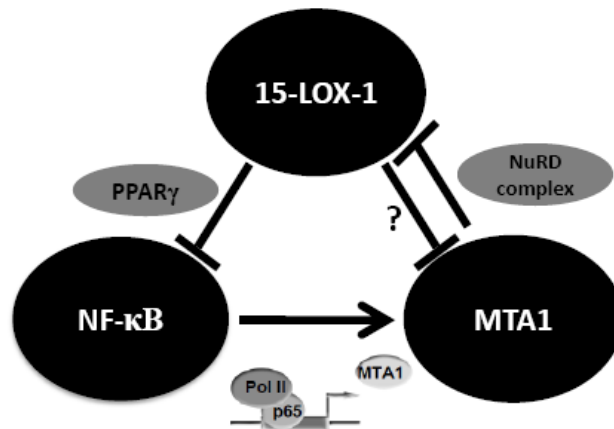


Figure 1. 2 Crosstalk between 15-LOX-1, NF- κ B and MTA1 proteins.

We believe this work will highlight the importance of MTA1 in the metastatic behaviour of colorectal cancer cells as well as epithelial mesenchymal transition. Moreover, explanation of possible mechanisms for MTA1 regulation by 15-LOX-1 will further underly tumor suppressor function of 15-LOX-1 gene in human colorectal cancer and help us to improve novel strategies to target and regulate the expression of MTA1 in colorectal cancer.

CHAPTER 2

MATERIALS AND METHODS

2.1 Cell culture

2.2 Cell culture

Human CRC cells HCT-116 were obtained from Deutsche Sammlung von Mikroorganismen und Zellkulturen (Braunschweig, Germany), HT-29 and Caco-2 cells were obtained from Şap Enstitüsü, (Ankara, Turkey), SW620 and LoVo cells were obtained from ATCC (Middlesex, England) and HUVEC were obtained from Lonza (Basel, Switzerland).

Human colorectal cancer cells HCT-116 were grown in phenol red free complete RPMI-1640 culture medium; HT-29 cells were grown in McCoy's 5A (Modified); SW620 cells were grown in Lebovitz-15 medium; Caco-2 cells were grown in EMEM medium and Lovo cells were grown in Ham's F12 medium. All media (Biochrom, Berlin, Germany) was supplemented with 10% fetal bovine serum (FBS) (Thermoscientific, Waltham MA, United States), 2 mM L-glutamine and 1% penicillin/streptomycin. The cells were grown in humidified atmosphere containing 5% CO₂ at 37°C. Cell culture media were supplemented with 1% penicillin/streptomycin. HUVEC cells were grown in EBM medium supplemented with growth factors (Lonza, Basel, Switzerland).

2.3 Transfection of cell lines

2.3.1 Cloning MTA1 silencing oligo (shRNA) into pSuper plasmid

2.3.1.1 Annealing of shRNA oligos

The forward and reverse shRNA oligos specific to MTA1 gene (5'GATCCCCGAACATCTACGACATCTCCTTCAAGAGAGGAGATGTCGTAGATGTTCTTTTAA3' and 5'AGCTTAAAAAGAACATCTACGACATCTCCTCTCTTGAAGGAGATGTCGTAGATGTTTCGGG 3') were annealed to each other in the presence of annealing buffer (Appendix B.1). The annealed oligo inserts were used immediately in the ligation reaction.

2.3.1.2 Linearization of the pSUPER.retro.neo+gfp vector:

pSUPER.retro.neo+gfp (received as a gift from Dr Elif Erson-Bensan, METU) vector (Appendix A.1) was linearized by double digestion using HindIII and BglII restriction enzymes. The reaction mixture was incubated at 37 °C O/N then at 80 °C for 20 min and EDTA was added to inactivate BglII. Digestion products were separated in 1% agarose gel in order to remove the fragment between two restriction enzyme BglII and HindIII, and to help separating the preparation from any undigested circular plasmid and to reduce the background in ligation and transformation (Appendix B.1). The linearized vector was obtained by using gel purification kit (Roche, Mannheim, Germany) according to the manufacturer's protocol. The protocol for gel purification is given in Appendix C.

2.3.1.3 Ligation into pSUPER.retro.neo+gfp vector

Annealed MTA1 shRNA oligos were ligated into pSUPER vector by using T4 DNA ligase (Roche, Mannheim, Germany) enzyme in the presence of T4 Ligation buffer. The mixture was incubated at 16°C, O/N and then transformed into *E.coli* Top10 competent cells (Competent cell preparation and transformation protocols are given in Appendix E and F, respectively), plated and left at 37°C for 16 h. Colonies formed on the plates were seeded in LB in the presence of ampicillin as the selection agent and left shaking at 37°C. The plasmid isolation was carried out by using plasmid isolation kit (Qiagen, Hilden, Germany) according to the manufacturer's protocol (Appendix G). Finally, the presence of positive clones was checked by double digestion with HindIII and EcoRI (Fermentas, Lithuania) as recommended in pSUPER RNAi system protocol and selected colonies were sent for sequencing (MCLab, South San Francisco, United States). Sequencing results are also shown in Appendix B.1.

2.3.2 Generation of pcDNA3.1/V5-His-TOPO (empty vector) from MTA1-pcDNA3.1/ V5-His-TOPO plasmid

MTA-1-pcDNA3.1/V5-His-TOPO vector (Appendix A.2) was kindly provided by Dr. Ansgar Brüning (Ludwig-Maximilians University; Munich, Germany). In order to generate empty vector from MTA1-pcDNA3.1/V5-His-TOPO, the vector was double digested with HindIII and XhoI restriction enzymes (Fermentas, Lithuania) for 4 h at 37°C. The digested products were separated in 1% agarose gel and appropriate band was obtained from the gel by using gel elution kit. Then, products were digested with S1 nuclease to remove overhangs and then ligation reaction was carried out with T4 DNA ligase (Roche) enzyme in the presence of T4 Ligation buffer. The mixture was incubated at 16°C, O/N and then transformed into Top10

competent cells, plated and left at 37°C for 16 h. Colonies formed on the plates were seeded in LB in the presence of ampicillin as the selection agent and left shaking at 37°C. The plasmid isolation was carried out by using plasmid isolation kit according to the manufacturer's protocol. Isolated plasmids were linearized after digestion with XbaI and separated in agarose gel for confirmation by size. The plasmids were also double digested with HindIII and XhoI to confirm the absence of the MTA1 insert (Data is shown in Appendix B.2).

2.3.3 Geneticin (G-418) kill curve for HCT-116 cells

Geneticin kill curve assay was done for HCT-116 cells by treating cells with changing concentrations of Geneticin (G-418). 0, 100, 200, 400, 600, 800, 1000 µg/ml geneticin was used in order to determine the minimum concentration required to kill untransfected HCT-116 cells. HCT-116 cells were plated in 6- well plates the day before antibiotic treatments (1,000,000 cells /well). The treatments were carried out in RPMI-1640 medium containing with 10% FBS, 2 mM L-glutamine and no penicillin-streptomycin. The medium containing G418 were replenished every 2 days. At the end of the assay cells were counted for each concentration and the kill curve was obtained as shown in Appendix M.

2.3.4 Stable Transfections

MTA-1-pcDNA3.1/V5-His-TOPO, pcDNA3.1/V5-His-TOPO (empty vector), MTA1-shRNA-pSUPER.retro.neo+gfp and pSUPER.retro.neo+gfp vectors (empty vector) were transfected into HCT-116 cells by using Lipofectamine transfection reagent as well as PLUS reagent to achieve high transfection performance. The day before transfection 5×10^5 HCT-116 cells per well was counted and plated in RPMI-1640 complete media without pen-strep. The confluency reached 60-80% on the day

of transfection. 2 µg plasmid DNA was mixed with 20 µl Lipofectamine PLUS Reagent and completed to 125 µl with reduced serum 1X OPTIMEM medium (Invitrogen, Carlsbad, CA, USA) and incubated at room temperature for 15 min. 7,5 µl Lipofectamine Reagent was completed to 125 µl serum-free dilution medium in a second tube and mixed. Then pre-complexed DNA and diluted Lipofectamine was mixed and incubated for 15 min at room temperature. As complexes were forming, medium on the cells was replaced with 1000 µl 1X OPTIMEM. Finally, DNA-PLUS-Lipofectamine Reagent complexes were added to each well, mixed into the medium gently and incubated at 37°C at 5% CO₂ over night. The medium of cells were changed with RPMI-1640 complete medium without antibiotics after 24 h of transfection and cells were left at 37°C at 5% CO₂. On day two G418 was added to select transfected cells. Finally, polyclones were obtained for MTA-1-pcDNA3.1/V5-His-TOPO and pcDNA3.1/V5-His-TOPO (empty vector) expressing cells; and monoclones were obtained for MTA1-shRNA-pSUPER.retro.neo+gfp and pSUPER.retro.neo+gfp (empty vector) expressing cells.

2.3.5 Transient Transfections

Cells were transiently transfected with pcDNA3.1-15-LOX-1 or pcDNA3.1 empty vector (Appendix A.3) for 48 h in 6 well plates (5 µg DNA) for protein isolations; in 10 cm dishes (24 µg DNA) for ChIP assays and in 12 well plates (2,5 µg) for luciferase assays. The pcDNA3.1-15-LOX-1 vector was obtained as a gift from Dr Uddhav Kelavkar, Mercer University School of Medicine, Savannah, GA, USA. Before the transfections, complete culture medium was changed with 1X antibiotic free OptiMEM medium.

X-tremeGENE HP (Roche, Mannheim, Germany) was used as a transfection reagent in ratio of 3:1 of X-tremeGENE HP to plasmid. Transfection mixes were

prepared in 1X OptiMEM. The ingredients were added into a sterile eppendorf tube in the order of OptiMEM, DNA and X-tremeGENE HP. Mixtures were left at RT for 15 min and added accordingly by swirling onto 80-90 % confluent cells.

DNA was precomplexed with the PLUS Reagent and incubated at room temperature for 15 min. Pre-complexed DNA and prediluted LIPOFECTAMINE Reagent was mixed and incubated for 15 min at room temperature. DNA-PLUS-LIPOFECTAMINE Reagent complexes were added to each well containing fresh medium on cells (60-80% confluency).

2.4 Protein expression analysis

2.4.1 Total Protein isolation and quantification

Proteins were extracted by using M-PER protein isolation kit (Pierce, Rockford, IL, USA) in the presence of protease inhibitors (Roche, Mannheim, Germany) according to the manufacturer's guidelines (M-PER protein isolation protocol is given in Appendix H). The protein content was measured by using modified Bradford Assay (Assay protocol and the standard curve is given in Appendix K).

2.4.2 Nuclear /cytoplasmic protein isolation and quantification

For isolation of nuclear and cytoplasmic proteins cells were collected in pre-chilled 1.5 ml eppendorph tubes and centrifuged suspended cells at 300 x g for 5 minutes at 4 °C. Supernatant was discarded and cells were resuspended in PBS/Phosphatase Inhibitor Solution and centrifuged at 300 x g for 5 min at 4°C (2X). Following the removal of supernatant, 500 µl ice-cold 1X Hypotonic Buffer, prepared from 10X

Hypotonic Buffer (100mM HEPES (pH 7.5), 40 mM NaF, 100 μ M Na₂MoO₄, 1mM EDTA) in the presence of protease and phosphatase inhibitors, was added and after gentle pipetting incubated pellet on ice for 15 minutes allowing cells to swell. 100 μ l of 10% Nonidet P-40 was added and mixed gently, centrifuged for 30 s at 4°C and supernatant (cytosolic fraction) was transferred into a new tube, stored at -80 °C. The pellet was resuspended in 1X ice-cold Complete Nuclear Extraction Buffer (1X) prepared from 2X Nuclear extraction buffer (20 mM HEPES (pH 7.9) 0.2 mM EDTA, 3 mM MgCl₂, 840 mM NaCl and 20% glycerol) in the presence of protease and phosphatase inhibitors as well as DTT (10 mM); vortexed 15 s at highest setting then gently rocked the tube on ice for 5 min using a shaking platform (2X). Lysate was centrifuged at 14000 x g for 10 min at 4 °C; supernatant was collected as nuclear fraction.

The protein content was measured by using modified Bradford Assay (Assay protocol and the standard curve is given in Appendix K).

2.4.3 Western blotting

Whole-cell extracts (50-80 μ g) and prestained Pageruler protein ladder (Fermentas, Lithuania) were separated in a 10% polyacrylamide gel (Appendix R) and transferred onto a nitrocellulose membrane (Bio-Rad, Hercules, CA, USA) at 4°C for 1.30 hours. The membrane was blocked in 5-10% skim milk and probed with appropriate antibodies in required dilutions. The 15-LOX-1 antibody was obtained from Cayman Chemical (Ann Arbor, MI, USA). XIAP, Bcl-xl, procaspase, E-cadherin, ZO-1, SNAI1, SLUG, Vimentin, β -catenin, p65, β -actin and GAPDH antibodies were obtained from Santa Cruz (CA, USA). Primary antibody incubation was followed by a horseradish peroxidase-conjugated (1:2000 dilution) secondary antibody incubation. After incubations, membrane was washed 3X using PBS-T

(Appendix P). Finally the bands were visualized by using an enhanced chemiluminescence kit ECL Plus (Pierce, Rockford, IL, USA) according to the manufacturer's instructions and Kodak X-ray processor.

In order to show equal protein loading, membranes were stripped by using a stripping buffer (Appendix P), at 65°C for 15 minutes with shaking and then probed with horseradish peroxidase-conjugated β -actin monoclonal antibody (1:1000 dilution). After membrane washing with PBS-T, the bands were visualized as described previously.

2.5 mRNA expression analysis

2.5.1 RNA isolation

Total cellular RNA was extracted from cells by using the RNeasy Minikit (Qiagen, Hilden, Germany) according to manufacturer's guidelines (Appendix I). RNA isolates were kept at -80°C till cDNA synthesis. The amount and purity of total RNA obtained from cells was measured spectrophotometrically at 260 and 280 nm in a quartz cuvette after dilution in molecular biology grade water in 1:20 ratio (Absorbance $\mu\text{g/ml} = 40 \times \text{Measured OD}_{260} \times \text{dilution factor}$). RNA samples with $\text{OD } 260 \text{ nm} / \text{OD } 280 \text{ nm} = 1.8$ and above was used in the downstream applications.

2.5.2 DNase-1 Treatment

In order to remove any contaminating genomic DNA from the RNA isolate, DNase-1 treatment was carried out with Fermentas DNase-1 treatment kit. 1 μg RNA, 1 μl 10X Reaction Buffer with MgCl_2 , 1 μl DNase-1 was completed to 9 μl in a RNase-

free tube and incubated at 37 °C for 30 minutes. Next, 1µl 25 mM EDTA was added into the reaction mixture and incubated at 65°C for 10 minutes. The treated RNA was used as a template for reverse transcriptase.

2.5.3 cDNA synthesis

First strand cDNA synthesis was carried out with Revert Aid cDNA Synthesis kit from total RNA (1µg) using oligo dT primers according to manufacturer's guidelines (Revert Aid cDNA Synthesis kit protocol is given in Appendix J).

2.5.4 Reverse transcriptase PCR

Amplification of cDNA was carried out using a 30 µl reaction mixture containing 3µl of 10X buffer, 0.2mM of each dNTP, 2.5mM MgCl₂, 0.5 µM forward and reverse primer pairs, 1U Taq DNA polymerase (Fermentas) and 3µl of cDNA (100 ng/ µl) and PCR grade water in thermal cycler (Applied Biosystems). Primers used for each particular experiment was listed under the relevant protocol.

For duplex PCR reactions, 0.5 µM GAPDH was added to the PCR mix as an internal control. Negative control was also included which does not contain template. 10 µl of the final PCR products were electrophoresed on a 2% agarose gel at 100V and photographed under UV light.

2.5.5 Quantitative (Real Time PCR)

Amplification of cDNA was carried out using a 20 µl reaction mixture containing 10 µl of 2X Fast Start SYBR Green Mastermix, 0.5 µM forward and reverse primers and 2 µl cDNA in Corbett (Qiagen) or Applied Biosystem 7500 Real Time

PCR machine. The housekeeping gene β -actin primers were used for calibration. Standard curves were constructed by using different dilutions of cDNAs and the delta Ct values were calculated. The fold change was calculated by using delta delta Ct method (Pfaffl, 2001).

2.6 Cell viability assay

2.6.1 MTT assay

The effects of MTA1 overexpression and silencing expression on cell proliferation was measured by using the Vybrant MTT colorimetric assay kit (Invitrogen Carlsbad, CA, USA) according to manufacturer's instructions which is a simple method for determination of the viable cell number using a microplate absorbance reader. The water soluble MTT (3-(4, 5-dimethylthiazol-2-yl)-2, 5-diphenyltetrazolium bromide) is converted to an insoluble formazan by mitochondrial reductase in the mitochondria of viable cell. The formazan is then solubilized by adding SDS solution and the concentration is determined by optical density at 570 nm.

Briefly, MTA1 overexpressing cells (MTA1 oex polyclone I), empty vector transfected cells (EV(pcDNA3.1); MTA1 silenced cells (shMTA1b1 and shMTA1d1), empty vector transfected cells (EV(pSUPER) were seeded in 96 well plates (15,000 cells/ well) and 24 hours later 10 μ l of MTT labeling reagent was added in fresh RPMI-1640 medium. Following incubation with MTT labeling reagent for 4 hours, 100 μ l SDS-HCL solution prepared by dissolving 1 g of SDS in 10 ml 0.01 M HCl solution was added to the wells and incubated for 18 hours. The medium with MTT reagent was used as a blank. The absorbance of each well was

read at 570nm in a Bio-Rad 680 microplate reader. Experiment was performed with 10 replicates.

2.7 Cell proliferation assay

2.7.1 BrdU assay:

Cellular proliferation was assayed by using BrdU assay kit (Roche, Mannheim, Germany) according to the manufacturer's instructions. The assay is based on the principle of detection of BrdU incorporation into the genomic DNA of proliferating cells. Briefly, MTA1 overexpressing cells (MTA1 oex polyclone I), empty vector transfected cells (EV pcDNA3.1); MTA1 silenced cells (shMTA1b1 and shMTA1d1), empty vector transfected cells (EV pSUPER) were seeded in (10,000 cells/ well) in 96-well tissue-culture black microplates were labeled by the addition of BrdU for 2 h. During this labeling period, BrdU was incorporated in place of thymidine into the DNA of proliferating cells. Following labeling, the cells were fixed, and the DNA was denatured by adding FixDenat. Subsequently, the anti-BrdU-POD antibody was added which binds to the BrdU incorporated newly synthesized cellular DNA. Finally, the immune complexes were detected after the substrate addition by measuring the light emission using a multi-well scanning luminometer (Turner Biosystems).

2.8 Cellular motility

2.8.1 *In vitro* scratch wound healing assay

Cellular motility was measured by *in vitro* scratch wound healing assay. MTA1 overexpressing cells (MTA1 oex polyclone I), empty vector transfected cells (EV(pcDNA3.1); MTA1 silenced cells (shMTA1b1 and shMTA1d1), empty vector transfected cells (EV(pSUPER)) were plated in six-well plates, incubated until 90% confluency was reached and then scratched with a sterile pipette tip. Wells were washed 2X with PBS, and the cells were then incubated in RPMI-1640 complete medium. Subsequent to wounding, images were taken with an inverted microscope with 10X objective (Olympus, Hamburg, Germany), Wound closure was monitored with microscopy for 24 hours after the wound was formed. The distances between the wound edges were measured from wound images using the ImageJ 1.42 program.

2.9 Apoptosis assay

2.9.1 Annexin V Staining

Movement of phosphatidylserine (PS) from the inner side of the plasma membrane to the outer layer, exposing PS at the surface of the cell is one of the alterations that occur in the early stages of apoptosis. Annexin V is a Ca^{2+} -dependent phospholipid-binding protein with a high affinity for PS. Annexin V staining was carried out according to the manufacturer's instructions. Briefly, MTA1 over-expressing cells (MTA1 oex polyclone I), empty vector transfected cells (EV (pcDNA3.1)); MTA1 silenced cells (shMTA1d1) and empty vector transfected cells (EV (pSUPER)) were

grown in 6 well plates and then trypsinized and collected as well as their supernatants. Cells are washed with PBS, centrifuged and the supernatant was removed. Finally the pellet was resuspended in 100 μ l of Annexin-V-FLUOS labeling solution, incubated 10-15 minutes at RT and read by flow cytometer after addition of 300 μ l incubation buffer. The flow cytometry experiments were conducted in the Department of Molecular Biology and Genetics, Bilkent University with the guidance of Dr. İhsan Gürsel and Dr. Tamer Kahraman.

2.10 Anchorage independent growth

2.10.1 Soft Agar Assay

To evaluate the ability of cells to grow in an anchorage-independent manner, MTA1 over-expressing cells (MTA1 oex polyclone I), empty vector transfected cells (EV(pcDNA3.1)); MTA1 silenced cells (shMTA1d1) and empty vector transfected cells (EV(pSUPER)) were grown on noble agar (Difco, BD Biosciences, San Jose, CA, USA). Briefly, a bottom noble agar layer was prepared by layering 1 ml of complete RPMI-1640 medium containing 0.6% agar and allowed to solidify for 1h at room temperature in a 6-well plate. Then HCT-116 cells were mixed with RPMI-1640, G-418 and 0.33 % noble agar. This mixture (1ml) was added onto the solidified bottom layer. After 2 weeks the plates were stained with crystal violet (0.005%) and the colonies were counted manually under a Leica light microscope.

2.11 Cell Adhesion Assay

In order to investigate the effect of MTA1 expression on the ability of HCT-116 cells to metastasize cell adhesion assay was carried out with MTA1 over-expressing

cells (MTA1 oex polyclone I), empty vector transfected cells (EV(pcDNA3.1)); MTA1 silenced cells (shMTA1d1) and empty vector transfected cells (EV(pSUPER)). 96 well plates were treated with 75 μ l of fibronectin at a concentration of 50 μ g/ml and left at 37°C in a CO₂ incubator for 1 hour. Some wells were left untreated to be used as negative controls. Then, the 96 well plates were washed 2X with washing buffer (0.1% BSA in RPMI-1640 medium). The plate was blocked with 1% blocking buffer (1% BSA in RPMI-1640) by adding 100 μ l of blocking buffer into the wells previously coated with fibronectin (Biological Industries, Israel) and incubated at 37°C in a CO₂ incubator for 1 h. After incubation, the plate was washed one more time with washing buffer and chilled on ice. The cells were washed with PBS, and seeded as 40,000 cells/ well in RPMI-1640 medium. Uncoated empty wells were also plated with 40,000 cells/well as negative controls. Additionally, 40,000 cells/well were seeded in a second 96 well plate treated with fibronectin as a total cell control. Both plates were left at 37°C in a CO₂ incubator for 2h. At the end of the incubation, the first 96-well plate (containing both fibronectin coated and uncoated wells) was washed twice with PBS and inverted on a filter paper gently to remove non-adherent cells.

Finally, MTT assay was carried out to measure cell number in each well. Adhesion values for each sample was calculated by dividing the obtained absorbance value in fibronectin treated wells by untreated, total cell wells corresponding to each particular sample. The ratios were multiplied by 100 and data was interpreted as % values.

2.12 Boyden chamber Cell Migration Assay

We investigated whether there is a difference in the migration ability of HCT-116 cells upon MTA1 over-expression or silencing by Boyden chamber cell migration

assay. Trans-well (Corning, NY, USA) cell migration assays were done in a two-chamber 24 well migration assay plate which includes of upper and lower chambers. Firstly, MTA1 over-expressing cells (MTA1 oex polyclone I), empty vector transfected cells (EV(pcDNA3.1)); MTA1 silenced cells (shMTA1d1) and empty vector transfected cells (EV(pSUPER)) were harvested by the use of Trypsin/EDTA and washed 3X in RPMI-1640 media with 1% FBS. Next, 100 μ l of the cell suspension containing 50,000 cells was applied onto the 8 μ m Transwell filters (upper chamber). For stimulation of the cell migration through the 8 μ m pored membranes, 300 μ l RPMI-1640 complete media containing 5 μ g/ml fibronectin as a chemoattractant was added to the lower chamber. The cells were left at 37°C in a CO₂ incubator for 48 hours. At the end of incubation period transwells were removed from the 24-well plates and the unmigrated cells and the media on the upper face of the Transwell membrane filters was swabbed of by using sterile cotton swabs. The swabbing repeated at least 2X with fresh swabs.

Subsequently, the Transwells were fixed and stained in 100% methanol for 10 minutes and in Giemsa solution for 2 minutes at RT, respectively. Finally, the Transwells were washed in sterile distilled water to remove excess stain and left to air dry inside the laminar flow hood. After the membrane filters were dry, they were removed out and transferred to a glass slide. The total number of cells that had migrated through transwell filters was counted under a Leica light microscope.

2.13 Boyden chamber Cell Invasion Assay

To study the effect of MTA1 expression on metastatic potential of HCT-116 cells, the Boyden chamber invasion assay was carried out which mimics the *in vivo* metastasis process. Invasive capacities of cancer cells can be determined by establishing a barrier of extracellular matrix (ECM) through which the cells are

expected to invade. Matrigel is a basement membrane matrix preparation and composed of mostly laminins and collagen IV isolated from the Englebreth-Holm-Swarm mouse sarcoma and used as an ECM barrier in these assays. Invasion of tumor cells into Matrigel (BD Biosciences, San Jose, CA, USA) has been used to investigate the enrollment of ECM receptors and matrix degrading enzymes in tumor progression. Firstly, Matrigel (thawed overnight at 4°C) was diluted in 1:5 ratio (400 µl Matrigel was mixed with 1600 µl serum free cold RPMI-1640 media) and then applied onto the upper chamber of the 24-well Transwell plates. Matrigel coated transwells are kept at 37°C in CO₂ incubator for 4 h.

Matrigel preparation steps were carried out on ice and all materials used were maintained at 4°C as matrigel solidifies very quickly. MTA1 over-expressing cells (MTA1 oex polyclone I), empty vector transfected cells (EV(pcDNA3.1)); MTA1 silenced cells (shMTA1d1) and empty vector transfected cells (EV(pSUPER)) were harvested by the use of Trypsin/EDTA and washed 3X in RPMI-1640 media with 1% FBS. Subsequently, gelled Matrigel prepared before was gently washed with warmed serum free culture media and 100 µl of the cell suspension containing 100,000 cells was applied onto the matrigel. For stimulation of invasion through matrigel coated Transwell filter membranes, 300 µl RPMI-1640 complete media containing 5µg/ml fibronectin as a chemoattractant is added to the bottom chamber of the Transwells.

The invasive cells invade through the matrix barrier and the pores of Transwell filter membrane. The incubation was carried out for 72 h at 37°C in a CO₂ incubator. At the end of the incubation, the upper chambers of Transwells were swabbed 3X by using cotton swabs.

By doing so, the entire surface of the filter was swabbed and all of the cells that have not invaded were removed. Subsequently, the Transwells were fixed and

stained in 100% methanol for 10 minutes and in Giemsa solution for 2 minutes at RT, respectively. Finally, the Transwells were washed in sterile distilled water to remove excess stain and left to air dry inside the laminar flow hood. After the transwell membranes were dry; they were removed out and transferred to a glass slide. The total number of cells that had migrated through transwell filters was counted under a Leica light microscope.

2.14 VEGF ELISA Assay

Human VEGF Immunoassay (Quantikine, R&D Systems) was used by following the manufacturer's instructions. Briefly, HCT-116 cells (1.5×10^6 cells/well) were seeded in 12 well plates and conditioned medium was collected after 48 h. Standards and samples were added into the assay plates wells which carries immobilized antibody for determination of VEGF present in the applied standards and samples. After incubation, color development was measured at 450 nm and 570 nm by the use of substrate reaction. Standard curve for VEGF concentration is given in Appendix L.

2.15 In vitro angiogenesis assay:

HCT-116 cells (1×10^6) cells were seeded in 500 μ l medium without antibiotics and the conditioned medium was collected after 48 hours. HUVECs (3×10^4 cells) were collected in EBM and mixed with previously collected conditioned medium in a 1:1 ratio which is then placed in Matrigel pre-coated 96 wells plates. After incubation of assay plates at 37°C for 16h, 4X microscope images were taken for the evaluation of number of tubes, branch points, nodal structures, and total skeleton length formed. Analyses were performed by S.CoLifesciences <http://www.sco-lifescience.com/trial.php5> (Munich, Germany).

2.16 Determination of NF- κ B binding sites on the MTA1 promoter region

To identify NF- κ B binding sites on the MTA1 promoter, we extracted ~ 2 kb sequence from NCBI database and analysed in Alibaba 2.1 Transcription factor binding site detection program <http://www.gene-regulation.com/pub/programs/alibaba2/index.html>. The program offered several binding sites between the regions -1874 and -730 upstream of the MTA1 transcription start site.

2.17 Chromatin Immunoprecipitation (ChIP) Assay:

For ChIP assays, cells were grown in T25 plates or 10 cm dishes to confluency and crosslinked with 0.75% final concentration of paraformaldehyde at room temperature for 7 minutes. Crosslinking was stopped by addition of 2 mM Glycine. After centrifuge and washing steps chromatin was sheared to an average size of 500-1000 bp by probe sonication (7 times with 30s pulses for HCT-116 cells or 9 times with 30s pulses for HT-29 cells and 20% output). After input control was spared from the lysate; the rest was snap-frozen and kept at -80°C. Input DNA was quantitated after RNase A (1 h, 37°C), Proteinase K (O/N,60°C) incubations followed by isolation of input DNA by using Roche High Pure PCR purification kit (Roche, Mannheim,Germany) according to manufacturer's instructions. Isolation protocol is given in Appendix D. According to the input DNA amount obtained, lysates corresponding to 25 μ g chromatin for each sample were immunoprecipitated with 10 μ g of SNAI1, SLUG or p65 (polyclonal) antibodies and normal goat or normal rabbit IgG by rotating overnight at 4°C. Protein A/G sepharose beads saturated with bovine serum albumin (BSA) and single-stranded calf thymus DNA were added to the lysate to isolate the antibody-bound complexes. The beads were washed several times to remove nonspecific binding, and the antibody-bound chromatin was eluted. The eluate was RNase treated for 1 hour at 37°C and with

proteinase K, O/N at 60 °C to digest the immunoprecipitated proteins, and finally, the DNA extracted using Roche High Pure PCR purification kit (Appendix D) was used in PCR reactions.

PCRs for Region I and Region II were carried out with promoter specific primers and control primers which are shown in Table 2. PCR thermal cycling conditions for ChIP PCRs are given in Appendix N. Negative control reaction mixture, without template was included for all PCR reactions. 10 µl of the final PCR products were electrophoresed at 100V, in a 2% agarose gel and photographed under UV light.

Table 2 Primers used for ChIP assays

Primer	Sequence
MTA1proR1F_ChIP	5'GGACAGCCTTGACTGTCTCC 3'
MTA1proR1R_ChIP	5'ACACCACTGGGACACATCCT 3'
MTA1proR2F_ChIP	5'TCTCTCCCCAGAGACAGCAC 3'
MTA1proR2R_ChIP	5'CACCTGTCAGGATGCCTTC 3'
controlprimerF_ChIP	5'ATGGTTGCCACTGGGGATCT 3'
controlprimerR_ChIP	5'TGCCAAAGCCTAGGGGAAGA 3'
SNAI_SLUG_ChIP_F	5'GAACTGCAAAGCACCTGTGA 3'
SNAI_SLUG_ChIP_R	5'TGCGTCCCTCGCAAGTC 3'

2.18 Reporter gene assays

2.18.1 Construction of reporter plasmids

Possible binding sites (Region I and Region II in ChIP assays) were cloned into pLuc-MCS vector (Appendix A.4 and Appendix B.3) as explained below. Region I was cloned as oligo and Region II was PCR cloned, oligo and primer sequences used are given in Table 3.

Briefly, Region I oligos were dissolved as 10 mg/ml stock concentration. In order to reach 0.1 µg/µl concentration of insert DNA, 1 µl from each oligos were mixed with 198 ul annealing buffer and heated at 95 °C for 5 min and gradually cooled down to room temperature after 95 °C for 5 min, 85°C for 4 min, 80 °C for 4 min, 75°C for 4 min, 70°C for 4 min, 60°C for 4 min, 50°C for 4 min 37 °C for 4 min, 20 °C for 4 min, 10 °C for 4 min till 4°C. Region II (~600 bp) containing 5 possible NFkB binding sites was PCR amplified with the cloning primers (Appendix B.3).

Table 3 Oligo and primer sequences used for generation of reporter vectors

Primer	Sequence
Oligo R1F	5'CCCAAGCTTGGCCAGGGAAGGCCAGGGAAGGCC AGGGAAGCTCGAGCCCCC 3'
Oligo R1R	5'CCCCCCTCGAGTTCCTGGCCTTCCTGGCCTTCC CTGGCCAAGCTTCCC 3'
Cloning primer R2F	5'CCCAAGCTTTCTCTCCCCAGAGACAGCAC 3'
Cloning primer R2R	5'CCCCCCTCGAGCACCTGTCAGGATGCCTTC 3'

Region I annealed oligos and PCR amplified Region II and pLuc- MCS plasmid was double digested by using HindIII and XhoI restriction enzymes in the presence of Buffer R by incubation at 37 °C for 16 h and inactivation at 80 °C for 20 min 1 unit from each. After confirmation of digestion and clearing steps inserts were ligated into pLuc-MCS vector by using T4 DNA ligase and incubating at 16°C, 16 h and 65°C, 10 minutes for inactivation. Generated plasmids were confirmed for carrying Region I or Region II by sequencing (Central Laboratory, METU). Sequencing results are shown in Appendix B.3.

2.18.2 Luciferase/renilla dual system assays

Luciferase assays were carried out by using Dual-Glo® Luciferase Assay System according to the manufacturer's instructions. The Dual-Glo® Luciferase Assay System provides analysis of mammalian cells containing genes for firefly and *Renilla* luciferases.

Transfection ratios of pLuc-MCS vectors to pHRLTK were optimized in pcDNA3.1-15-LOX-1 and pcDNA3.1-EV pre-transfected LoVo cells (1:200) in 96 wells. The transfection efficiency graph can be found in Appendix O. Transfection ratios for the HT-29 cells were previously optimized (1:5) in our laboratory.

Cells previously transfected with 15-LOX-1 and EV plasmids were transfected with pLuc-R1, pLuc-R2 or pLuc-MCS plasmids together with pHRLTK plasmid for 24 h. The Dual-Glo® Luciferase reagent which induces cell lysis and acts as a substrate for firefly luciferase was added onto the cells and luminescence of the lysate was measured in white plates. Then Dual-Glo® Stop & Glo® Reagent, substrate for *Renilla* luciferase, was added and luminescence was measured again.

2.19 Electrophoretic mobility shift assay (EMSA)

Nuclear proteins were extracted from 15-LOX-1 or empty pcDNA3.1 vector transfected HT-29 and LoVo cells as described above. NF- κ B DNA binding sequences were designed as three repeats together with their mutated oligos (mainly Gs were converted to A's in original oligo sequences) and obtained commercially (Iontek, Turkey). Oligos containing the binding or mutated sequences for sense and antisense strands were biotinylated at the 3' end of each oligo by using Biotin 3' End DNA Labeling Kit (Thermo Scientific Pierce, USA). 25 μ l ultrapure water, 10 μ l terminal transferase reaction buffer (5X), 5 μ l oligo (1 μ M), 5 μ l biotin-11-UTP, 5 μ l terminal transferase enzyme (2U/ μ l) and 1 μ M of each oligo was mixed and reaction was incubated for 30 minutes at 37°C, and then stopped by the addition of 2.5 μ l 0.2M EDTA. The products were subjected to phenol:chloroform:isoamylalcohol (25:24:1) extraction in order to remove terminal deoxynucleotidyl transferase (TdT). Equal amounts of the oligos were annealed by heating to 95°C and then cooling down gradually. Unlabeled strands were also annealed to be used as cold probes.

In EMSA binding reactions 5-10 μ g of protein was mixed with 2 μ l 10X binding buffer, 1 μ l of 50% glycerol, 1 μ l of 1 μ g/ μ l Poly (dI•dC), 1 μ l of 1% NP-40, 1 μ l of 100mM MgCl₂, 1 μ l of 1M KCl, 1 μ l of 200mM EDTA, 20 fmol labeled oligo and ultrapure water.

For confirmation of reaction specificity, 200 fold molar excess (4 pmol) of cold probe was used which should cause a loss of the gel shift. Another reaction was also included containing p65 monoclonal antibody, causing to a supershift of the oligo-protein-antibody complex. Finally, 5 μ l of 4X Loading Dye was mixed with reactions and loaded in the gel. A positive control (EBNA, provided in the kit) was also included in the experiments.

The products were loaded and separated in 8% polyacrylamide gel (Appendix R) in 0.5X TBE buffer (Preparation of TBE buffer is given in Appendix P) at 100 V for 1 h at 4°C. Then, a transfer was carried out using Biodyne A or B membranes (Thermo Scientific Pierce, USA) in 0.5X TBE buffer at 100 V, for 30 minutes at 4°C.

Next, membrane was placed on UV transilluminator as DNA side down for 15 minutes to achieve cross linking reaction. The membrane was then incubated in streptavidin containing solution and finally detection was achieved using luminol enhanced hydrogen peroxide substrate. The signals were reflected on X-ray films by the use of Kodak X-Ray film developer machine.

NF- κ B binding oligo and mutated oligo sequences used in EMSA are shown in Table 4.

Table 4. EMSA oligo sequences

Primer	Sequence
Oligo1F	5' GGCCAGGGAAGGCCAGGGAAGGCCAGGGAA 3'
Oligo1R	5' TTCCCTGGCCTTCCCTGGCCTTCCCTGGCC 3'
Oligo2F	5' GGGGCTTTCGGGGCTTTCGGGGCTTTC 3'
Oligo2R	5' GGAAAGCCCCGGAAAGCCCCGGAAAGCCCC 3'
Oligo3F	5' CTGGCTTTCCTCCTGGCTTTCCTCCTGGCTTTCCT C 3'
Oligo3R	5'GAGGAAAGCCAGGAGGAAAGCCAGGAGGAAAG CCAG 3'
Oligo4F	5'GGGATGTCCC GGGATGTCCC GGGATGTCCC 3'
Oligo4R	5'GGGACATCCC GGGACATCCC GGGACATCCC 3'
Oligo5F	5'GGGAAGCCCC GGAAGCCCC GGAAGCCCC 3'
Oligo5R	5'GGGGCTTCCC GGGGCTTCCC GGGGCTTCCC 3'
Oligo6F	5'TGGA CTCTCC TGA CTCTCC TGA CTCTCC 3'
Oligo6R	5'GGAGAGTCCA GGAGAGTCCA GGAGAGTCCA 3'
Mutated_Oligo1F	5'GGCCAATTCA GGCCAATTCA GGCCAATTCA 3'
Mutated_Oligo1R	5'TGAATTGGCCTGAATTGGCCTGAATTGGCC 3'
Mutated_Oligo6F	5'TAATCTCAACTAATCTCAACTAATCTCAAC 3'
Mutated_Oligo6R	5'GTTGAGATTAGTTGAGATTAGTTGAGATTA 3'

2.20 Microarray data analysis

Publicly available cancer dataset GSE41258 were used for analyzing the correlation between 15-LOX-1 and MTA1 transcript levels in colorectal cancer patients as wells as other forms of cancer and healty individuals. These datasets were downloaded from Gene Expression Omnibus (GEO) which can be accessed at: <http://www.ncbi.nlm.nih.gov/geo/>.

Dataset GSE41258 was downloaded and analyzed using GeneSpring GX 11.0. The raw intensity values were pre-processed, summarized and normalized with using RMA algorithm. The resulting values were log transformed and expression levels for each of the probesets representing MTA1 and 15-LOX-1 were extracted. Correlation was evaluated by calculation of Pearson's coefficient (r) in Graphpad Prism 5 Software.

2.21 TissueScan Aray

Human TissueScan Colon Cancer Tissue qPCR Panel IV, containing 48 samples covering 8-normal, 5-Stage I, 8-IIA, 1-II, 1-IIIA, 6-IIIB, 3-IIIC, 6-III, 10-IV patients dried colon first strand cDNA, was purchased from Origene (Rockville, USA). 3 identical plates were used for 15-LOX-1, MTA1 and b-actin (calibrator gene) expressions.

Prior to the start of the experiment, the TissueScan plate was removed from -20°C storage and allowed to warm to room remperature. A SYBR Green pre-mix was prepared by using 2X SYBR Green Master Mix, 10 pmol/μl of gene specific forward and reverse primers (shown in Table 5) and PCR grade water completing the reaction mixture up to 30 μl/well. After aliquoting 30 μL of the PCR pre-mix

into the wells, the top of the plate was covered with adhesive cover sheet and left on ice for 15 min to allow the dried cDNA to dissolve. Finally, the plate was mounted into the heating unit of 96 well ABI 7500 Real-Time machine (Department of Molecular Biology and Genetics, Bilkent University). The particular thermal cycling program optimized and used for the primers is given in Appendix S. Melt curves are shown in Appendix T

Table 5. RT-PCR primers used in TissueScan array

Primer	Sequences
15-LOX-1_Q-PCR_F	GTCTTCCTTCTATGCCCAAGAT
15-LOX-1_Q-PCR_R	CACAGCCACGTCTGTCTTATAG
MTA1_Q-PCR_F	TGCTCAACGGGAAGTCCTACC
MTA1_Q-PCR_F	GGGCATGTAGAACACGTCACC

2.22 Statistical analysis

Each assay was repeated independently at least 3 times with several technical replicates. Results are expressed as the mean \pm standard deviation. One-way ANOVA with Tukey's post hoc test, Student's t-test or Mann–Whitney U-test was used for statistical analysis, and differences at $P < 0.05$ were considered significant.

CHAPTER 3

RESULTS

3.1 MTA1 expression in CRC cell lines

In order to determine the expression of MTA1 protein in different CRC cell lines, a Western blot for MTA1 was carried out using protein lysates from HT-29, LoVo, HCT-116, SW620 and Caco-2 cells (Figure 3. 1). We observed high expression of MTA-1 in HT-29 and LoVo cell; a moderate expression in HCT-116 and very low expression in Caco-2 cell line. HCT-116 cells were chosen for both overexpression and silencing of MTA1.

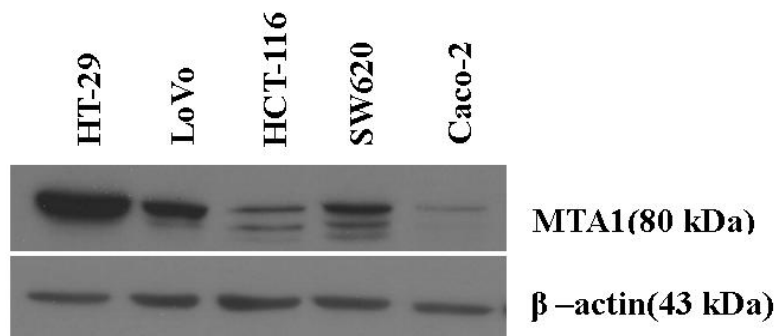


Figure 3. 1 Western blot of MTA1 protein expression in five different CRC cell lines including HT-29, LoVo, HCT-116, SW620 and Caco-2.

The multiple bands seen with the MTA1 antibody most likely stems from methylated and demethylated forms of MTA1 protein at lysine 532 residue, which have been shown to be involved in NuRD and NuRF complexes respectively (Nair et al., 2013).

3.2 MTA1 expression in transfected HCT-116 cells

HCT-116 cells were transfected with MTA1-pcDNA3.1/V5-His-TOPO or pcDNA3.1/V5-His-TOPO empty vector to generate stable polyclones of MTA1-overexpressing and empty vector transfected HCT-116 cells. Specific shRNA targeting of MTA1 was carried out by transfecting HCT-116 cells with MTA1-shRNA-pSUPER.retro.neo+gfp vector or with pSUPER.retro.neo+gfp vector as control.

In order to confirm the overexpression and silencing of MTA1 in the transfected cells, a western blot analysis was carried out. The corresponding empty vector transfected cells served as controls. As shown in Figure 3. 2, MTA1 protein levels were higher in MTA1 overexpressing polyclones (MTA1oex polyclone I and II) compared to the empty vector transfected cells (EV pcDNA3.1), whereas the protein levels in the MTA1 silenced HCT-116 monoclonal cells (shMTA1b1 and shMTA1d1) were reduced considerably compared to the corresponding empty vector transfected cells (EV(pSUPER)).

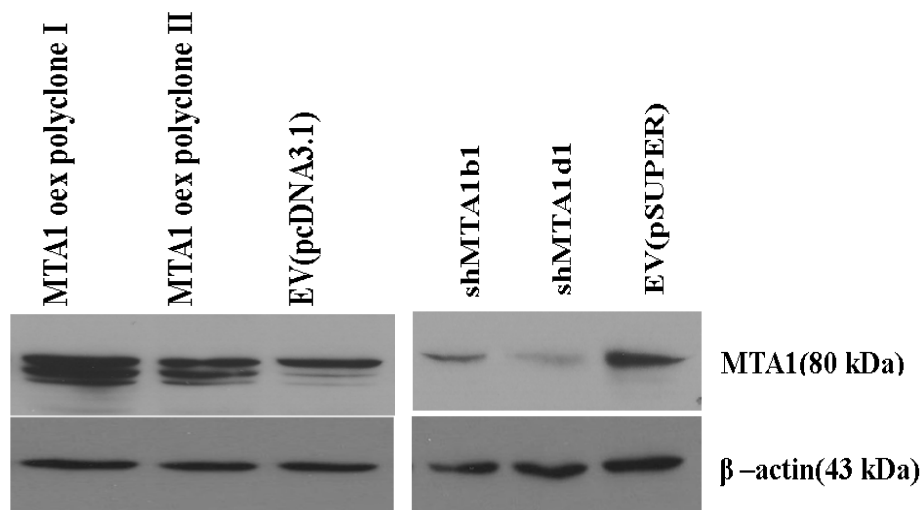


Figure 3. 2 Western blot analysis of MTA1 overexpressing (MTA1 oex polyclone I and II), MTA1 silenced (shMTA1b1 and shMTA1d1) and corresponding empty vector carrying control HCT-116 cells EV(pcDNA3.1) and EV(pSUPER).

3.3 Cell viability assay

3.3.1 MTT

In order to understand the functional changes in the cells as a result of overexpression or silencing of MTA1, the proliferation of the cells was determined by an MTT assay.

MTA1 over-expression in HCT-116 cells increased cell viability at 24, 48 and 72 hour time points (** $p < 0,01$ and *** $p < 0,001$) compared to empty vector transfected cells (Figure 3. 3). MTA1 silenced HCT-116 monoclonal shMTA1b1 and shMTA1d1 showed a significant reduction in cell viability compared empty vector

transfected cells ($***p<0,001$) at all time points (24-72h) as shown in Figure 3. 4. The reduction in proliferation in MTA1 silenced monoclones was proportional to the extent of reduction in MTA1 expression for both time points.

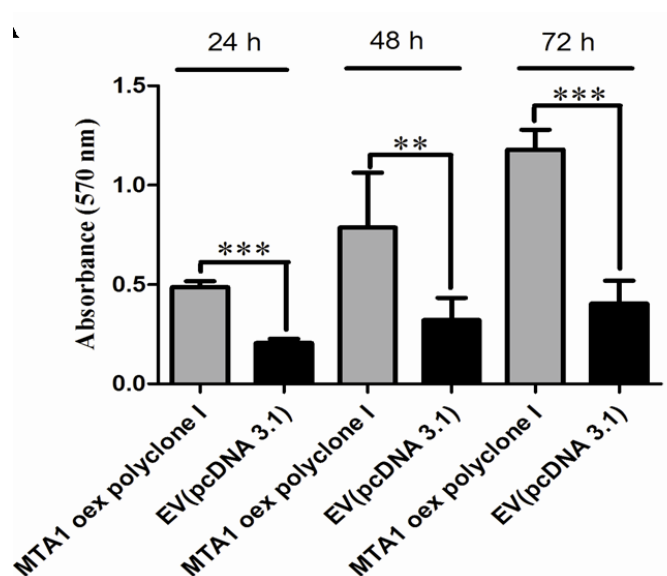


Figure 3. 3 MTT assay showing a significant increase ($***p<0.001$ and $**p<0.01$) in cell viability in MTA1 overexpressing cells (MTA1 oex polyclone I) compared to control cells in 24, 48 and 72 h. Data are presented as mean \pm SD of three independent experiments. Statistical significance was determined with one-way ANOVA and Tukey's posthoc test.

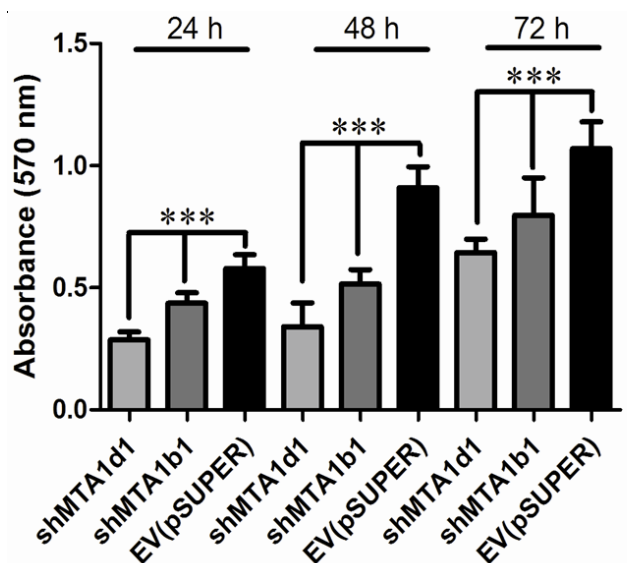


Figure 3. 4 MTT assay showing significant decrease (***) $p < 0.001$ in cell viability in MTA1 silenced HCT-116 cells (shMTA1d1 and shMTA1b1) compared to control cells (EV(pSUPER)) in 24, 48 and 72 h. Data are presented as mean \pm SD of three independent experiments. Statistical significance was determined with one-way ANOVA and Tukey's posthoc test.

3.4 Cell proliferation assay

3.4.1 BrdU assay

To further confirm whether the overexpression or silencing of MTA1 were reflected functionally in cell proliferation, we carried out the chemiluminescent BrdU incorporation assay for at 24 and 48 h. We have observed a significant increase in proliferation in MTA1 overexpressing cells at both 24 and 48 hours of proliferation

(** $p < 0.01$ and *** $p < 0.001$). Concurrently, we have observed a significant decrease in proliferation at all time points when MTA1 was silenced ($*p < 0.05$ and *** $p < 0.001$) as shown in Figure 3. 5. The reduction in proliferation in the MTA1 silenced monoclonal cell populations were proportional to the level of MTA1 silencing at both time points. These data further confirmed the oncogenic nature of MTA1 and have reaffirmed the importance of this protein in functional characteristics of cancer cells.

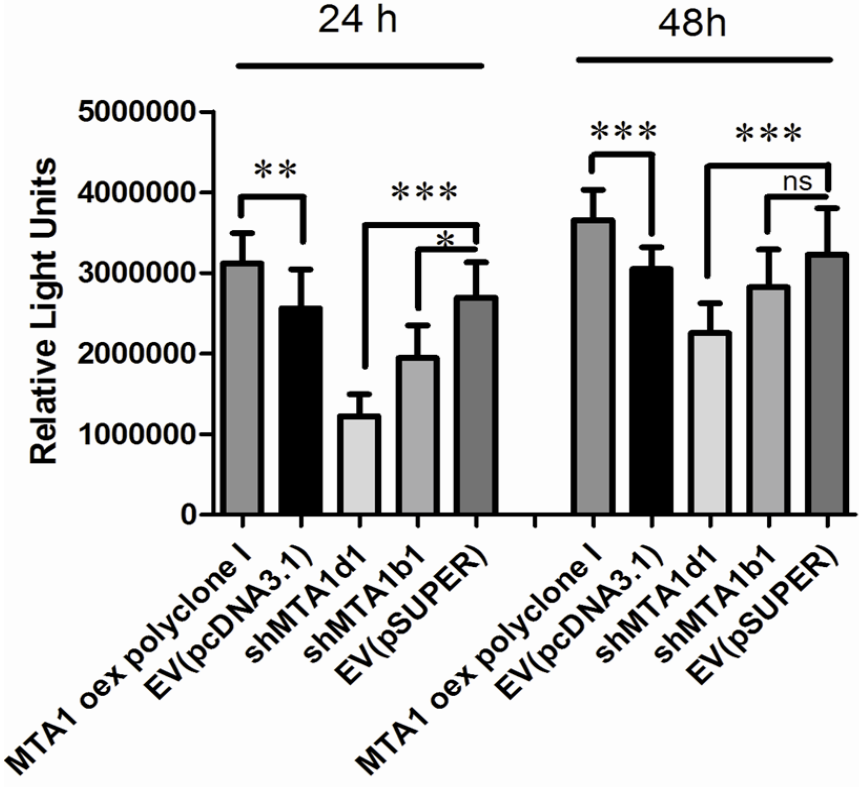


Figure 3. 5 BrdU incorporation assay (chemiluminescent) showing a significant increase in cellular proliferation in MTA1 overexpressing (MTA1 oex polyclone I), and a significant decrease in proliferation in the MTA1 silenced HCT-116

(shMTA1d1 and shMTA1b1) cells compared to the corresponding empty vector transfected cells for 24 and 48h. Data are presented as mean \pm SD of three independent experiments. Statistical significance was determined with one-way ANOVA and paired t-test (** $p < 0.001$, ** $p < 0.01$ and * $p < 0.05$).

3.5 Anchorage Independent Cell Growth

Anchorage-independent growth is one of the hallmarks of transformation which occurs due to a loss of both external and internal signals that normally restrain growth. This assay is also widely accepted as one the most accurate and stringent *in vitro* assay for detecting malignant transformation of cells.

3.5.1 Soft Agar colony formation assay

Soft agar assay was carried out in order to monitor anchorage independent growth properties of MTA1 overexpressing and MTA1 silenced HCT-116 cells with their corresponding empty vector transfected cells. MTA1 overexpression significantly (** $p < 0.01$) increased the number of colonies formed by HCT-116 cells compared to empty vector transfected cells (Figure 3. 6 and Figure 3. 7). On the other hand, the MTA1 silencing (shMTA1d1) caused a significant reduction in both size and number of the colonies formed as shown in Figure 3. 6 and Figure 3. 7 (** $p < 0.01$ and * $p < 0.05$).

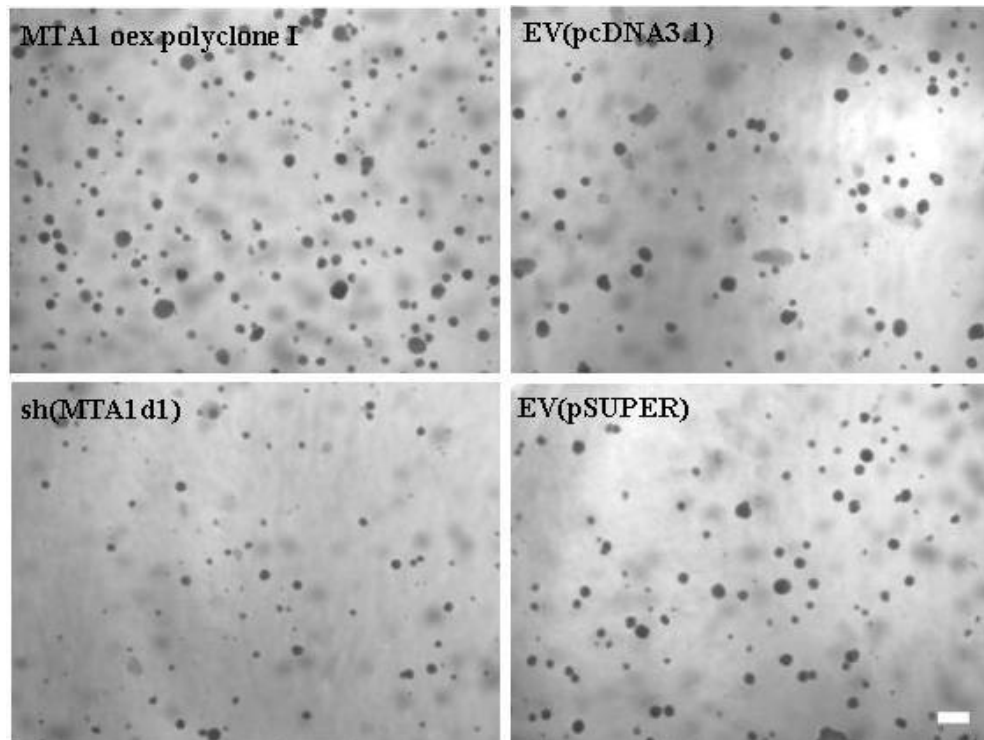


Figure 3. 6 Representative images (10X objective) of colonies formed in soft agar, showing the anchorage independent growth potential of MTA1 overexpressing, MTA1 silenced and the control cells. Significantly higher and larger colonies were observed in the MTA1 overexpressing cells compared to its empty vector transfected cells. Smaller and significantly fewer colonies were observed when MTA1 was silenced. Scale bar: 100 μ m.

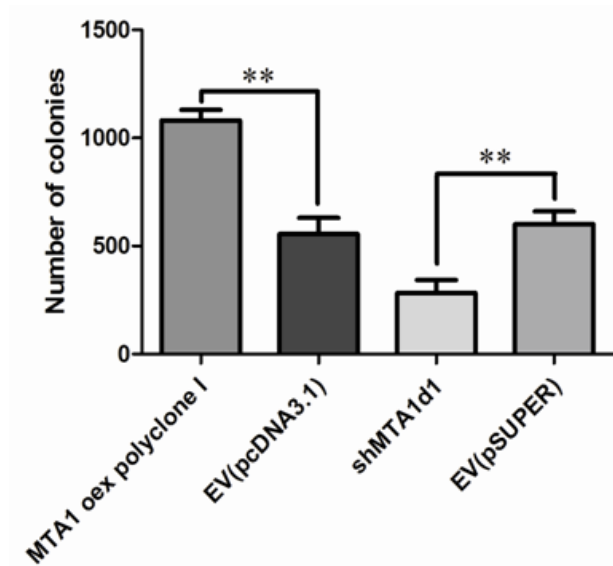


Figure 3. 7 Quantitative analysis of colonies formed in soft agar, showing significantly increased and decreased anchorage independent growth of MTA1 overexpressing (MTA1 oex polyclone I) and MTA1 silenced (shMTA1d1) cells respectively, compared to the the control cells. Statistical significance was determined with Mann–Whitney U-test (** $p < 0.01$).

3.6 Cell adhesion assay

MTA1 overexpression significantly increased the ability of HCT-116 cells to adhere to fibronectin (** $p < 0.001$) compared to empty vector transfected cells, while MTA1 silencing caused a significant reduction in the ability of HCT-116 cells to adhere to fibronectin as shown in Figure 3. 8 ($p < 0.05$).

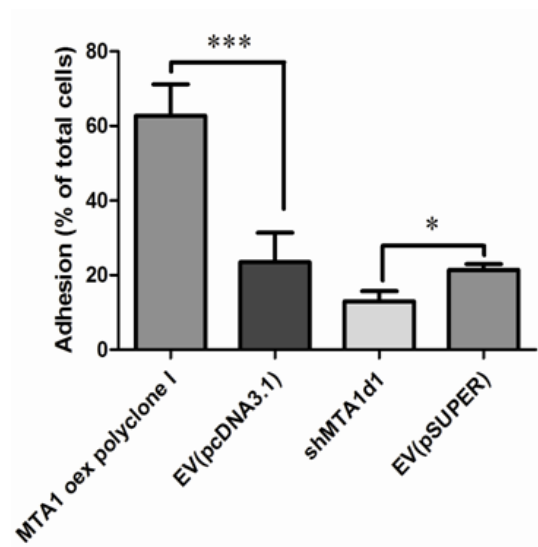


Figure 3. 8 Adhesion assay showing increased and decreased cell adhesion to an extracellular matrix component fibronectin in MTA1 overexpressing and MTA1 silenced cells, respectively, compared to the control cells. Statistical significance was determined with Mann–Whitney U-test (* $p < 0.05$ and *** $p < 0.001$).

3.7 Wound healing

In order to determine the role of MTA1 in the motility of HCT-116 cells, an *in vitro* scratch wound healing assay was carried out. The results indicate that after allowing the cells to grow over 24 h, MTA1 overexpressing HCT-116 cells were much more motile compared to the control cells (Figure 3. 9). In contrast, MTA1 silencing in HCT-116 cells resulted in significantly less motile cells (Figure 3. 9) which could close much less area of the wound compared to the control cells.

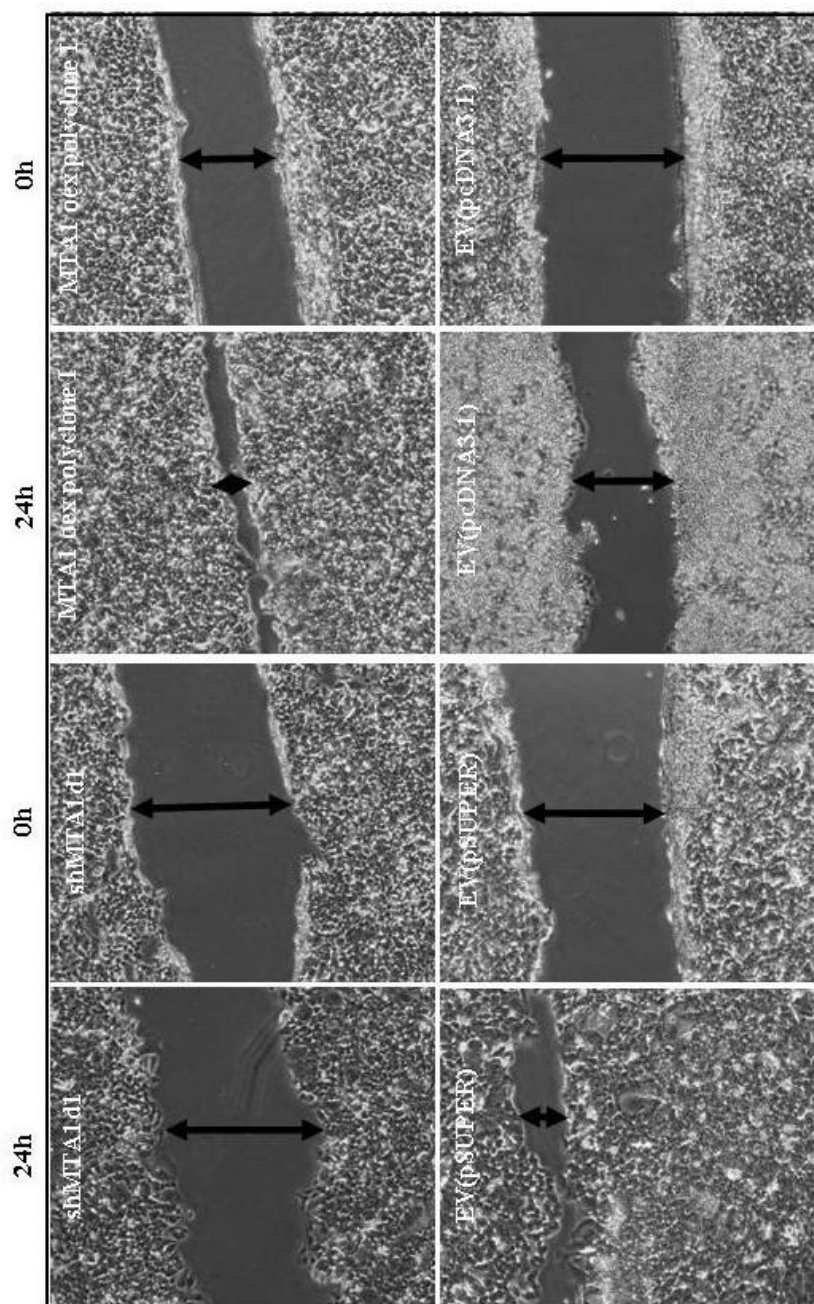


Figure 3. 9 Wound closure representative pictures showing increased wound closure, representing increased motility in MTA1 overexpressing (MTA1 oex polyclone I), and decreased wound closure, representing decreased motility in MTA1 silenced (shMTA1d1) cells compared to control cells.

The quantitative evaluation of wound closure in MTA1 overexpressing, MTA1 silenced and the respective empty vector transfected HCT-116 cells is shown in Figure 3. 10. Differences were observed in the motility of empty vector transfected control cells EV(pcDNA3.1) and EV(pSUPER) with the latter being more motile than the former. This could be because the EV(pSUPER) cells were selected as monoclones from a single cell; while the EV(pcDNA3.1) cells were selected as polyclones which results in the generation of heterogenic population of cells that may alter cellular characteristics in different ways. Both controls, however, were significantly different from their corresponding MTA1 transfected cells.

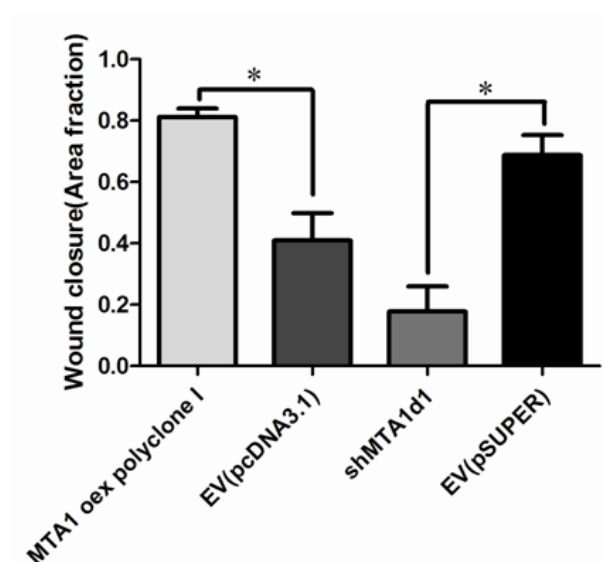


Figure 3. 10 Quantification of motility in the scratch wound healing assay in MTA1 overexpressing (MTA1 oex polyclone I), MTA1 silenced (shMTA1d1) and the control cells. Analysis was done with Image J (<http://rsb.info.nih.gov/ij/>). Statistical significance was determined with Mann–Whitney U-test (* $p < 0.05$).

3.8 Boyden chamber migration and invasion assays

In order to demonstrate the effect of MTA1 expression on the migration and invasion of HCT-116 cells, *in vitro* Transwell migration and Matrigel invasion assays were performed based on the principle of the Boyden chamber assay. The assay was continued for 24 h (for migration assay using MTA1 overexpressing HCT-116 cells), 48 h (for migration assay in MTA1 silenced HCT-116 cells) and 72 h (for invasion assay in HCT-116 cells with overexpressed and silenced MTA1). A significant increase was observed in both migration (Figure 3. 11) and invasion (Figure 3. 13) of MTA1 overexpressing HCT-116 cells compared to empty vector transfected cells as shown in quantitatively Figure 3. 12 and Figure 3. 14. Conversely, MTA1 silencing could significantly decrease the number of cells that were able to migrate (Figure 3. 11) and invade across Matrigel-coated membranes (Figure 3. 13) compared to empty vector transfected cells. Thus, MTA1 expression had a remarkable effect on the migration and invasion capability of HCT-116 cells, further confirming the ability of this protein to induce metastasis in CRC cells.

Interestingly, the invasion ability of the two control cells were different with the pcDNA3.1 empty vector transfected cells invading in much lower numbers compared to the pSUPER transfected cells (Figure 3.12). This could have resulted from the fact that the pcDNA3.1 empty vector transfected cells were obtained as a polyclone with a heterogenous population of cells, whereas the pSUPER transfected cells were obtained from a monoclonal where the cells are expected to behave in a more homogenous manner. It should be pointed out, however, that both the control cells were significantly different in the invasion ability when compared to the experimental cells.

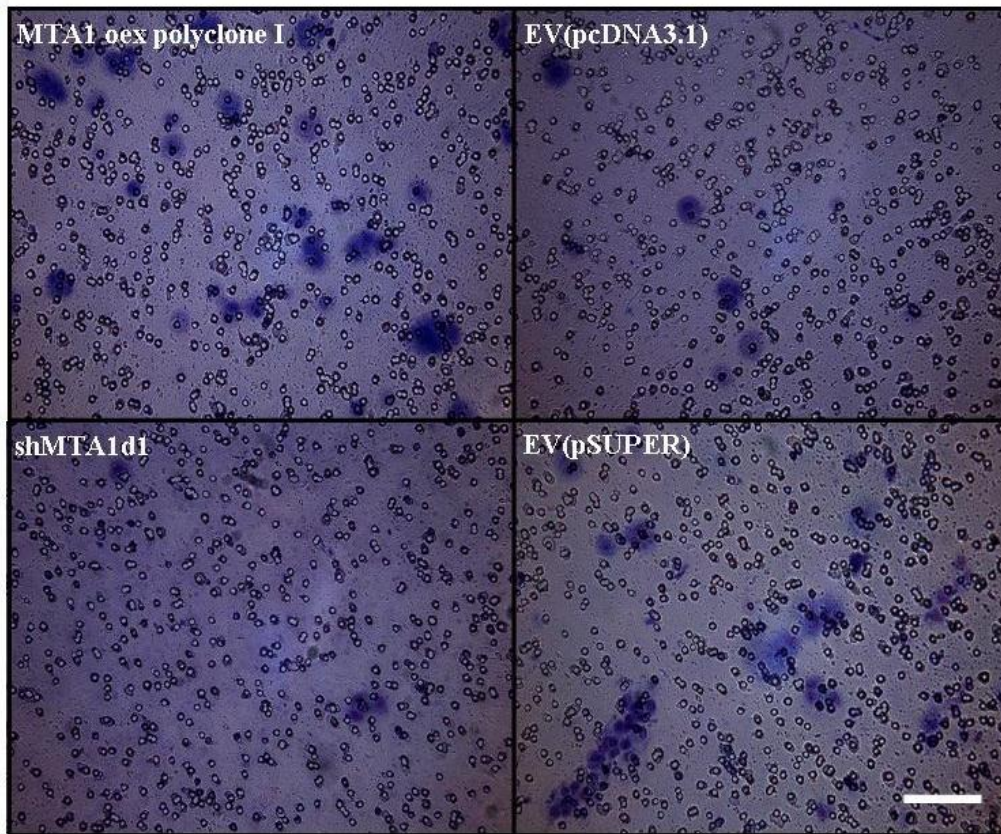


Figure 3. 11 A representative image from the migration assay (20X objective) showing higher migration in MTA1 overexpressing cells (MTA1 oex polyclone I) and lower migration in MTA1 silenced (shMTA1d1) cells, compared to the control HCT-116 cells EV(pcDNA3.1) and EV(pSUPER) respectively. Scale bar: 40 μ m.

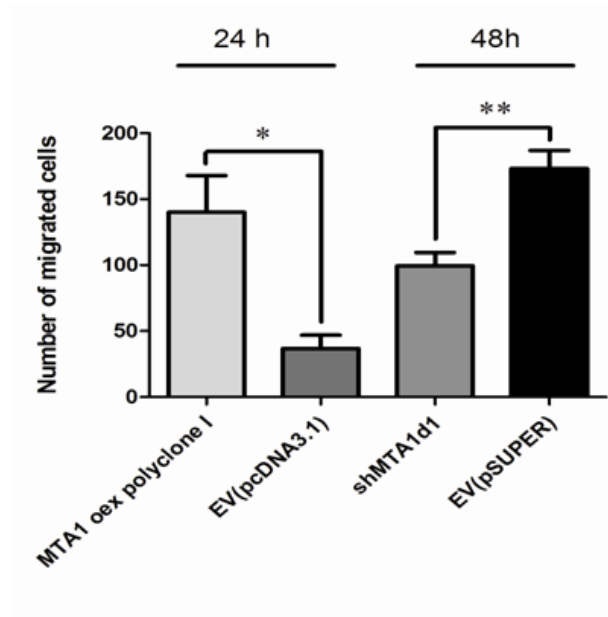


Figure 3. 12 Quantitative analysis of cell migration through the Transwell. Data are presented as mean \pm SD of three independent experiments. Statistical significance was determined with Mann–Whitney U-test (* p < 0.05 and ** p < 0.01).

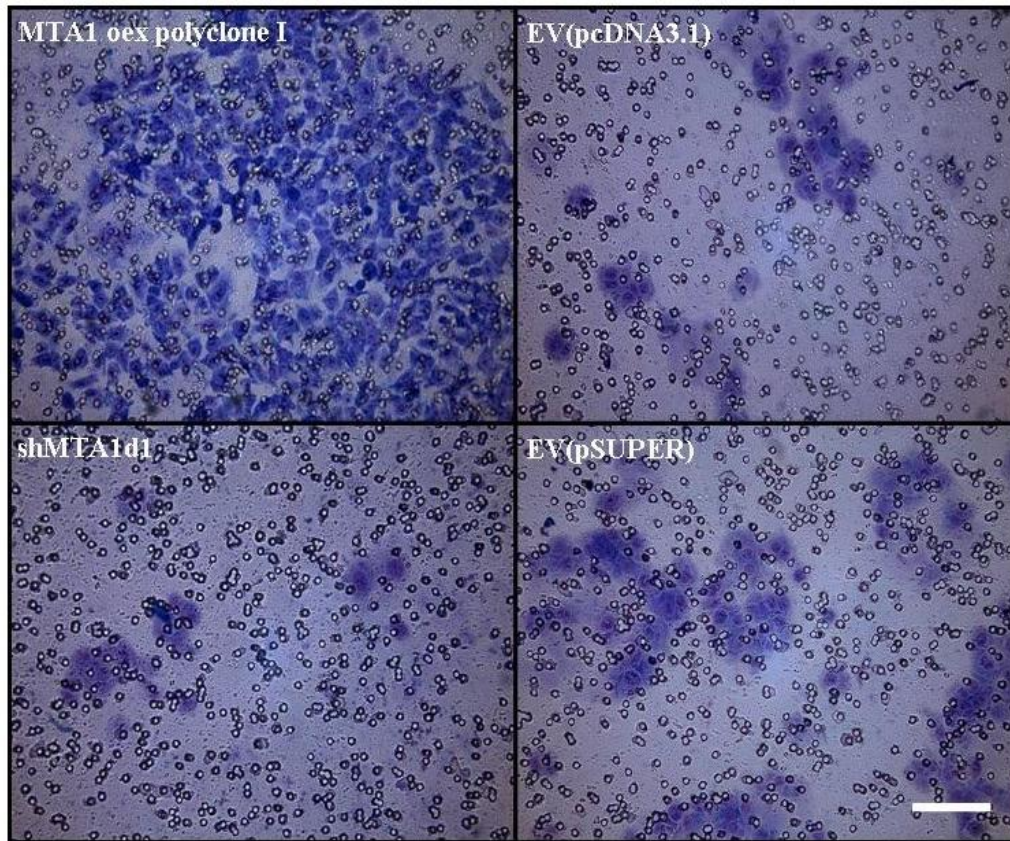


Figure 3. 13 A representative image of the invasion assay (20X objective) showing higher invasion across Matrigel in the MTA1 overexpressing cells (MTA1 oex polyclone I) and lower invasion in the MTA1 silenced (shMTA1d1) cells, compared to the control HCT-116 cells EV(pcDNA3.1) and EV(pSUPER), respectively. Scale bar: 40 μ m.

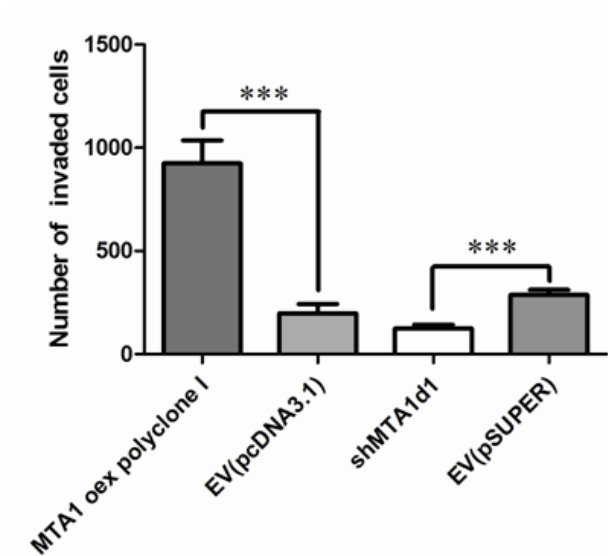


Figure 3. 14 Quantitative analysis of number of cells that invaded through Transwells and Matrigel. Data are presented as mean \pm SD of three independent experiments. Statistical significance was determined with Mann–Whitney U-test (** $p < 0.001$).

3.9 MTA1 induces survival signals in CRC cell lines

3.9.1 Apoptosis assay

One of the hallmarks of cancer is the rise of capability of escape from apoptosis (Hanahan, 2000).

3.9.1.1 Annexin V staining

Annexin V staining followed by flow cytometry of HCT-116 cells showed that MTA1 overexpression resulted in a decrease in the number of early and late apoptotic cells compared to the empty vector transfected cells as shown in Figure 3. 15(a-b) and Figure 3. 16 (* $p < 0.05$). MTA1 silenced HCT-116 cells exhibited significantly increased total apoptotic events, with a dramatic increase in early apoptotic cells (lower right quadrant) (* $p < 0.05$ and ** $p < 0.01$) compared to the empty vector transfected cells as shown in Figure 3. 15 (c-d) and Figure 3. 17).

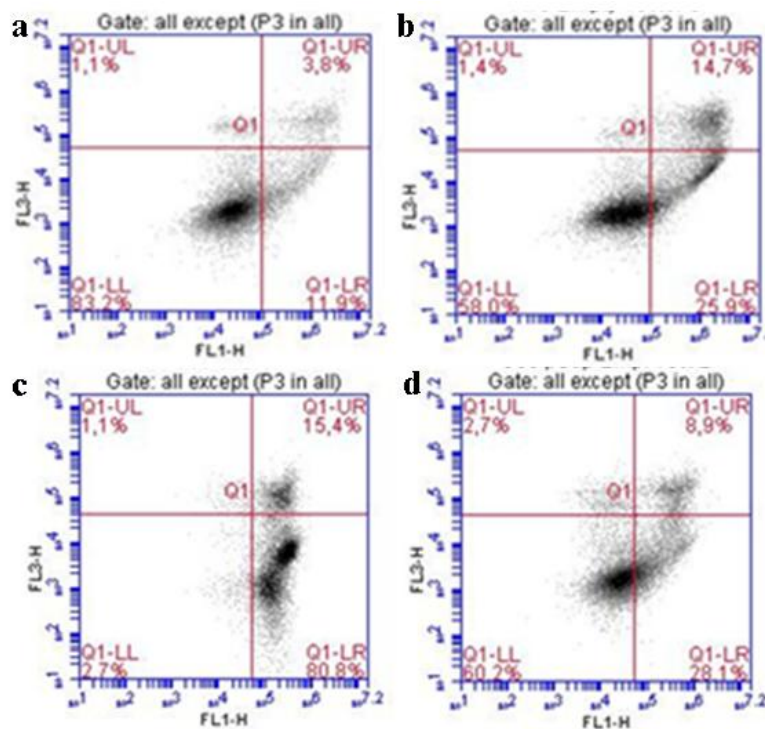


Figure 3. 15 MTA1 expression reduces apoptosis of HCT-116 cells. Distribution of early, late and total apoptotic cells percentages in (a) MTA1 overexpressing (MTA1

oex polyclone I) and (b) empty vector transfected (pcDNA3.1) (c) MTA1 silenced (shMTA1d1) and d) empty vector transfected EV(pSUPER) cells. The cell populations shifted towards the apoptotic cells when MTA1 was silenced and towards viable cells when MTA1 was overexpressed.

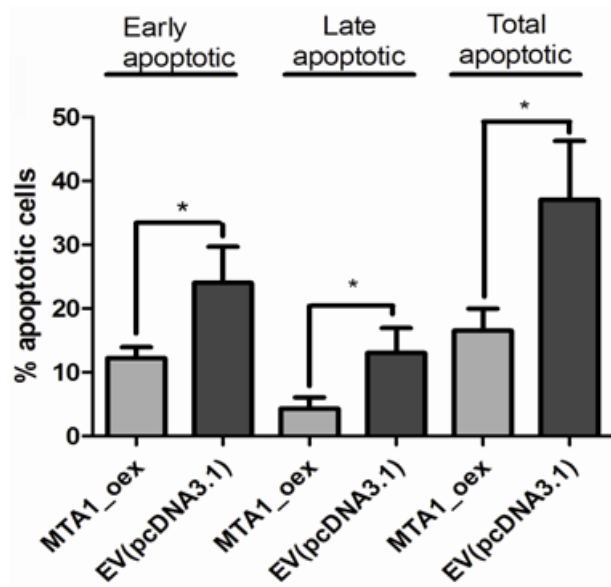


Figure 3. 16 Quantitative analysis of early, late and total apoptotic cells percentages showing reduced number of apoptotic cells in MTA1 overexpressing (MTA1 oex polyclone I) cell population compared to empty vector transfected (EV(pcDNA3.1)) cell population. Statistical significance was determined with Mann–Whitney U-test ($*p < 0.05$).

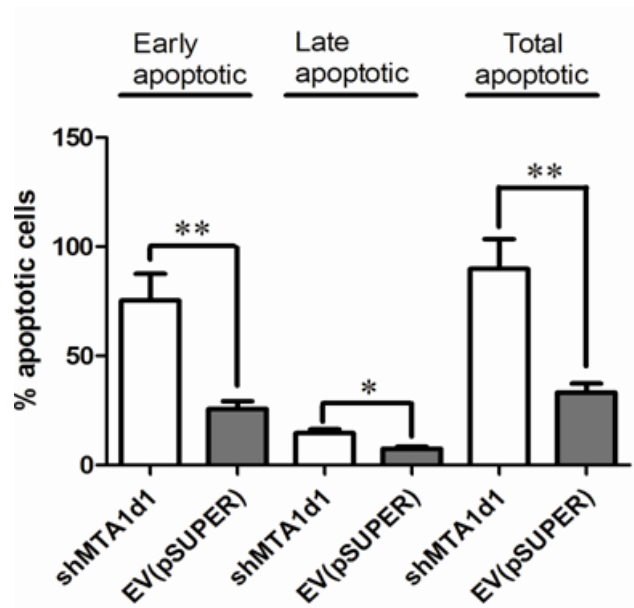


Figure 3. 17 Quantitative analysis of early, late and total apoptotic cells percentages showing increased number of apoptotic cells in MTA1 silenced (shMTA1d1) cell population compared to empty vector transfected EV(pSUPER) cell population. Statistical significance was determined with Mann–Whitney U-test (* $p < 0.05$, ** $p < 0.01$).

3.9.1.2 Bcl-xl and XIAP levels

To further confirm the role of MTA1 in induction of apoptosis of HCT-116 cells, we determined the expression of the antiapoptotic proteins Bcl-xl and XIAP. We have observed that MTA1 overexpression, especially clone I where MTA1 was overexpressed more, resulted in a greater increase in the expression of Bcl-xl. On the other hand, the expression of Bcl-xl was decreased in proportion to the level of MTA1 silencing, with shMTA1d1 where MTA1 was silenced to a greater extent

showing a greater decrease in the levels of Bcl-xl as shown in Figure 3. 18. Furthermore, MTA1 silencing in HCT-116 cells resulted in a slight decrease of the anti-apoptotic protein XIAP (Figure 3. 19). These data indicate that MTA1 decreases apoptosis in cancer cells, at least in part by increasing the levels of antiapoptotic proteins.

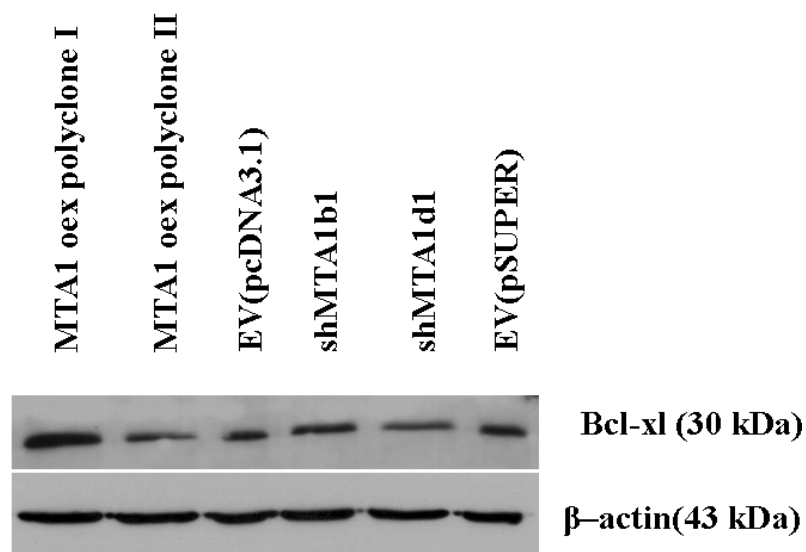


Figure 3. 18 Western blot analysis showing increased expression of the antiapoptotic protein Bcl-xl protein in MTA1 overexpressing cells and decreased expression in MTA1 silenced HCT-116 cells. β -actin was used as a loading control.

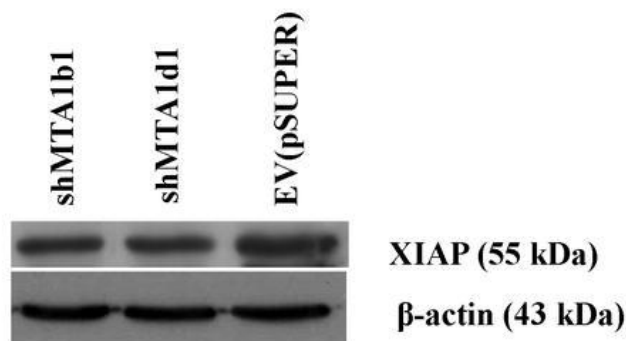


Figure 3. 19 Western blot analysis of the antiapoptotic XIAP protein showing reduced amounts of protein in MTA1 silenced monoclonal cells compared to corresponding empty vector transfected cells

3.9.2 Angiogenesis assays

MTA1 has been shown to induce angiogenesis by stabilizing hypoxia inducible factor 1alpha (HIF-1 α) (Yoo et al., 2006). Moreover, MTA1 has been associated with angiogenesis in a number of different cancer types (Jang et al., 2006; Kai et al., 2011; Li et al., 2012b) and with lymphangiogenesis in CRC (Du et al., 2011). However, whether MTA1 expression is also associated with angiogenesis in CRC has not been established to date.

3.9.2.1 Secreted VEGF levels

Secreted VEGF levels were determined by an ELISA-based assay. We have observed that the MTA1 overexpressing cells secreted significantly higher amounts of VEGF into the conditioned medium compared to empty vector transfected cells.

On the contrary, VEGF secretion in the MTA1 silenced cells was significantly less when compared to the control cells (Figure 3. 20, * $p < 0.05$ and ** $p < 0.01$).

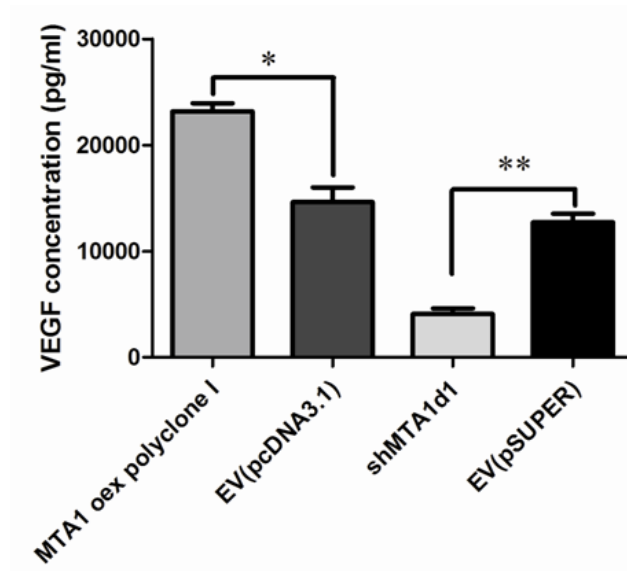


Figure 3. 20 VEGF concentrations (pg/ml) determined by VEGF immunoassay showing higher levels of secreted VEGF in conditioned medium obtained from MTA1 overexpressing (MTA1 oex polyclone I) cells and lower levels of secreted VEGF in conditioned medium obtained from MTA1 silenced (shMTA1d1) cells compared to corresponding empty vector transfected cells. Data are presented as mean \pm SD of three independent experiments. Statistical comparisons were carried out using paired t-test (* $p < 0.05$ and ** $p < 0.01$).

3.9.2.2 Endothelial Tube Formation assay

To determine whether the secreted VEGF was functional, an endothelial tube formation assay was carried out. Since LoVo cells express very low amounts of VEGF (Kondo et al., 2000), these experiments were carried out with HCT-116 cells. The endothelial tube formation assay depends on the principle of incubating subconfluent HUVEC in Matrigel with conditioned medium and allowing for the formation of capillary like structures or tubes. Conditioned medium collected from MTA1 overexpressing cells after 72 h caused HUVEC to form tubes with significantly higher total skeleton length, number of branching points and nodal structures but not number of tubes compared to empty vector transfected cells (Figure 3. 21, Figure 3. 22, Figure 3. 23; ** $p < 0.01$ and * $p < 0.05$). Conditioned medium collected from the MTA1 silenced cells, on the other hand, resulted in tubes with significantly reduced total skeleton length, number of branching points, nodal structures and tubes compared to empty vector transfected HCT-116 cells (Figure 3. 21, Figure 3. 23, Figure 3. 24; ** $p < 0.01$ and * $p < 0.05$).

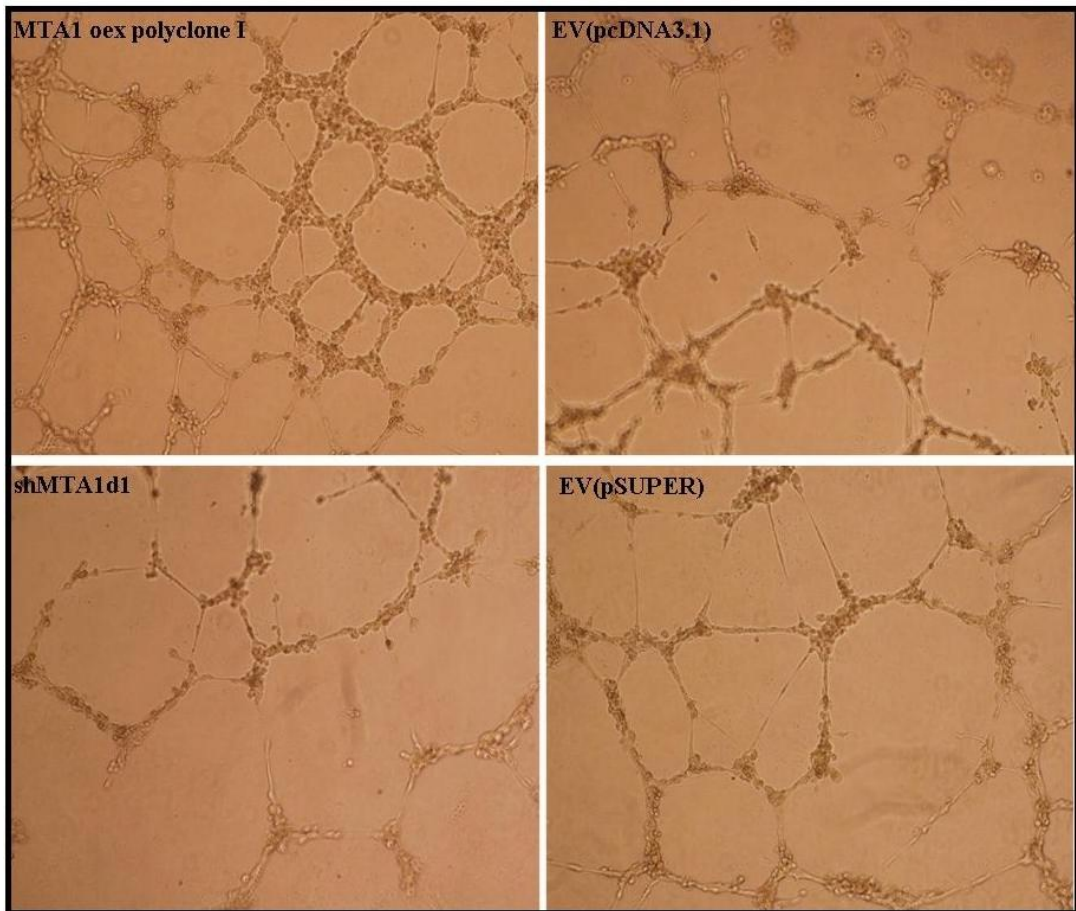


Figure 3. 21 Endothelial Tube Formation assay 10X objective representative images in MTA1 overexpressing, MTA1 silenced and control cells.

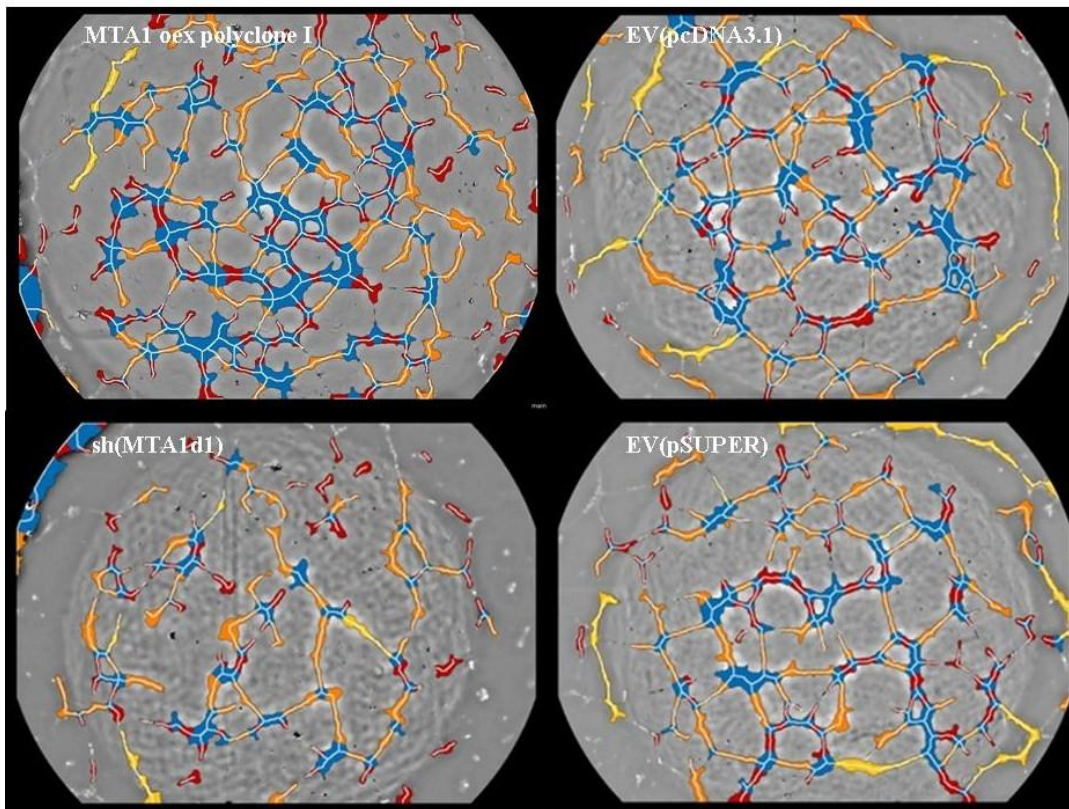


Figure 3. 22 Endothelial Tube Formation assay 4X objective representative images (evaluated by by S.Co Lifesciences) in MTA1 overexpressing, MTA1 silenced and control cells. Skeleton and branching points are shown in white; tubes are shown in yellow, orange and red, while the nodal structures are shown in blue.

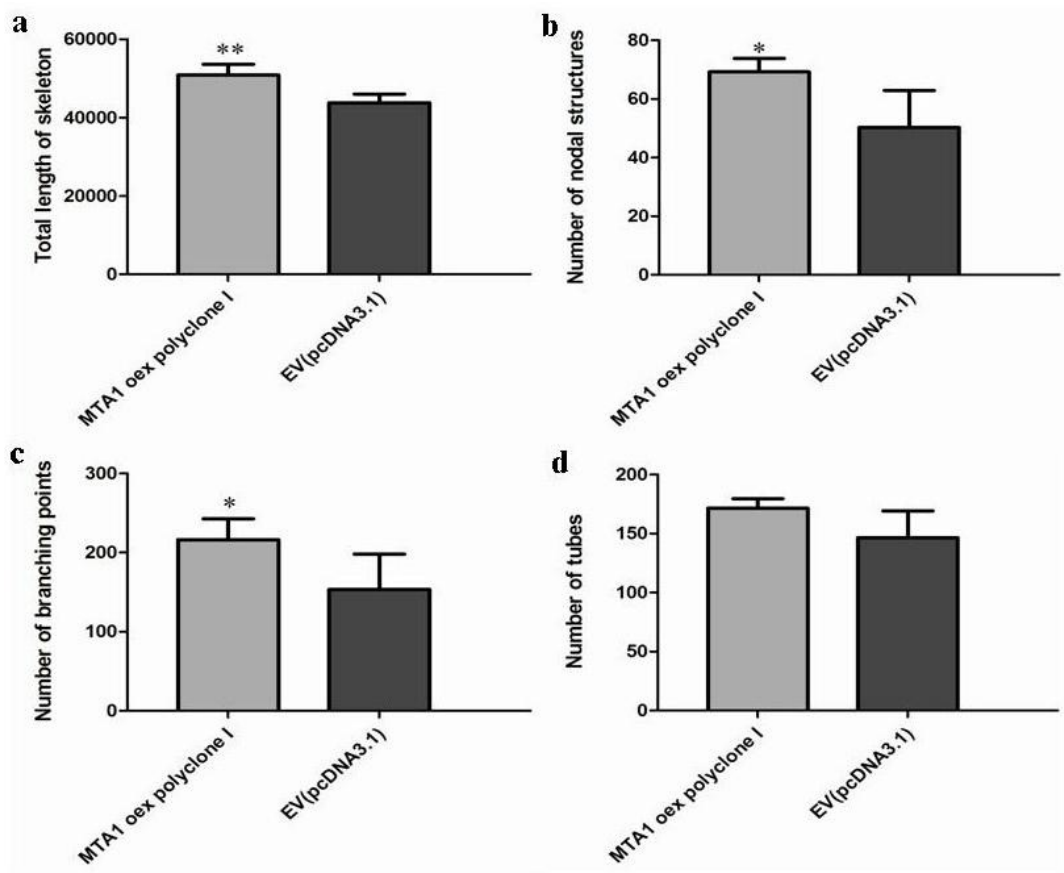


Figure 3. 23 Endothelial Tube Formation assay showing higher amount of a) Total Length of skeleton (Mean=50849, Std error=1364 and Mean=41009, Std error 2911), b) Number of nodal structures (Mean=69.25, Std error=2.287 and Mean=50.33, Std error 7.265), c) Number of branching points (Mean=216.3, Std error=13.25 and Mean=153.3, Std error 22.50), (d) Number of tubes (Mean=171.5, Std error=4.052 and Mean=146.5, Std error 11.41) in MTA1 overexpressing cells compared to control cells. Data are presented as mean \pm SD of three independent experiments. Statistical comparisons were carried out using or paired t-test (* $p < 0.05$, ** $p < 0.01$). Mean and standard errors are shown the order of MTA1 oex polyclone I and EV(pcDNA3.1) cells, respectively.

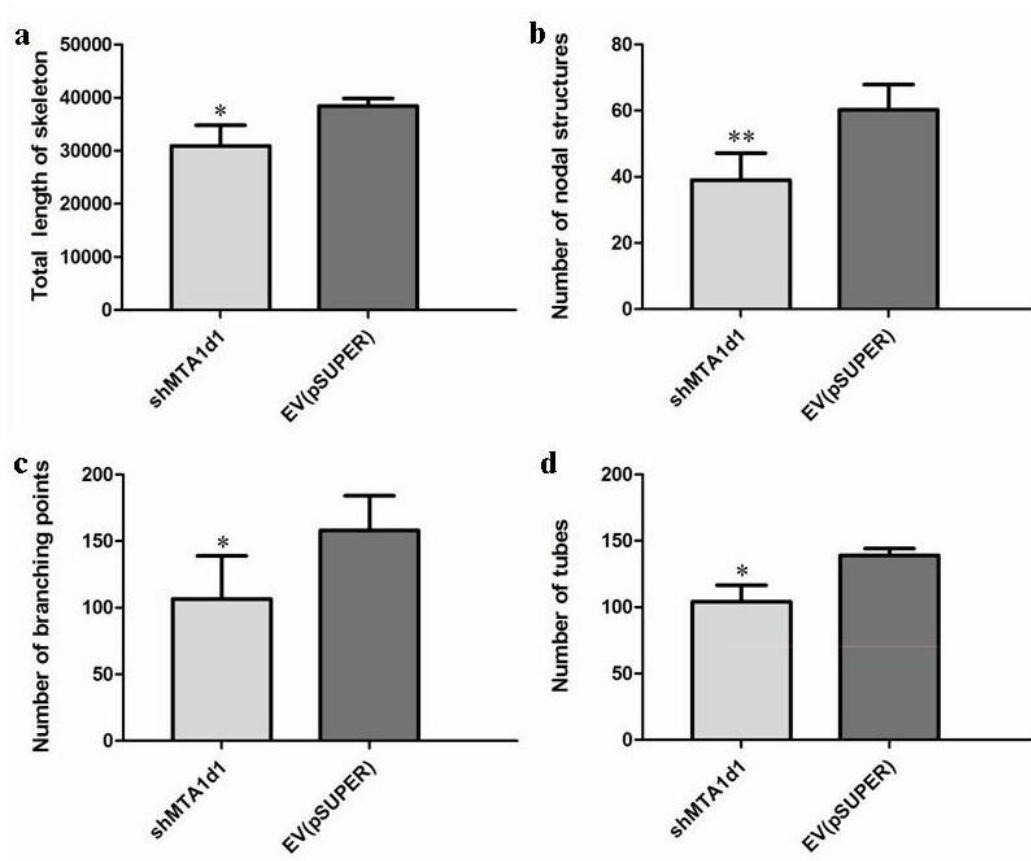


Figure 3. 24 Endothelial Tube Formation assay showing lower a) Total Length of skeleton (Mean=30941, Std error=2247 and Mean=38432, Std error 822.7), b) Number of nodal structures (Mean=39, Std error=4.726 and Mean=60.33, Std error 4.372), c) Number of branching points (Mean=106.7, Std error=18.67 and Mean=158.0, Std error 15.04), (d) Number of tubes (Mean=104.0, Std error=7.234 and Mean=139.0, Std error 3.055) in MTA1 silenced cells compared to control cells. Data are presented as mean \pm SD of three independent experiments. Statistical comparisons were carried out using or paired t-test ($*p < 0.05$, $**p < 0.01$). Mean and standard errors are shown the order of shMTA1d1 and EV(pSUPER) cells, respectively.

3.10 MTA1 expression induces Epithelial Mesenchymal Transition (EMT) in CRC cell lines

In order to explain the mechanism behind the functional changes observed above and based on recent reports regarding the involvement of MTA1 in EMT in breast cancer cells (Pakala et al., 2011), we wanted to examine whether MTA1 was responsible for EMT-like changes in colon cancer cells. For this, we first determined the expression of common molecular markers of EMT such as E-cadherin, ZO-1, β -catenin and vimentin in MTA1 overexpressing HCT-116 cells as well as MTA1 silenced HCT-116 and LoVo (MTA1 silenced monoclonal LoVo-1F2 and 1F7 as well as corresponding empty vector carrying polyclonal LoVo-EV were generated in our laboratory) cells. E-cadherin and ZO-1, which are markers of an epithelial phenotype, were expressed significantly more in the MTA1 silenced HCT-116 and LoVo cells compared to the respective empty vector transfected cells. Conversely, the expression of vimentin, a mesenchymal marker, was decreased in both HCT-116 and LoVo when MTA1 was silenced. When MTA1 was overexpressed, however, no change in E-cadherin and ZO-1 expression levels were observed, however, an increase in the expression of vimentin compared to empty vector transfected cells could be seen. On the other hand, the expression of β -catenin did not show any change in MTA1 overexpressing or MTA1 silenced cells compared to empty vector transfected cells in both cell lines (Figure 3. 25 and Figure 3. 26).

We next determined the expression of the EMT master regulators Snai1 and Snai2 (Slug) in MTA1 overexpressing and silenced HCT-116 cells. We observed that both Snai1 and Slug protein levels were reduced in MTA1 silenced cells, whereas no difference in expression was seen in the HCT-116 cells overexpressing MTA1 (Figure 3. 25 and Figure 3. 26). To confirm whether the increased E-cadherin expression in the MTA1 silenced cells was due to the decreased recruitment of

Snail and Slug onto the E-cadherin promoter, we carried out a Chromatin immunoprecipitation (ChIP) assay in the MTA1 silenced HCT-116 cells (shMTA1d1) and the control EV(pSUPER) transfected cells. The results showed that both Snail and Slug were recruited less to the E-boxes on the proximal E-cadherin promoter when MTA1 was silenced (Figure 3. 27), resulting in a loss of repression and thereby increased expression of E-cadherin.

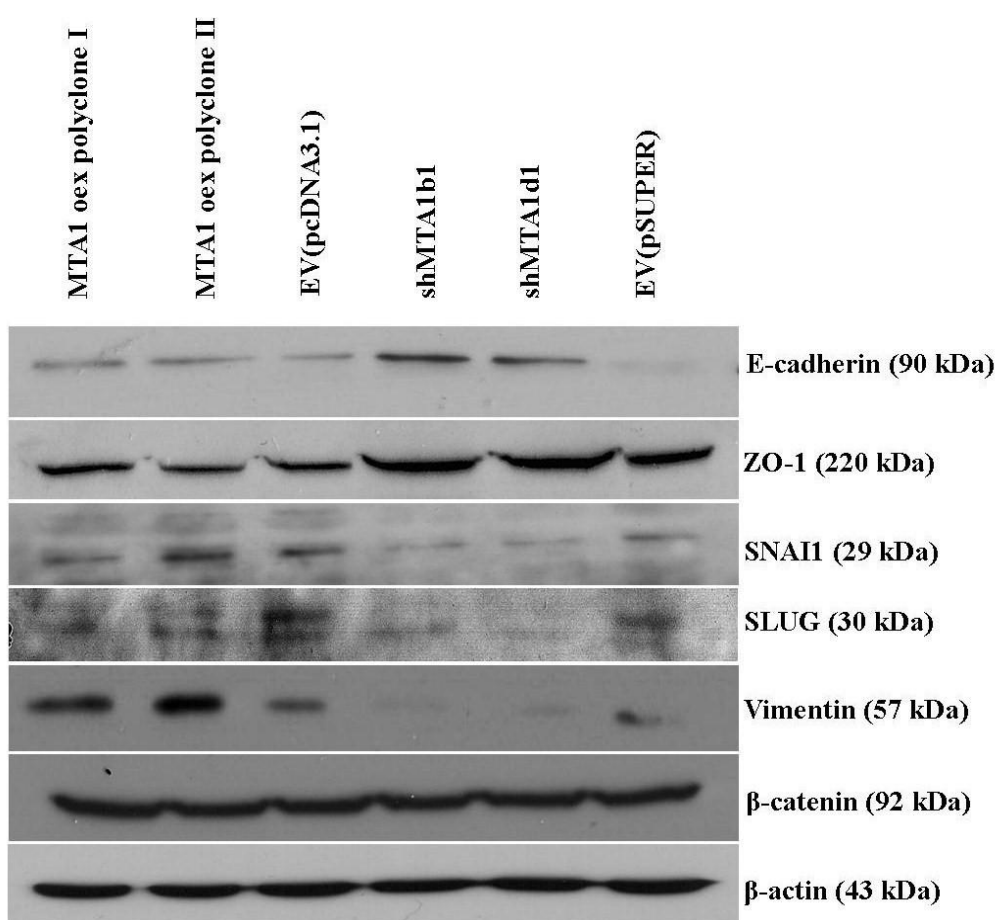


Figure 3. 25 MTA1 expression affects the expression levels of EMT markers EMT regulator transcription factors. Western blot analysis of E-cadherin, ZO-1, SNAI1,

SLUG, vimentin and β -catenin proteins in MTA1 overexpressing (MTA1 oex polyclone I and II), MTA1 silenced HCT-116 (shMTA1d1 and shMTA1b1) and the corresponding control cells. β -actin was used as a loading control.

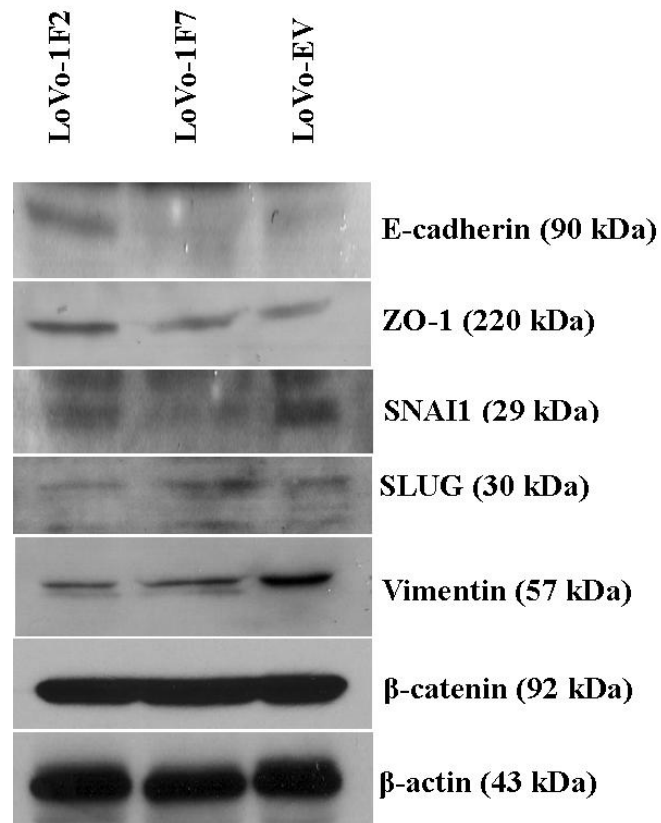


Figure 3. 26 Western blot analysis of E-cadherin, ZO-1, SNAI1, SLUG, vimentin and β -catenin proteins in MTA1 silenced LoVo (LoVo-1F7 and 1F2) and the control cells. β -actin was used as a loading control.

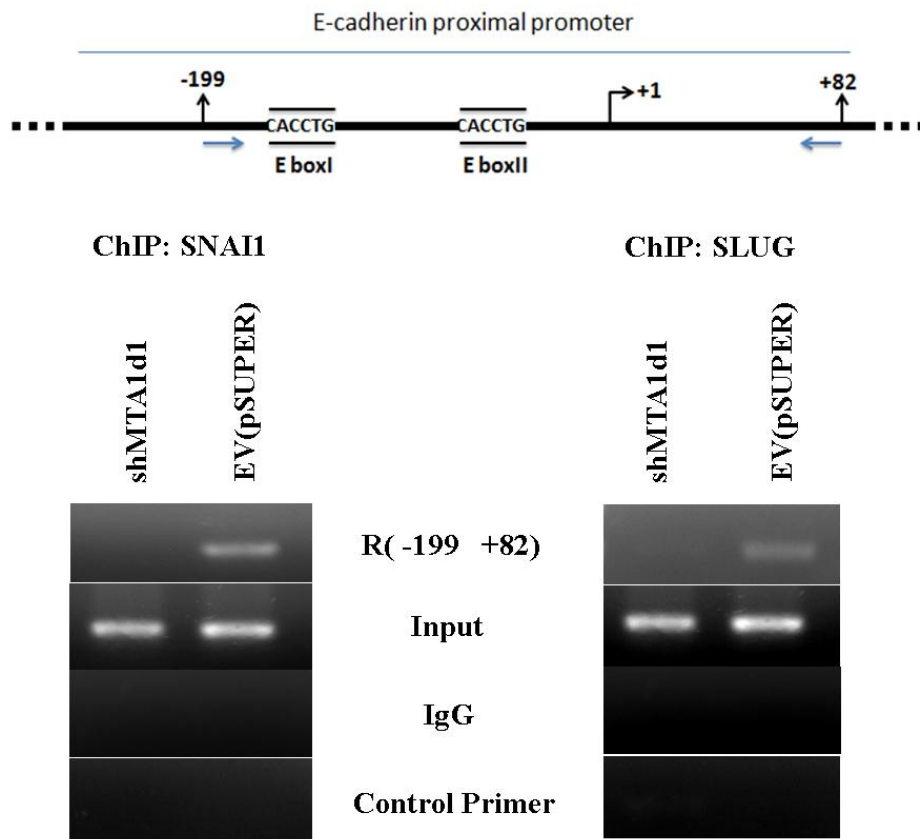


Figure 3. 27 ChIP assay showed a reduction in recruitment of SNAI1 and SLUG proteins onto the E-cadherin promoter E-box elements in MTA1 silenced shMTA1d1 cells compared to empty vector transfected EV(pSUPER) control cells (IgG and control primers served as the negative controls for the assay in the PCR reactions). Reduced recruitment of SNAI1 and SLUG resulted in increased expression of E-cadherin.

3.11 MTA1 expression levels in 15-LOX-1 transfected cells

In our previous studies we have shown that expression of 15-LOX-1 in HT-29 and HCT-116 CRC cell lines resulted in a decrease in expression has an inhibitory effect on the MTA1 expression at both in mRNA and protein levels thesis (Cimen et al., 2009a; Tuncay, 2009). The same cells were also less motile and with slower migration and invasion through Matrigel (Cimen et al., 2009a). We therefore hypothesized that the anti-metastatic properties of 15-LOX-1 expression could be due to the inhibition in the expression of MTA1 and set out to determine the mechanism here.

In order to reconfirm the loss of MTA1 expression when 15-LOX-1 is expressed in CRC cell lines, we transfected LoVo, Caco-2 and SW620 cells with pcDNA3.1-15-LOX-1 expression vector and corresponding pcDNA3.1 empty vector. As shown in Figure 3. 28, LoVo cells showed significantly decreased levels of MTA1 in 15-LOX-1 transfected cells. In Caco-2 and SW620 cells, which express low endogenous levels of MTA1, 15-LOX-1 expression did not result in a significant change in MTA1 expression levels.

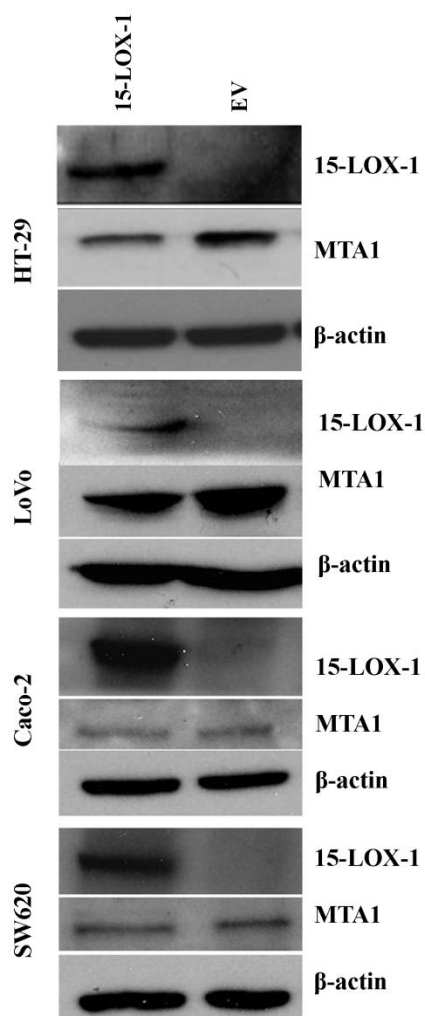


Figure 3. 28 Western blot analysis of 15-LOX-1 (75 kDa) and MTA-1 proteins (80 kDa) in different cell lines. A reduction in MTA1 levels was observed when 15-LOX-1 was expressed in HT-29 and LoVo cells. The same effect was not seen in Caco-2 or SW620 cells. Lane 1: 15-LOX-1 expressing cells, lane 2: empty vector expressing cells. Equal protein loading was shown by β -actin (43 kDa) levels.

3.12 Nuclear translocation of NF- κ B in the cells expressing 15-LOX-1

Having established that the expression of 15-LOX-1 resulted in a decrease in MTA1 expression in the CRC cell lines, we next wanted to examine the mechanism behind it. Recent studies have indicated that MTA1 is transcriptionally upregulated by NF- κ B (Pakala et.al., 2010), and we and others have also shown that 15-LOX-1 expression results in an inhibition in NF- κ B activity (Cimen et al., 2011; Shureiqi, 2012). We have therefore examined the hypothesis that 15-LOX-1 inhibits MTA1 expression through the inhibition of NF- κ B.

First, we examined the nuclear translocation NF- κ B in the presence of 15-LOX-1 expression using western blot. For this purpose, nuclear and cytoplasmic extracts isolated from the 15-LOX-1 expressing HT-29 and LoVo cells were probed with a p65 monoclonal antibody. The results show that forced expression of 15-LOX-1 in both HT-29 and LoVo cell lines could decrease the nuclear translocation of the NF- κ B subunit p65 (65 kDa) when compared to the empty vector transfected cells (Figure 3. 29).

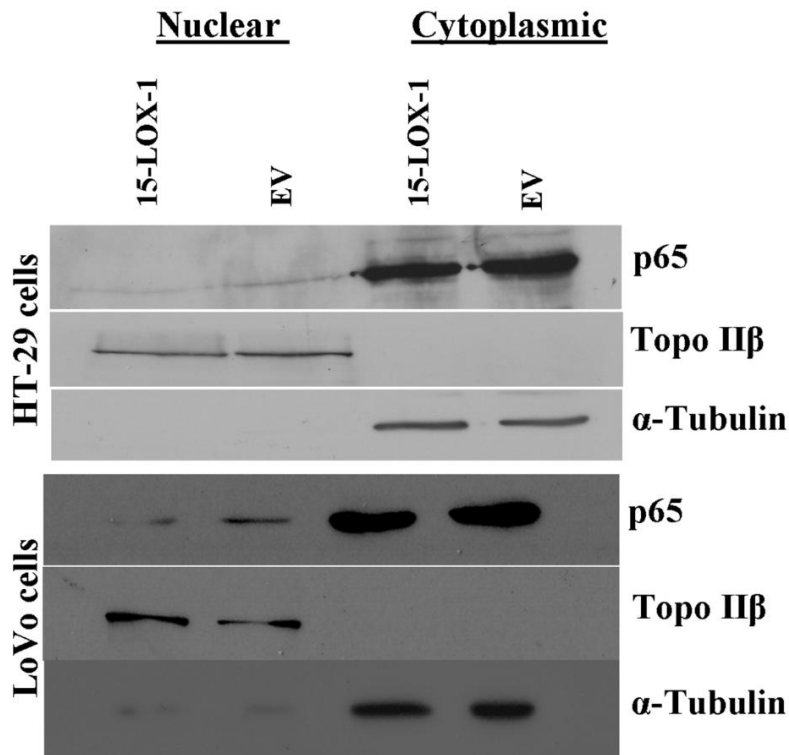


Figure 3. 29 Western blot analysis of nuclear and cytoplasmic extracts isolated from 15-LOX-1 expressing HT-29 and LoVo cells. Reduced translocation of p65 to the nucleus was seen in cells expressing 15-LOX-1 indicating an inhibition of NF- κ B.

3.13 Detection of NF- κ B binding regions on the MTA1 promoter region

A 2 kb sequence including upstream of the start site including the proximal promoter of MTA1 gene was gathered from NCBI database and subjected to analysis for determination of possible NF- κ B binding sites by using transcription factor binding program Alibaba 2.1. In Figure 3. 30 possible binding sequences for NF- κ B on the MTA1 promoter are shown.

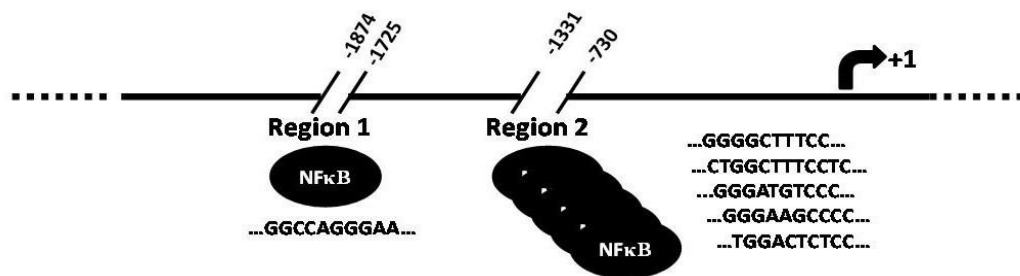


Figure 3. 30 Schematic diagram of NF- κ B binding sites in the region between chr14: 105884100-105886185 on the MTA1 promoter, detected by AliBaba 2.1 Program.

3.14 NF- κ B recruitment onto the MTA1 promoter in the presence of 15-LOX-1 expression

In order to analyze the physical interaction of the NF- κ B p65 subunit with the binding sequences identified through bioinformatic means, ChIP primers were designed to amplify the region between -1874 to -1725 (Region I, containing one NF- κ B binding sequence) and -1331 to -730 (Region II, containing five different NF- κ B binding sequences). 15-LOX-1 or EV transfected HT-29, LoVo and SW620 cells were crosslinked and cell lysates were probe sonicated. For each sample equal amounts of chromatin were immunoprecipitated with p65 polyclonal antibody. Amplification of immunoprecipitated DNA along with IgG immunoprecipitated (negative control) and input DNA (positive control) showed that p65 could bind to both Region I and Region II on the MTA1 promoter (Figure 3. 31, Figure 3. 32, Figure 3. 33). As another negative control, immunoprecipitated DNA was subjected

to PCR amplification by a primer set specific for an off target region gene desert. Importantly, 15-LOX-1 transfected HT-29 cells showed reduced recruitment onto the both Regions I and II (Figure 3. 31), while LoVo cells showed reduced recruitment on Region I only compared to empty vector transfected cells (Figure 3. 32). Furthermore, ChIP analysis of SW620 cells showed no change in 15-LOX-1 or EV transfected cells p65 recruitment onto the either of the regions as shown in Figure 3. 33. SW620 cells had very low MTA1 expression which did not show any variation when 15-LOX-1 was expressed (Figure 3. 28).

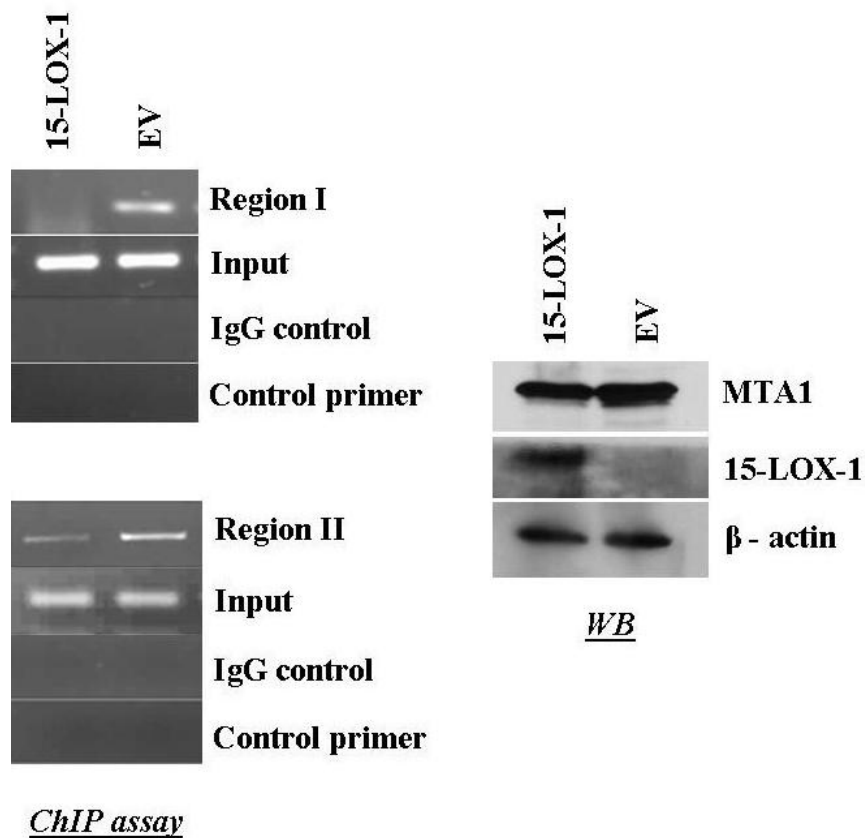


Figure 3. 31 15-LOX-1 expression decreases p53 recruitment onto the MTA1 promoter (Region I (chr14:105884312-105884461); and Region II (chr 14: 105884853-105885464)) as shown by ChIP assay in HT-29 cells. 15-LOX-1 expression in the ChIP lysates was confirmed by western blot.

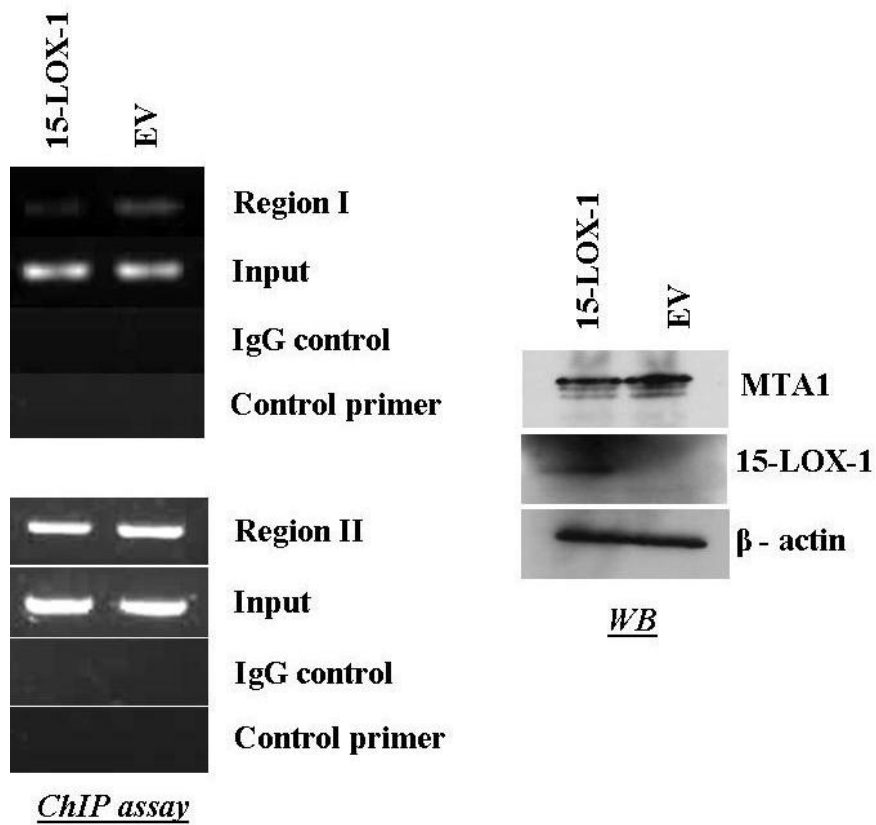


Figure 3. 32 15-LOX-1 expression decreases p65 recruitment onto the MTA1 promoter (Region I (chr14:105884312-105884461); and Region II (chr 14: 105884853-105885464)) as shown by ChIP assay in LoVo cells. 15-LOX-1 expression in the ChIP lysates was confirmed by western blot.

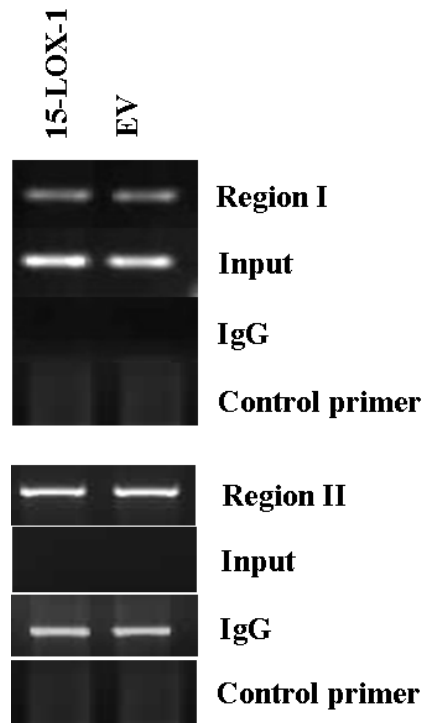


Figure 3. 33 15-LOX-1 expression does not change p65 recruitment onto the MTA1 promoter (Region I (chr14:105884312-105884461); and Region II (chr 14: 105884853-105885464)) in SW620 cells as shown by ChIP assay.

3.15 Transcriptional activity in region RI and RII in the presence of 15-LOX-1 expression

Next we decided to determine the transcriptional activity of NF- κ B in the 15-LOX-1 expressing HT-29 and LoVo cells. For this purpose, we cloned the binding sequence detected in Region I in five tandem repeats as an oligo in the luciferase reporter vector pLuc-MCS. Region II was PCR cloned into the luciferase reporter

vector pLuc-MCS. After transfecting cells with pcDNA3.1-15-LOX-1 and pcDNA3.1-EV plasmids; cells were also separately transfected with the pLuc-MCS-RI, pLuc-MCS- RII or pLuc-MCS-EV (empty vector). All the cells were transfected with pHRLTK plasmids for normalization. The transfection ratios were pre-optimized (Appendix O). We collected the cells and assayed them for luciferase and renilla signals. Results normalized to pLuc-MCS-EV (empty vector) /pHRLTK ratios are given in Figure 3. 34 for HT-29 cells and Figure 3. 35 for LoVo cells. Our data indicate that p65 transcriptional activity was reduced in 15-LOX-1 expressing HT-29 and LoVo cells both in Region I and II of the MTA1 promoter when compared to EV transfected cells.

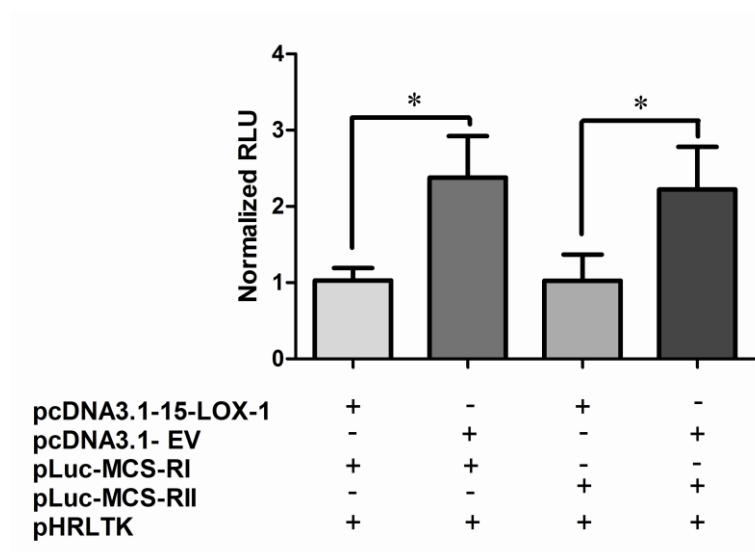


Figure 3. 34 MTA1 promoter activity in Region I and II containing NF- κ B binding sites was significantly is decreased in 15-LOX-1 expressing HT-29 cells. The data are nomalized to pLuc-MCS-EV (empty vector) /pHRLTK ratios. Three independent experiments were performed and statistical comparisons were carried out using paired t-test (* $p < 0.05$).

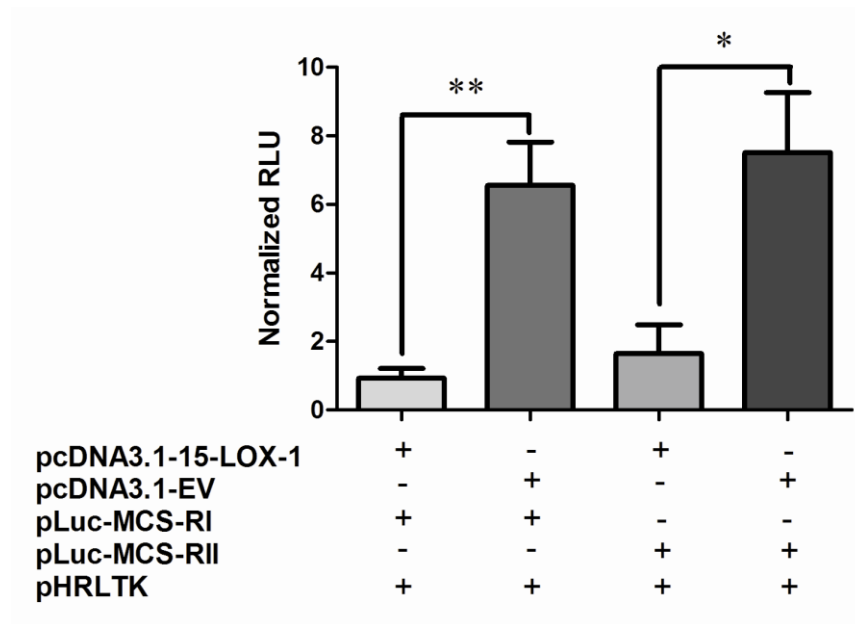


Figure 3. 35 MTA1 promoter activity containing NF- κ B binding sites was significantly decreased in Region I and II in 15-LOX-1 expressing LoVo cells. The data are normalized to pLuc-MCS-EV (empty vector) /pHRLTK ratios. Three independent experiments were performed and statistical comparisons were carried out using paired t-test ($*p<0.05$ and $**p<0.01$).

3.16 Electrophoretic mobility shift assay (EMSA) for NF- κ B binding on the MTA1 promoter

Considering the recruitment of p65 and its transcriptional activity observed on RI and RII regions of the MTA1 promoter DNA in ChIP and luciferase assays, we wanted to examine p65 binding to each of the identified sequences by using non radioactive EMSA.

Equal amounts of nuclear extracts from HT-29 were incubated with biotin labeled oligos (oligo sequences are given in Table 4). The biotin labeled oligo1, 2, 3 and 6 [corresponding to the NF- κ B binding sequences in RI (oligo 1) and RII (oligos 2, 3 4, 5 and 6)] were able to form complexes with the proteins in the nuclear extract from empty vector transfected cells (Figure 3. 36 and Figure 3. 37) with the strongest binding observed with oligos 1 and 6. However, when nuclear extracts from 15-LOX-1 expressing cells were incubated with the oligos, a loss in binding was observed. The presence of p65 protein in the proteins from the EV transfected cells binding to the oligos was confirmed by addition of a monoclonal p65 antibody, which resulted in a supershift of the complex. Moreover, the addition of corresponding unlabeled oligonucleotide (cold probe), led to the loss of the shifts due to the competition of excess unlabeled probe with complex formation.

The binding of p65 to Oligos 1 and 6 was also examined in the LoVo cells line and also further validated in HT-29 by mutating the oligos (Mutant oligo sequences are shown in Table 4). Results in Figure 3. 38 and Figure 3. 39 further validate the reduced p65 binding to the oligo sequence 1 and 6 in HT-29 cells. Incubation of EV nuclear proteins with the mutated oligos resulted in a loss of binding. For the LoVo cells, binding was observed in the EV transfected cells to the oligo 6, which was lost when the oligo was mutated, or when 15-LOX-1 was expressed. Although ChIP indicated a loss of recruitment to Region I in LoVo cells, NF- κ B binding to Oligo 1 could not be detected by EMSA.

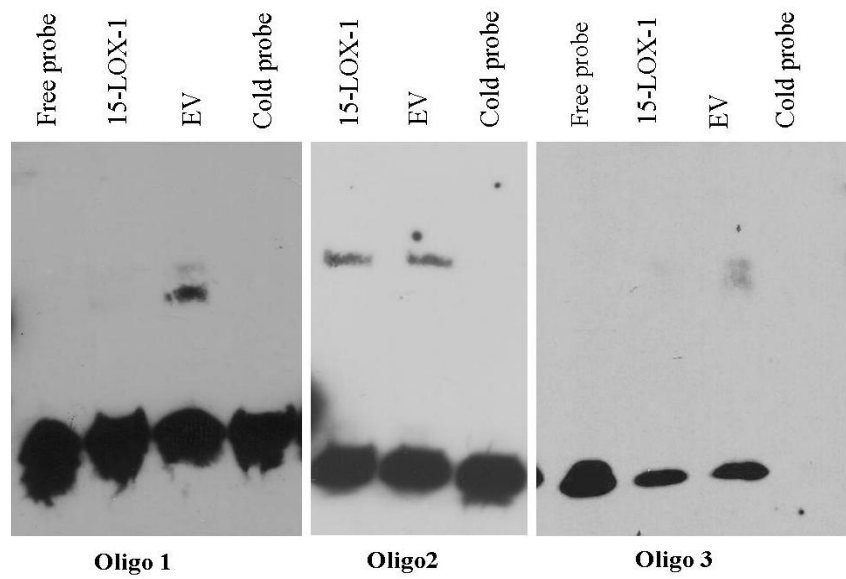


Figure 3. 36 EMSA using oligo 1, 2 and 3 in HT-29 cells. Reduced protein binding to NF- κ B consensus sequences in 15-LOX-1 expressing cells was observed with Oligo 1 (Region I), no difference in protein binding was observed with Oligo 2 (Region II) and no binding was observed in Oligo 3 (Region II).

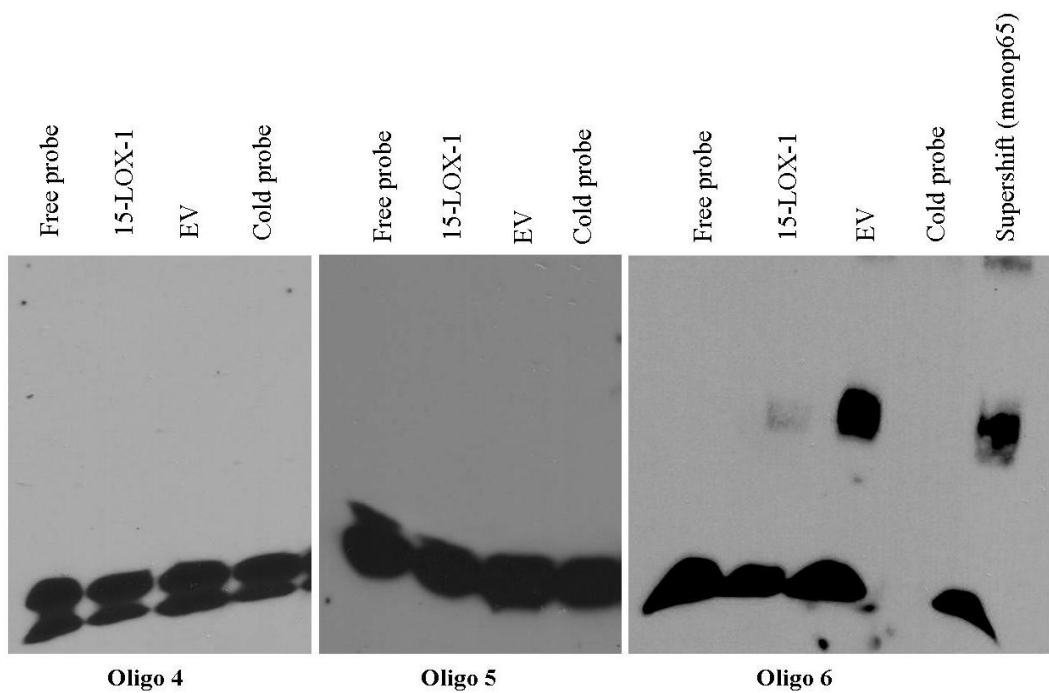


Figure 3. 37 EMSA using oligo 4, 5 and 6 in HT-29 cells. . Reduced protein binding to NF- κ B consensus sequences in 15-LOX-1 expressing cells was observed with Oligo 6 (Region II), and no binding was observed in Oligos 4 and 5 (Region II). Specificity of the binding was ensured by the use of the competitive cold probe. Supershift was observed when the lysate was incubated with a monoclonal p65 antibody.

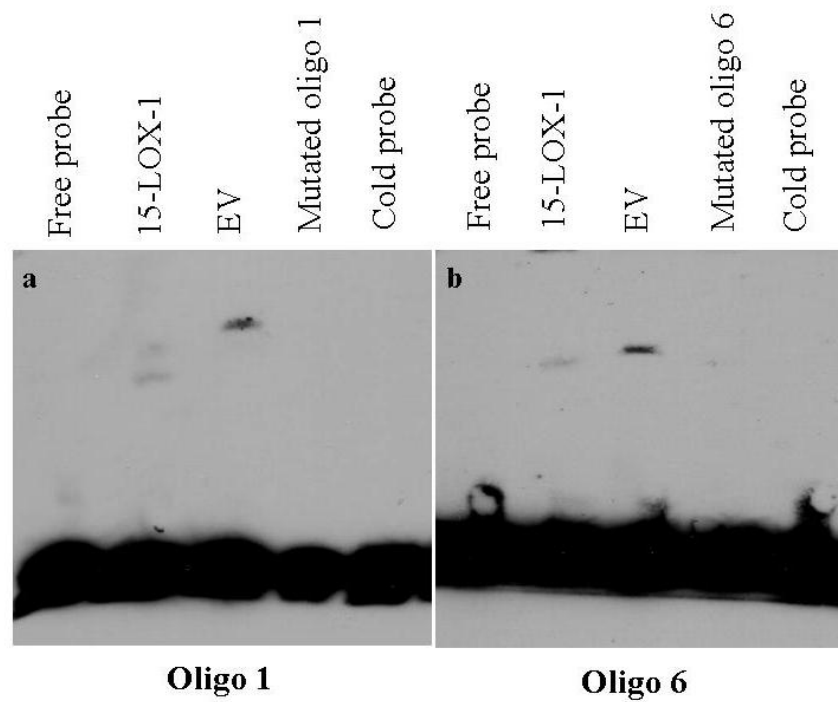


Figure 3. 38 Confirmation of protein binding to NF- κ B binding sequences in the promoter of MTA1 by EMSA using oligo 1&6 and the mutated sequences in HT-29 cells. Incubation of protein lysates from the empty vector transfected control cells with oligos 1 and 6 where the NF- κ B consensus sequence was mutated resulted in a loss of binding.

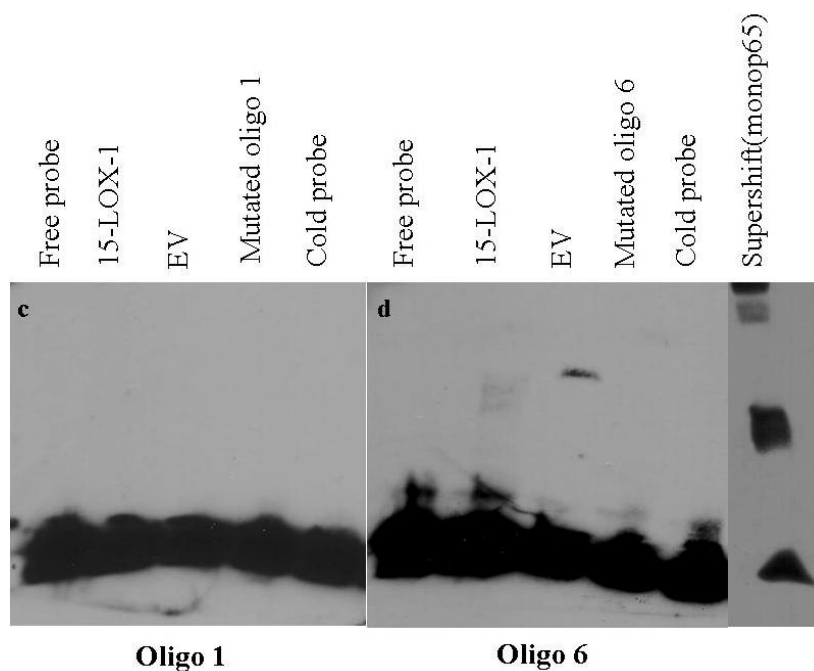


Figure 3. 39 Confirmation of protein binding to NF- κ B binding sequences in the promoter of MTA1 by EMSA using oligo 1 & 6 and the mutated sequences in LoVo cells. Incubation of protein lysates from the empty vector transfected control cells with oligos 1 and 6 where the NF- κ B consensus sequence was mutated resulted in a loss of binding Supershift was observed with the lysates incubated.

3.17 Correlation analysis of 15-LOX-1 and MTA1 expressions in CRC patients

To understand whether the negative correlation observed between MTA1 and 15-LOX-1 expressions observed in the cell lines was relevant in CRC patients; we investigated the publicly available microarray dataset (GSE41258) including 53 normal and 182 colorectal cancer patients. We observed no significant correlation

of the expression of the two genes in normal colon tissues (Figure 3. 40) or in Stage I and Stage II colorectal cancer patients (Figure 3. 41). However, as shown in Figure 3. 42, there is a significant negative correlation (evaluated by calculation of Pearson's coefficient (r)) between the expressions of 15-LOX-1 and MTA1 genes in Stage III and Stage IV colorectal cancer patients.

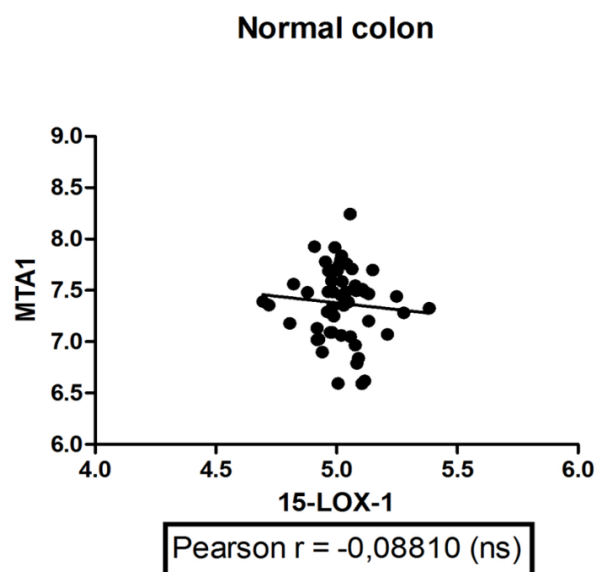


Figure 3. 40 Correlation analysis of 15-LOX-1 and MTA1 expressions in normal colon tissues obtained from publicly available microarray data set (GSE41258). No significant correlation was seen between the two genes. Evaluation was done by calculation of Pearson's coefficient (r).

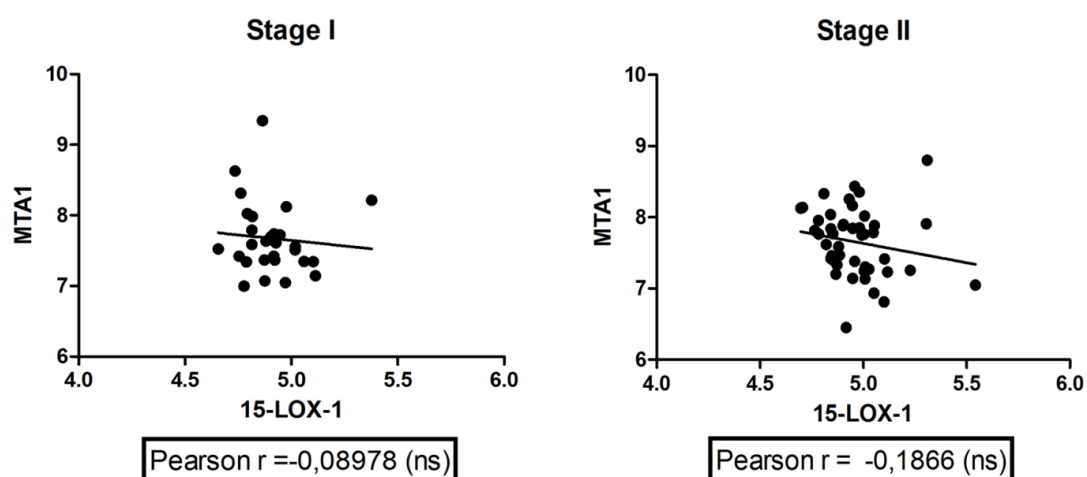


Figure 3. 41 Correlation analysis of 15-LOX-1 and MTA1 expressions in Stage I and Stage II CRC patients showing no significant correlation between two genes. Evaluation was done by calculation of Pearson's coefficient (r).

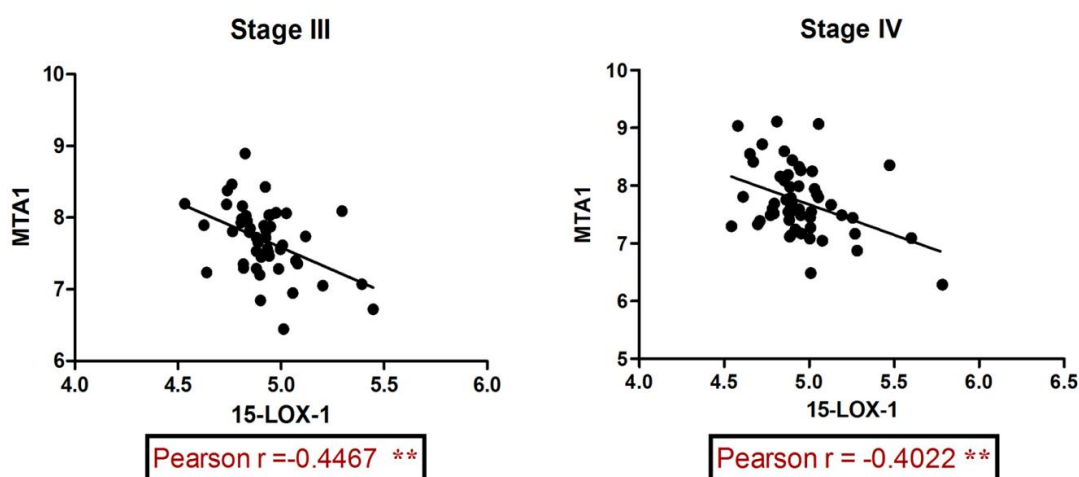


Figure 3. 42 Correlation analysis of 15-LOX-1 and MTA1 expressions in Stage III and IV CRC patients showing a significant negative correlation between two genes with Pearson r = -0.4467 and -0.4022 respectively.

3.18 Tissue scan array

To confirm the inverse correlation of 15-LOX-1 and MTA1 expressions in colorectal cancer patient tissues we carried out qRT-PCR analysis for *ALOX15* and *MTA1* expressions with a TissueScan cDNA array containing 48 samples. The array consisted of 8-normal, 5-Stage I, 8-IIA, 1-II, 1-IIIA, 6-IIIB, 3-IIIC, 6-III, 10-IV CRC patients' first strand cDNAs obtained from pathologist verified tissues. The results were verified and normalized to β -actin in sequential qRT-PCR analyses.

The $\Delta\Delta C_t$ values obtained were subjected to correlation analysis and the Pearson r values were calculated. The results in Figure 3. 43 - Figure 3. 46 show the presence of a negative correlation in Stage I (Pearson $r = -0.3896$) Stage II-IIA (Pearson $r = -0.5966$), Stage IIIA-IIIB-IIIC (Pearson $r = -0.2540$) and Stage IV (Pearson $r = -0.4001$) patients. None of these correlations reached statistical significance primarily because of the limited number of samples. No correlation was observed in the normal tissue samples (Pearson $r = -0.02317$) or in the Stage III samples (Pearson $r = 0.1019$).

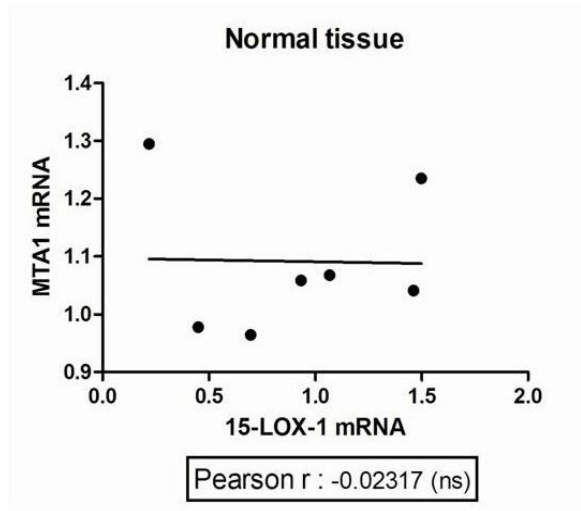


Figure 3. 43 Correlation analysis of 15-LOX-1 and MTA1 expressions in normal tissue with the data obtained from TissueScan array showing no correlation (Pearson r = -0.02317).

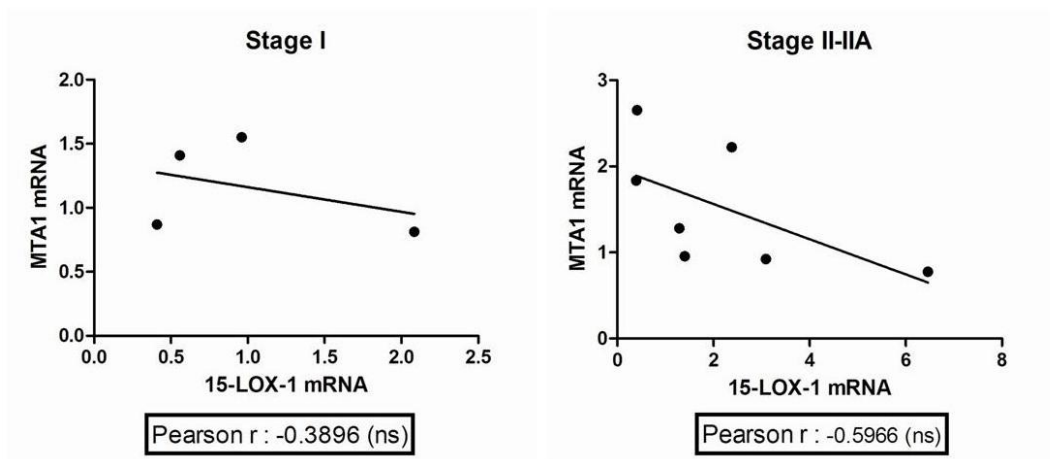


Figure 3. 44 Correlation analysis of 15-LOX-1 and MTA1 expressions in Stage I and II-IIA CRC patients with the data obtained from TissueScan array (Pearson r =

-0.3896 and -0.5966). A negative correlation was observed in Stage II-IIA, however, the correlation was statistically not significant due to the low sample number.

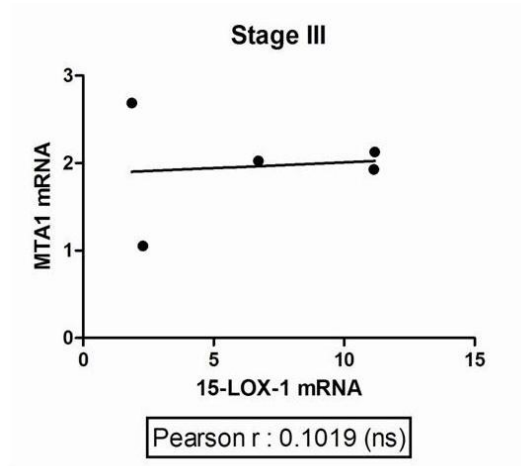


Figure 3. 45 Correlation analysis of 15-LOX-1 and MTA1 expressions in Stage III CRC patients with the data obtained from TissueScan array showing no correlation (Pearson $r = 0.1019$).

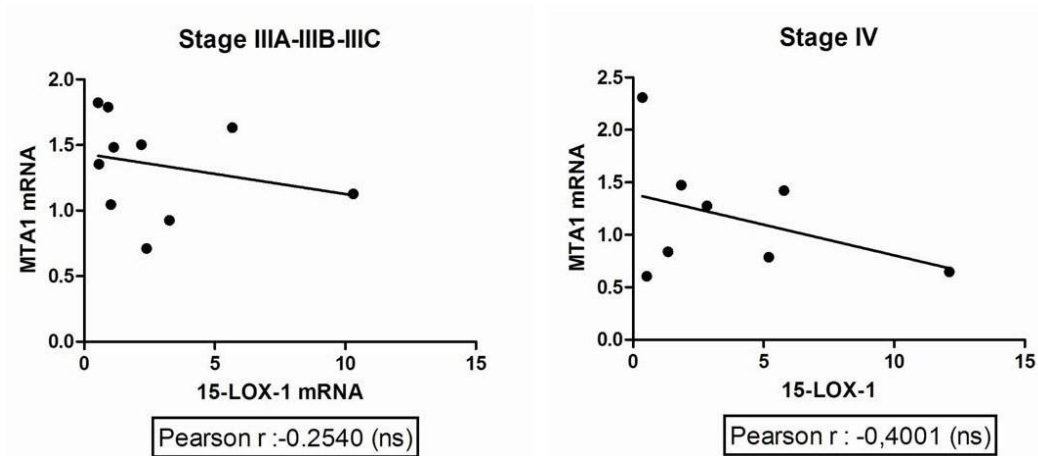


Figure 3. 46 Correlation analysis of 15-LOX-1 and MTA1 expressions in Stage IIIA-III B-III C and Stage IV CRC patients with the data obtained from TissueScan array (Pearson $r = -0.2540$ and -0.4001).

CHAPTER 4

DISCUSSION

Genes that are important for cancer progression are often controlled by deregulated coregulatory molecules to drive the process of growth and metastasis. One such coregulator protein is the chromatin remodeler Metastasis Associated Protein 1 (MTA1), which is a critical component of the repressive nucleosome remodeling and histone deacetylase (NuRD) complex and can act as both a coactivator and corepressor (Li et al., 2012a; Mazumdar et al., 2001). MTA1 has also been described as a master regulator of cancer progression and occupies a special place in cancer biology because of its widespread overexpression in human cancers (Li et al., 2012a). However, the importance of this protein in CRC has only recently been emerging.

15-lipoxygenase-1 (15-LOX-1) is a lipid metabolizing enzyme (Nagy et al., 1998; Zuo et al., 2006) that has tumor suppressive properties in many different cancer types (Cimen et al., 2009a; Shureiqi and Lippman, 2001; Shureiqi et al., 1999; Wu et al., 2008). The expression of *ALOX15* is repressed in colorectal cancer cells at the transcriptional level by various different mechanisms such as promoter hypermethylation (Liu et al., 2004), repression through GATA-6 (Kamitani et al., 2000), histone acetylation and demethylation (Zuo et al., 2008) as well as the NuRD complex (Zuo et al., 2009b). We have previously shown that re-expression of 15-LOX-1 inhibited metastasis in CRC (Cimen et al., 2009a; Tuncay, 2009) and resulted in reduced expression of MTA1 indicating the presence of a feedback loop.

4.1 MTA1 in CRC

Du et al. have shown that MTA1 expression correlated with Dukes staging and lymph node metastasis. (Du et al., 2011; Higashijima et al., 2011) have shown that MTA1 expression was correlated with worse prognosis in CRC patients and that coexpression of MTA1 and HDAC1 was related to the worst overall survival, compared to the expression of each protein individually. We have also established that MTA1 expression is enhanced in more invasive or higher grade tumors (Tuncay Cagatay et al., 2013). Recently, Zhu et al. have shown that MTA1 is upregulated by eukaryotic initiation factor 5A2 (EIF5A2) which led to EMT in CRC cells (Pakala et al., 2011; Zhu et al., 2012).

Based on these recent studies, we have aimed to first understand whether MTA1 was important for proliferation, metastasis and angiogenesis in CRC, and whether the observed functional changes stemmed from EMT like changes. For this, we generated HCT-116 CRC cells that stably overexpress MTA1, or used shRNA technology to stably silence MTA1 in HCT-116 cells. We used two populations of MTA1 overexpressing cells with increasing levels of MTA1 expression and two clones of MTA1 silenced cells with decreasing levels of MTA1 expression.

4.1.1 MTA1 enhances viability and proliferation in CRC cell lines

An increased viability and proliferation rate in the MTA1 overexpressing cells and a decrease in proliferation in the cells with silenced MTA1 confirmed that the overexpression and silencing were functional. Moreover, the viability and proliferation rate was proportional to the extent to which MTA1 was overexpressed or repressed in the cells.

4.1.2 MTA1 expression stimulates anchorage independent growth

Anchorage independent growth is a measure of the transformation of cells whereby they acquire the ability to grow in semi-solid medium (Clark et al., 1995). MTA1 overexpression in HCT-116 cells increased anchorage independent growth by forming more colonies in soft agar compared to empty vector expressing cells while MTA1 silencing caused much lower number of colonies compared to corresponding control cells.

4.1.3 MTA1 enhance metastatic phenotype, survival signals and angiogenesis

Metastasis results in cells that are more adherent to the extracellular matrix and migratory and are also associated with survival signals such as reduction in apoptosis and the expression of VEGF and neoangiogenesis, thereby resulting in a more aggressive tumor type (Bates et al., 2003; Bates et al., 2007; Friedl et al., 2004; van der Horst et al., 2012). Therefore, we next determined whether overexpression or silencing of MTA1 in CRC cells also showed functional changes that accompany the process of cellular motility, invasion and survival. MTA1 overexpression significantly increased the adhesion of HCT-116 to extracellular matrix component fibronectin; while silencing of the MTA1 gene caused a reduction in adhesion of the cells compared to corresponding empty vector transfected cells. Moreover, the MTA1 overexpressing HCT-116 cells also displayed higher motility and closed a scratch wound within 24 h, while the reverse was seen in the silenced cells. Furthermore, MTA1 overexpression enhanced cell migration through the Transwell pores and invasion through Matrigel, whereas silencing of MTA1 was accompanied by a substantial inhibition of cell migration and invasion.

A strong stimulus for apoptosis in normal epithelial cells is the loss of adhesive interactions (both cell–matrix and cell–cell) followed by the dissolution of the epithelial architecture (Bates et al., 1995). Moreover, loss of apoptosis is a survival signal that cells undergoing metastasis also possess, which most likely results in the resistance of migratory cells with stem cell like properties to chemotherapy protocols (Monteiro and Fodde, 2010). We therefore evaluated the effect of MTA1 overexpression and silencing on apoptosis of HCT-116 cells. Our data showed that MTA1 overexpression caused a robust inhibition of apoptosis whereas MTA1 silencing resulted in a strong stimulus for apoptosis, compared to the control cells. Furthermore, the anti-apoptotic protein Bcl-xl, which is a well-established target of MTA1 in mammary cell development (Bagheri-Yarmand et al., 2004), was seen to be expressed more in HCT-116 cells ectopically expressing MTA1 and reduced in MTA1 silenced HCT-116 cells. MTA1 silenced HCT-116 cells also showed decreased levels of the anti-apoptotic protein XIAP. Therefore, the reduction of both anti-apoptotic proteins in MTA1 silenced cells provides a mechanistic basis for the gain in apoptosis in these cells.

A second survival signal that is widely associated with MTA1 expression is the expression of VEGF-A, a secreted growth factor that results in the formation of new blood vessels in the hypoxic tumor microenvironment (Bates et al., 2003; Bertout et al., 2008; Jang et al., 2006; Kai et al., 2011; Li et al., 2012b) The role of MTA1 in neoangiogenesis in CRC has not been previously reported. We have observed that VEGF-A secretion was significantly decreased in MTA1 silenced cells, whereas MTA1 overexpression resulted in much higher secretion of VEGF-A. To further define whether the secreted VEGF-A resulted in neoangiogenesis, we carried out an endothelial tube formation assay. We have observed that the MTA1 overexpressing HCT-116 cells were capable of inducing HUVECs to form tubes with significantly more nodal structures, total skeleton lengths and branching points. On the contrary,

MTA1 silenced cells showed significantly decreased total skeleton length, number of branching points, nodal structures and tubes compared to control HCT-116 cells.

4.1.5 MTA1 induces Epithelial to Mesenchymal Transition (EMT) in CRC

Several of the functional changes described above can be associated with cells undergoing EMT. EMT promotes escape from the constraints of adhesion-dependent survival, thereby enhancing the process of metastasis (Bates et al., 2007). Moreover, overexpression of the transcription factor SLUG was shown to promote angiogenesis in glioblastoma in vivo and siRNA mediated silencing of MTA1 reduced angiogenesis in T24 human bladder cancer cells (Wang et al., 2011; Yang et al., 2010). Additionally, MTA1 has been shown to enhance EMT breast cancer cells via TGF β 1 mediated upregulation of MTA1 (Pakala et al., 2011), as well as in CRC cells via EIF5A2 mediated upregulation of MTA1 (Zhu et al., 2012). In order to confirm that MTA1 was involved in the process of EMT, we next determined whether MTA1 expression was related to the expression of epithelial and mesenchymal markers in MTA1 overexpressing or silenced HCT-116 cells as well as MTA1 silenced LoVo cells. We have observed that MTA1 silencing in HCT-116 and LoVo cells caused an increase in the junctional proteins E-cadherin and ZO-1. Interestingly, the expression of E-cadherin was related to the extent to which MTA1 was silenced in both LoVo and HCT-116 cells. Therefore, the cells where MTA1 was silenced more showed a greater recovery in the expression of E-cadherin. This was effect not seen for the mesenchymal markers for which a decrease in expression of MTA1 by 15 % in the clone shMTA1b1 was enough to completely abrogate the expression of several key EMT markers.

We have not observed a significant decrease in the expression of E-cadherin and ZO-1 or an increase in Snai1 and Slug transcription factors in MTA1 overexpressing cells either due to these cells being polyclones and therefore with

heterogeneous expression of MTA1, or due to the presence of hitherto unknown compensatory mechanisms. The Snail family proteins, including the highly homologous proteins Snai1 and Slug repress E-cadherin transcription by binding the E-box E-pal element on the E-cadherin promoter (Kang and Massague, 2004). We have therefore examined the expression of Snai1 and Slug in MTA1 silenced HCT-116 and LoVo cells and observed a downregulation in both proteins. Moreover, the recruitment of Snai1 and Slug to the E-box sequences on the E-cadherin promoter was also reduced, most likely due to this decrease in the expression of these transcription factors, providing a new mechanistic explanation for the increase in E-cadherin expression in the MTA1 silenced CRC cells. Although the MTA1/NuRD complex is known to induce repression of several different genes, MTA1 alone can also act as a transcriptional upregulator (Li et al., 2012a). Therefore, MTA1 may directly upregulate Snai1 and Slug, although this remains to be established. Alternatively, it has been previously suggested that MTA3, also a member of the NuRD complex, can repress the expression of Snai1 in breast cancer cells (Fujita et al., 2003). Furthermore, it was also reported that late stage breast carcinomas in PyV-mT transgenic mice showed very few MTA3 positive cells, whereas MTA1 was highly expressed in those cells (Zhang et al., 2006). Whether such a reciprocal expression of MTA1 and MTA3 exists in CRC remains to be seen.

We have also observed stable levels of β -catenin in MTA1 overexpressing or MTA1 silenced cells. Indeed, in almost all colorectal carcinomas β -catenin level or its activity is increased due to APC inactivation but in most of these tumors β -catenin is not enough or necessary to induce EMT (Polyak and Weinberg, 2009).

MMPs are enzymes that can degrade the extracellular matrix; therefore, increased expression of MMPs, especially MMP2 and MMP9, are associated with tumor invasion, metastasis, angiogenesis and poor clinical outcome (Bauvois, 2012). Emerging data show that mesenchymal cells contribute to ECM remodeling through

the production of MMPs (Egeblad and Werb, 2002; Radisky, 2005). On the other hand, MMP-9 can stimulate EMT by either interfering with E-cadherin mediated cell to cell junctions or by cooperating with Snail to reduce E-cadherin expression (Egeblad and Werb, 2002; Lin et al., 2011; Orlichenko and Radisky, 2008).

4.2 Interplay between 15-LOX-1, MTA1 and NF- κ B

We have previously reported that expression of 15-LOX-1 reduced the metastatic potential of colon cancer cell lines, at least in part by reducing the expression of MTA1, indicating the presence of a feedback loop (Cimen et al, 2009). Moreover, we have shown that 15-LOX-1 can inhibit the activity of NF- κ B (Cimen et al., 2011) while MTA1 can be transcriptionally upregulated by the inflammatory transcription factor Nuclear factor kappa B (NF- κ B) (Pakala et al., 2010a). Therefore, we aimed to investigate the crosstalk between MTA1 and 15-LOX-1 by evaluating the hypothesis that 15-LOX-1 can regulate the expression of MTA1 through NF- κ B.

4.2.1 15-LOX-1 expression reduces MTA1 expression and NF- κ B translocation

In a high throughput study where gene expression in p53 wildtype MTA1 knock out mouse embryonic fibroblasts (MEFs) was compared with the wild type MEFs, the genes regulated by MTA1 were primarily involved in the inflammatory response (Ghanta et al., 2011a). MTA1 was shown to be a co-regulator of Transglutaminase 2, a protein involved in the activation of the inflammatory transcription factor NF- κ B and the development of sepsis (Ghanta et al., 2011b). MyD88 expression and NF- κ B activation in LPS stimulated macrophages also involved MTA1 as a co-regulator with enhanced recruitment of MTA1, RNA polymerase II, and p65RelA complex to the NF- κ B consensus sites in the MyD88 promoter (Pakala et al., 2010b). Moreover, mouse model studies have shown that MTA1 can be

transcriptionally upregulated by the inflammatory transcription factor NF- κ B) (Pakala et al., 2010a), indicating the presence of extensive crosstalk between MTA1 expression and inflammation.

Recent work from our lab and others has shown that 15-LOX-1 expression can inhibit the activity of NF- κ B (Cimen et al., 2011; Zuo et al., 2012). Moreover, we have also observed that 15-LOX-1 expression in CRC cell lines resulted in reduced expression of MTA1 (Cimen et al., 2009b). Therefore we have hypothesized that mechanism behind the loss of metastatic potential in the 15-LOX-1 expressing cell lines was due to the loss of MTA1 following the reduced activation of NF- κ B.

A screen of 128 different human cancer cell lines from 20 different cancer types, including CRC, consistently showed reduced mRNA levels of 15-LOX-1 compared to the terminally differentiated cells (Moussalli et al., 2011). Therefore, we firstly expressed 15-LOX-1 in 4 different CRC cell lines that do not express 15-LOX-1 and observed a considerable reduction in MTA1 expression in HT-29 and LoVo cells, which express robust amounts of MTA1. Interestingly, Caco-2 and SW620 cells, which express very low amounts of MTA1, did not show such regulation when 15-LOX-1 was expressed. Even a modest decrease in MTA1 protein levels in cell lines expressing high amounts of MTA1 is of importance since we have recently shown that shRNA mediated silencing of MTA1 by just 35% was enough to almost completely abrogate migration and invasion through Transwells as well as anchorage independent growth in CRC cell lines (Tuncay Cagatay et al., 2013).

1.2.2 Forced expression of 15-LOX-1 regulates p65 binding in regions between -1874 to -1725 and -1331 to -730 on the MTA1 promoter

To determine whether the decrease in MTA1 levels in HT29 and LoVo cells where 15-LOX-1 was restored was due to an inhibition in NF- κ B activation, we have first confirmed the decreased nuclear translocation (indicating inhibition in activity) of p65 in the presence of 15-LOX-1 in these cells. Next, we aimed to understand the regulation of MTA1 by NF- κ B in human cells. Although the transcriptional regulation of MTA1 by NF- κ B has been reported in murine models (Pakala et al., 2010a), the MTA1 gene is at a different location in the human genome and the human MTA1 promoter has not been characterized yet for NF- κ B binding. Using bioinformatic approaches, we identified possible binding sites for p65 on the MTA1 promoter spanning a region of 2 kb upstream of the start site. Six putative binding sites were identified, five of which were clustered in one region (called Region II between -1331 and -730) and the remaining one site was located upstream of the cluster (Region I between -1874 to -1725). To understand whether these two regions were functional, we carried out ChIP and luciferase reporter gene assays. When 15-LOX-1 was expressed in HT-29 and LoVo cells, a reduction in the recruitment and transcriptional activity of p65 in these regions was observed. Interestingly, SW620 cells, which did not show any reduction in MTA1 levels when 15-LOX-1 was expressed, also did not show any difference in the recruitment of p65 in the presence or absence of 15-LOX-1. To further confirm the physical association of p65 with the MTA1 promoter we carried out EMSA using oligos representing the six different sequences from the MTA1 promoter predicted to bind to p65. Of these, the oligos representing sequence 1 in Region I and sequences 3 and 6 in Region II showed a reduction in binding of p65 on the MTA1 promoter in the presence of 15-LOX-1 when compared to the empty vector transfected cells.

4.3 Correlation of 15-LOX-1 and MTA1 gene expressions in patient data

To understand whether the loss in MTA1 expression when 15-LOX-1 was re-expressed had relevance in the clinical setting, we evaluated a publicly available microarray data set including 53 normal and 182 colorectal cancer patients representing various stages of the disease. Interestingly, we observed no significant correlation between the two genes in normal colon tissues or in Stage I and Stage II. However, a statistically significant negative correlation was observed in Stage III and Stage IV patients. MTA1 levels are generally high in later stages of the disease (Tuncay Cagatay et al., 2013) indicating that this negative correlation with 15-LOX-1 gene expression may be an important player in the late stages of colorectal carcinoma. To further confirm these microarray data, we next amplified the *MTA1* and *ALOX15* genes from an array consisting of cDNA from colon tissues of 48 patients including normal colon as well as representative samples from different stages. We have observed a negative correlation, albeit statistically non significant, in the expression of the genes at nearly all the stages except normal colon. These data indicate that the expressions of both *MTA1* and *ALOX15* are of importance in colon tumorigenesis. 15-LOX-1 reexpression using an adenoviral vector in LoVo colon cancer xenografts was shown to completely regress the tumors in 21% of the animals through the induction of apoptosis (Wu et al., 2008). Moreover, gut targeted expression of a human 15-LOX-1 transgene in mice also suppressed azoxymethane induced colon tumor formation and resulted in reduced levels of several inflammatory markers through the inhibition of NF- κ B (Zuo et al., 2012). Although neither of these studies examined the effect of 15-LOX-1 re-expression on metastasis, it is highly likely that the reduction in metastatic potential observed with the re-expression of 15-LOX-1 *in vitro* (Cimen et al., 2009a), will be replicated *in vivo*.

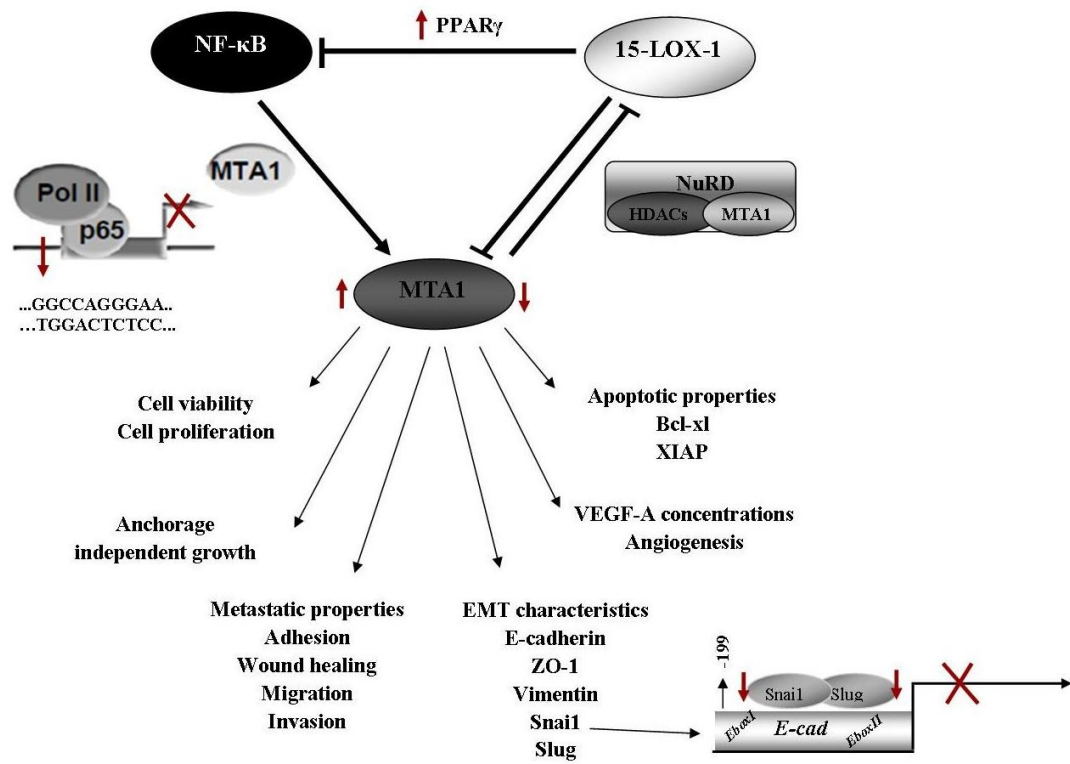


Figure 4. 1 Schematic summary of the study

CHAPTER 5

CONCLUSION

The primary aim of this study was to understand the mechanism of the reduction in motility of colon cancer cells ectopically expressing 15-LOX-1. Based on extensive reports in the literature on the importance of MTA1 in tumor progression and metastasis, we first characterized the effect of MTA1 on functional changes in colon cancer cells by overexpressing or silencing MTA1 in HCT-116 cells and reported the induction of epithelial to mesenchymal changes (EMT) in cells as a reason for the changes in motility, anchorage independent growth and angiogenesis observed in these cells.

When we examined the expression of MTA1 in colon tumor samples by immunohistochemistry, we observed higher MTA1 expression in Stages III and IV tumors (Tuncay Cagatay et al., 2013). Examination of publicly available microarray data for human colon tumor samples showed a significant negative correlation between the expression of MTA1 and 15-LOX-1, especially at Stages III and IV. The same negative correlation was observed in a colon cancer cDNA array where we amplified *ALOX15* and *MTA1* by RT-qPCR. These data indicated the likelihood for the presence of a crosstalk between MTA1 and 15-LOX-1. Re-expression of 15-LOX-1 in colon cancer cells resulted in a loss of MTA1, but only in those cell lines where MTA1 expression was high.

To understand whether the inhibition of NF- κ B through 15-LOX-1 re-expression (Cimen et al., 2009b) was implicated loss of MTA1 expression, we examined the promoter of the human MTA1 gene and determined several putative NF- κ B binding sequences. Well established techniques such as chromatin immunoprecipitation, luciferase reporter gene assays and electrophoretic mobility shift assays indicated the regulation of MTA1 by NF- κ B (primarily in the high MTA1 expressing cells, indicating the presence of other regulatory transcription factors as well) in human colon cancer cells. Moreover, we showed for the first time that in the presence of 15-LOX-1, this NF- κ B mediated transcriptional regulation of MTA1 was inhibited due to an overall inhibition of NF- κ B itself. We propose that this mechanism resulted, at least in part, in the lower MTA1 expression observed in the 15-LOX-1 expressing cells.

We believe these data further highlight the mechanisms behind the tumor suppressive functions of 15-LOX-1 and help us to understand novel strategies to regulate the expression MTA1, a master regulator of tumorigenesis, in colorectal cancer.

REFERENCES

- Adams, J. M., and S. Cory, 2007, The Bcl-2 apoptotic switch in cancer development and therapy: *Oncogene*, v. 26, p. 1324-37.
- Ara, G., and B. A. Teicher, 1996, Cyclooxygenase and lipoxygenase inhibitors in cancer therapy: *Prostaglandins Leukot Essent Fatty Acids*, v. 54, p. 3-16.
- Baer, A. N., P. B. Costello, and F. A. Green, 1991, In vivo activation of an omega-6 oxygenase in human skin: *Biochem Biophys Res Commun*, v. 180, p. 98-104.
- Baeuerle, P. A., and D. Baltimore, 1996, NF-kappa B: ten years after: *Cell*, v. 87, p. 13-20.
- Bagheri-Yarmand, R., A. H. Talukder, R. A. Wang, R. K. Vadlamudi, and R. Kumar, 2004, Metastasis-associated protein 1 deregulation causes inappropriate mammary gland development and tumorigenesis: *Development*, v. 131, p. 3469-79.
- Balasantil, S., R. R. Broaddus, and R. Kumar, 2006, Expression of metastasis-associated protein 1 (MTA1) in benign endometrium and endometrial adenocarcinomas: *Hum Pathol*, v. 37, p. 656-61.
- Barrallo-Gimeno, A., and M. A. Nieto, 2005, The Snail genes as inducers of cell movement and survival: implications in development and cancer: *Development*, v. 132, p. 3151-61.
- Bates, R. C., J. D. Goldsmith, R. E. Bachelder, C. Brown, M. Shibuya, P. Oettgen, and A. M. Mercurio, 2003, Flt-1-dependent survival characterizes the epithelial-mesenchymal transition of colonic organoids: *Curr Biol*, v. 13, p. 1721-7.
- Bates, R. C., L. F. Lincz, and G. F. Burns, 1995, Involvement of integrins in cell survival: *Cancer Metastasis Rev*, v. 14, p. 191-203.

- Bates, R. C., B. M. Pursell, and A. M. Mercurio, 2007, Epithelial-mesenchymal transition and colorectal cancer: gaining insights into tumor progression using LIM 1863 cells: *Cells Tissues Organs*, v. 185, p. 29-39.
- Bauvois, B., 2012, New facets of matrix metalloproteinases MMP-2 and MMP-9 as cell surface transducers: outside-in signaling and relationship to tumor progression: *Biochim Biophys Acta*, v. 1825, p. 29-36.
- Bertout, J. A., S. A. Patel, and M. C. Simon, 2008, The impact of O₂ availability on human cancer: *Nat Rev Cancer*, v. 8, p. 967-75.
- Bhattacharya, S., G. Mathew, D. G. Jayne, S. Pelengaris, and M. Khan, 2009, 15-lipoxygenase-1 in colorectal cancer: a review: *Tumour Biol*, v. 30, p. 185-99.
- Bhowmick, N. A., E. G. Neilson, and H. L. Moses, 2004, Stromal fibroblasts in cancer initiation and progression: *Nature*, v. 432, p. 332-7.
- Blasco, M. A., 2005, Telomeres and human disease: ageing, cancer and beyond: *Nat Rev Genet*, v. 6, p. 611-22.
- Brash, A. R., 1999, Lipoxygenases: occurrence, functions, catalysis, and acquisition of substrate: *J Biol Chem*, v. 274, p. 23679-82.
- Brash, A. R., W. E. Boeglin, and M. S. Chang, 1997, Discovery of a second 15S-lipoxygenase in humans: *Proc Natl Acad Sci U S A*, v. 94, p. 6148-52.
- Burkhardt, D. L., and J. Sage, 2008, Cellular mechanisms of tumour suppression by the retinoblastoma gene: *Nat Rev Cancer*, v. 8, p. 671-82.
- Carmeliet, P., 2005, VEGF as a key mediator of angiogenesis in cancer: *Oncology*, v. 69 Suppl 3, p. 4-10.
- Chan, A. O., K. M. Chu, S. K. Lam, B. C. Wong, K. F. Kwok, S. Law, S. Ko, W. M. Hui, Y. H. Yueng, and J. Wong, 2003, Soluble E-cadherin is an independent pretherapeutic factor for long-term survival in gastric cancer: *J Clin Oncol*, v. 21, p. 2288-93.
- Cheng, N., A. Chytil, Y. Shyr, A. Joly, and H. L. Moses, 2008, Transforming growth factor-beta signaling-deficient fibroblasts enhance hepatocyte

- growth factor signaling in mammary carcinoma cells to promote scattering and invasion: *Mol Cancer Res*, v. 6, p. 1521-33.
- Cimen, I., E. Astarci, and S. Banerjee, 2011, 15-lipoxygenase-1 exerts its tumor suppressive role by inhibiting nuclear factor-kappa B via activation of PPAR gamma: *J Cell Biochem*, v. 112, p. 2490-501.
- Cimen, I., S. Tuncay, and S. Banerjee, 2009a, 15-Lipoxygenase-1 expression suppresses the invasive properties of colorectal carcinoma cell lines HCT-116 and HT-29: *Cancer Sci*.
- Cimen, I., S. Tuncay, and S. Banerjee, 2009b, 15-Lipoxygenase-1 expression suppresses the invasive properties of colorectal carcinoma cell lines HCT-116 and HT-29: *Cancer Sci*, v. 100, p. 2283-91.
- Clark, G. J., A. D. Cox, S. M. Graham, and C. J. Der, 1995, Biological assays for Ras transformation: *Methods Enzymol*, v. 255, p. 395-412.
- Cortes Sempere, M., V. Rodriguez Fanjul, I. Sanchez Perez, and R. Perona, 2008, The role of the NFkappaB signalling pathway in cancer: *Clin Transl Oncol*, v. 10, p. 143-7.
- Dannenmann, C., N. Shabani, K. Friese, U. Jeschke, I. Mylonas, and A. Bruning, 2008, The metastasis-associated gene MTA1 is upregulated in advanced ovarian cancer, represses ERbeta, and enhances expression of oncogenic cytokine GRO: *Cancer Biol Ther*, v. 7, p. 1460-7.
- Daret, D., P. Blin, and J. Larrue, 1989, Synthesis of hydroxy fatty acids from linoleic acid by human blood platelets: *Prostaglandins*, v. 38, p. 203-14.
- Deshpande, A., P. Sicinski, and P. W. Hinds, 2005, Cyclins and cdks in development and cancer: a perspective: *Oncogene*, v. 24, p. 2909-15.
- Dorudi, S., J. P. Sheffield, R. Poulson, J. M. Northover, and I. R. Hart, 1993, E-cadherin expression in colorectal cancer. An immunocytochemical and in situ hybridization study: *Am J Pathol*, v. 142, p. 981-6.
- Du, B., Z. Y. Yang, X. Y. Zhong, M. Fang, Y. R. Yan, G. L. Qi, Y. L. Pan, and X. L. Zhou, 2011, Metastasis-associated protein 1 induces VEGF-C and

- facilitates lymphangiogenesis in colorectal cancer: *World J Gastroenterol*, v. 17, p. 1219-26.
- Egeblad, M., and Z. Werb, 2002, New functions for the matrix metalloproteinases in cancer progression: *Nat Rev Cancer*, v. 2, p. 161-74.
- Evan, G., and T. Littlewood, 1998, A matter of life and cell death: *Science*, v. 281, p. 1317-22.
- Ferlay, J., H. R. Shin, F. Bray, D. Forman, C. Mathers, and D. M. Parkin, 2010, Estimates of worldwide burden of cancer in 2008: GLOBOCAN 2008: *Int J Cancer*, v. 127, p. 2893-917.
- Ferrara, N., 2009, Vascular endothelial growth factor: *Arterioscler Thromb Vasc Biol*, v. 29, p. 789-91.
- Ferrara, N., and T. Davis-Smyth, 1997, The biology of vascular endothelial growth factor: *Endocr Rev*, v. 18, p. 4-25.
- Folkman, J., 2002, Role of angiogenesis in tumor growth and metastasis: *Semin Oncol*, v. 29, p. 15-8.
- Forsythe, J. A., B. H. Jiang, N. V. Iyer, F. Agani, S. W. Leung, R. D. Koos, and G. L. Semenza, 1996, Activation of vascular endothelial growth factor gene transcription by hypoxia-inducible factor 1: *Mol Cell Biol*, v. 16, p. 4604-13.
- Friedl, P., Y. Hegerfeldt, and M. Tusch, 2004, Collective cell migration in morphogenesis and cancer: *Int J Dev Biol*, v. 48, p. 441-9.
- Fujita, N., D. L. Jaye, M. Kajita, C. Geigerman, C. S. Moreno, and P. A. Wade, 2003, MTA3, a Mi-2/NuRD complex subunit, regulates an invasive growth pathway in breast cancer: *Cell*, v. 113, p. 207-19.
- Funk, C. D., 1996, The molecular biology of mammalian lipoxygenases and the quest for eicosanoid functions using lipoxygenase-deficient mice: *Biochim Biophys Acta*, v. 1304, p. 65-84.
- Ghanta, K. S., D. Q. Li, J. Eswaran, and R. Kumar, 2011a, Gene profiling of MTA1 identifies novel gene targets and functions: *PLoS One*, v. 6, p. e17135.

- Ghanta, K. S., S. B. Pakala, S. D. Reddy, D. Q. Li, S. S. Nair, and R. Kumar, 2011b, MTA1 coregulation of transglutaminase 2 expression and function during inflammatory response: *J Biol Chem*, v. 286, p. 7132-8.
- Giannini, R., and A. Cavallini, 2005, Expression analysis of a subset of coregulators and three nuclear receptors in human colorectal carcinoma: *Anticancer Res*, v. 25, p. 4287-92.
- Gong, Z., J. R. Hebert, R. M. Bostick, Z. Deng, T. G. Hurley, D. A. Dixon, D. Nitcheva, and D. Xie, 2007, Common polymorphisms in 5-lipoxygenase and 12-lipoxygenase genes and the risk of incident, sporadic colorectal adenoma: *Cancer*, v. 109, p. 849-57.
- Gould Rothberg, B. E., and M. B. Bracken, 2006, E-cadherin immunohistochemical expression as a prognostic factor in infiltrating ductal carcinoma of the breast: a systematic review and meta-analysis: *Breast Cancer Res Treat*, v. 100, p. 139-48.
- Hamberg, M., and B. Samuelsson, 1974, Prostaglandin endoperoxides. Novel transformations of arachidonic acid in human platelets: *Proc Natl Acad Sci U S A*, v. 71, p. 3400-4.
- Hanahan, D., and J. Folkman, 1996, Patterns and emerging mechanisms of the angiogenic switch during tumorigenesis: *Cell*, v. 86, p. 353-64.
- Hanahan, D., and R. A. Weinberg, 2011, Hallmarks of cancer: the next generation: *Cell*, v. 144, p. 646-74.
- Heidt, M., G. Furstenberger, S. Vogel, F. Marks, and P. Krieg, 2000, Diversity of mouse lipoxygenases: identification of a subfamily of epidermal isozymes exhibiting a differentiation-dependent mRNA expression pattern: *Lipids*, v. 35, p. 701-7.
- Hennig, R., T. Kehl, S. Noor, X. Z. Ding, S. M. Rao, F. Bergmann, G. Furstenberger, M. W. Buchler, H. Friess, P. Krieg, and T. E. Adrian, 2007, 15-lipoxygenase-1 production is lost in pancreatic cancer and

- overexpression of the gene inhibits tumor cell growth: *Neoplasia*, v. 9, p. 917-26.
- Heslin, M. J., A. Hawkins, W. Boedefeld, J. P. Arnoletti, A. Frolov, R. Soong, M. M. Urist, and K. I. Bland, 2005, Tumor-associated down-regulation of 15-lipoxygenase-1 is reversed by celecoxib in colorectal cancer: *Ann Surg*, v. 241, p. 941-6; discussion 946-7.
- Higashijima, J., N. Kurita, T. Miyatani, K. Yoshikawa, S. Morimoto, M. Nishioka, T. Iwata, and M. Shimada, 2011, Expression of histone deacetylase 1 and metastasis-associated protein 1 as prognostic factors in colon cancer: *Oncol Rep*, v. 26, p. 343-8.
- Hofer, M. D., R. Kuefer, S. Varambally, H. Li, J. Ma, G. I. Shapiro, J. E. Gschwend, R. E. Hautmann, M. G. Sanda, K. Giehl, A. Menke, A. M. Chinnaiyan, and M. A. Rubin, 2004a, The role of metastasis-associated protein 1 in prostate cancer progression: *Cancer Res*, v. 64, p. 825-9.
- Hofer, M. D., A. Menke, F. Genze, P. Gierschik, and K. Giehl, 2004b, Expression of MTA1 promotes motility and invasiveness of PANC-1 pancreatic carcinoma cells, *Br J Cancer*, v. 90: England, p. 455-62.
- Hofer, M. D., C. Tapia, T. J. Browne, M. Mirlacher, G. Sauter, and M. A. Rubin, 2006, Comprehensive analysis of the expression of the metastasis-associated gene 1 in human neoplastic tissue: *Arch Pathol Lab Med*, v. 130, p. 989-96.
- Ikawa, H., H. Kamitani, B. F. Calvo, J. F. Foley, and T. E. Eling, 1999, Expression of 15-lipoxygenase-1 in human colorectal cancer: *Cancer Res*, v. 59, p. 360-6.
- Il Lee, S., X. Zuo, and I. Shureiqi, 2011, 15-Lipoxygenase-1 as a tumor suppressor gene in colon cancer: is the verdict in?: *Cancer Metastasis Rev*, v. 30, p. 481-91.
- Iwatsuki, M., K. Mimori, T. Yokobori, H. Ishi, T. Beppu, S. Nakamori, H. Baba, and M. Mori, 2010, Epithelial-mesenchymal transition in cancer development and its clinical significance: *Cancer Sci*, v. 101, p. 293-9.

- Jang, K. S., S. S. Paik, H. Chung, Y. H. Oh, and G. Kong, 2006, MTA1 overexpression correlates significantly with tumor grade and angiogenesis in human breast cancers: *Cancer Sci*, v. 97, p. 374-9.
- Jiang, Q., H. Zhang, and P. Zhang, 2011, ShRNA-mediated gene silencing of MTA1 influenced on protein expression of ER alpha, MMP-9, CyclinD1 and invasiveness, proliferation in breast cancer cell lines MDA-MB-231 and MCF-7 in vitro: *J Exp Clin Cancer Res*, v. 30, p. 60.
- Jiang, W. G., G. Watkins, A. Douglas-Jones, and R. E. Mansel, 2006, Reduction of isoforms of 15-lipoxygenase (15-LOX)-1 and 15-LOX-2 in human breast cancer: *Prostaglandins Leukot Essent Fatty Acids*, v. 74, p. 235-45.
- Jostarndt, K., N. Gellert, T. Rubic, C. Weber, H. Kuhn, B. Johansen, N. Hrboticky, and J. Neuzil, 2002, Dissociation of apoptosis induction and CD36 upregulation by enzymatically modified low-density lipoprotein in monocytic cells: *Biochem Biophys Res Commun*, v. 290, p. 988-93.
- Kai, L., J. Wang, M. Ivanovic, Y. T. Chung, W. B. Laskin, F. Schulze-Hoepfner, Y. Mirochnik, R. L. Satcher, Jr., and A. S. Levenson, 2011, Targeting prostate cancer angiogenesis through metastasis-associated protein 1 (MTA1): *Prostate*, v. 71, p. 268-80.
- Kamitani, H., M. Geller, and T. Eling, 1998, Expression of 15-lipoxygenase by human colorectal carcinoma Caco-2 cells during apoptosis and cell differentiation: *J Biol Chem*, v. 273, p. 21569-77.
- Kamitani, H., H. Kameda, U. P. Kelavkar, and T. E. Eling, 2000, A GATA binding site is involved in the regulation of 15-lipoxygenase-1 expression in human colorectal carcinoma cell line, caco-2: *FEBS Lett*, v. 467, p. 341-7.
- Kang, Y., and J. Massague, 2004, Epithelial-mesenchymal transitions: twist in development and metastasis: *Cell*, v. 118, p. 277-9.
- Karin, M., 2006, Nuclear factor-kappaB in cancer development and progression: *Nature*, v. 441, p. 431-6.

- Kessenbrock, K., V. Plaks, and Z. Werb, 2010, Matrix metalloproteinases: regulators of the tumor microenvironment: *Cell*, v. 141, p. 52-67.
- Kim, J. H., J. H. Chang, J. H. Yoon, J. G. Lee, J. H. Bae, and K. S. Kim, 2006, 15-Lipoxygenase-1 induced by interleukin-4 mediates apoptosis in oral cavity cancer cells: *Oral Oncol*, v. 42, p. 825-30.
- Klymkowsky, M. W., and P. Savagner, 2009, Epithelial-mesenchymal transition: a cancer researcher's conceptual friend and foe: *Am J Pathol*, v. 174, p. 1588-93.
- Kondo, Y., S. Arii, A. Mori, M. Furutani, T. Chiba, and M. Imamura, 2000, Enhancement of angiogenesis, tumor growth, and metastasis by transfection of vascular endothelial growth factor into LoVo human colon cancer cell line: *Clin Cancer Res*, v. 6, p. 622-30.
- Kowalski, P. J., M. A. Rubin, and C. G. Kleer, 2003, E-cadherin expression in primary carcinomas of the breast and its distant metastases: *Breast Cancer Res*, v. 5, p. R217-22.
- Kuhn, H., and B. J. Thiele, 1999, The diversity of the lipoxygenase family. Many sequence data but little information on biological significance: *FEBS Lett*, v. 449, p. 7-11.
- Kumar, R., S. Balasenthil, B. Manavathi, S. K. Rayala, and S. B. Pakala, 2010, Metastasis-associated protein 1 and its short form variant stimulates Wnt1 transcription through promoting its derepression from Six3 corepressor: *Cancer Res*, v. 70, p. 6649-58.
- Kumar, R., R. A. Wang, A. Mazumdar, A. H. Talukder, M. Mandal, Z. Yang, R. Bagheri-Yarmand, A. Sahin, G. Hortobagyi, L. Adam, C. J. Barnes, and R. K. Vadlamudi, 2002, A naturally occurring MTA1 variant sequesters oestrogen receptor-alpha in the cytoplasm: *Nature*, v. 418, p. 654-7.
- Lehembre, F., M. Yilmaz, A. Wicki, T. Schomber, K. Strittmatter, D. Ziegler, A. Kren, P. Went, P. W. Derksen, A. Berns, J. Jonkers, and G. Christofori,

- 2008, NCAM-induced focal adhesion assembly: a functional switch upon loss of E-cadherin: *EMBO J*, v. 27, p. 2603-15.
- Li, D. Q., S. B. Pakala, S. S. Nair, J. Eswaran, and R. Kumar, 2012a, Metastasis-associated protein 1/nucleosome remodeling and histone deacetylase complex in cancer: *Cancer Res*, v. 72, p. 387-94.
- Li, S. H., H. Tian, W. M. Yue, L. Li, C. Gao, W. J. Li, W. S. Hu, and B. Hao, 2012b, Metastasis-associated protein 1 nuclear expression is closely associated with tumor progression and angiogenesis in patients with esophageal squamous cell cancer: *World J Surg*, v. 36, p. 623-31.
- Li, S. H., H. Tian, W. M. Yue, L. Li, W. J. Li, Z. T. Chen, W. S. Hu, Y. C. Zhu, and L. Qi, 2011, Overexpression of metastasis-associated protein 1 is significantly correlated with tumor angiogenesis and poor survival in patients with early-stage non-small cell lung cancer: *Ann Surg Oncol*, v. 18, p. 2048-56.
- Lin, C. Y., P. H. Tsai, C. C. Kandaswami, P. P. Lee, C. J. Huang, J. J. Hwang, and M. T. Lee, 2011, Matrix metalloproteinase-9 cooperates with transcription factor Snail to induce epithelial-mesenchymal transition: *Cancer Sci*, v. 102, p. 815-27.
- Liotta, L. A., P. S. Steeg, and W. G. Stetler-Stevenson, 1991, Cancer metastasis and angiogenesis: an imbalance of positive and negative regulation: *Cell*, v. 64, p. 327-36.
- Liu, C., D. Xu, J. Sjoberg, P. Forsell, M. Bjorkholm, and H. E. Claesson, 2004, Transcriptional regulation of 15-lipoxygenase expression by promoter methylation: *Exp Cell Res*, v. 297, p. 61-7.
- Lowe, S. W., E. Cepero, and G. Evan, 2004, Intrinsic tumour suppression: *Nature*, v. 432, p. 307-15.
- Mac Gabhann, F., and A. S. Popel, 2008, Systems biology of vascular endothelial growth factors: *Microcirculation*, v. 15, p. 715-38.

- Mahoney, M. G., A. Simpson, M. Jost, M. Noe, C. Kari, D. Pepe, Y. W. Choi, J. Uitto, and U. Rodeck, 2002, Metastasis-associated protein (MTA)1 enhances migration, invasion, and anchorage-independent survival of immortalized human keratinocytes: *Oncogene*, v. 21, p. 2161-70.
- Manavathi, B., and R. Kumar, 2007, Metastasis tumor antigens, an emerging family of multifaceted master coregulators, *J Biol Chem*, v. 282: United States, p. 1529-33.
- Manavathi, B., K. Singh, and R. Kumar, 2007, MTA family of coregulators in nuclear receptor biology and pathology: *Nucl Recept Signal*, v. 5, p. e010.
- Mani, S. A., W. Guo, M. J. Liao, E. N. Eaton, A. Ayyanan, A. Y. Zhou, M. Brooks, F. Reinhard, C. C. Zhang, M. Shipitsin, L. L. Campbell, K. Polyak, C. Briskin, J. Yang, and R. A. Weinberg, 2008, The epithelial-mesenchymal transition generates cells with properties of stem cells: *Cell*, v. 133, p. 704-15.
- Martin, M. D., K. Fischbach, C. K. Osborne, S. K. Mohsin, D. C. Allred, and P. O'Connell, 2001, Loss of heterozygosity events impeding breast cancer metastasis contain the MTA1 gene: *Cancer Res*, v. 61, p. 3578-80.
- Martin, M. D., S. G. Hilsenbeck, S. K. Mohsin, T. A. Hopp, G. M. Clark, C. K. Osborne, D. C. Allred, and P. O'Connell, 2006, Breast tumors that overexpress nuclear metastasis-associated 1 (MTA1) protein have high recurrence risks but enhanced responses to systemic therapies: *Breast Cancer Res Treat*, v. 95, p. 7-12.
- Maxwell, P. H., G. U. Dachs, J. M. Gleadle, L. G. Nicholls, A. L. Harris, I. J. Stratford, O. Hankinson, C. W. Pugh, and P. J. Ratcliffe, 1997, Hypoxia-inducible factor-1 modulates gene expression in solid tumors and influences both angiogenesis and tumor growth: *Proc Natl Acad Sci U S A*, v. 94, p. 8104-9.
- Mazumdar, A., R. A. Wang, S. K. Mishra, L. Adam, R. Bagheri-Yarmand, M. Mandal, R. K. Vadlamudi, and R. Kumar, 2001, Transcriptional repression

- of oestrogen receptor by metastasis-associated protein 1 corepressor: *Nat Cell Biol*, v. 3, p. 30-7.
- Micalizzi, D. S., S. M. Farabaugh, and H. L. Ford, 2010, Epithelial-mesenchymal transition in cancer: parallels between normal development and tumor progression: *J Mammary Gland Biol Neoplasia*, v. 15, p. 117-34.
- Mishra, S. K., Z. Yang, A. Mazumdar, A. H. Talukder, L. Larose, and R. Kumar, 2004, Metastatic tumor antigen 1 short form (MTA1s) associates with casein kinase I-gamma2, an estrogen-responsive kinase: *Oncogene*, v. 23, p. 4422-9.
- Miyake, K., T. Yoshizumi, S. Imura, K. Sugimoto, E. Batmunkh, H. Kanemura, Y. Morine, and M. Shimada, 2008, Expression of hypoxia-inducible factor-1alpha, histone deacetylase 1, and metastasis-associated protein 1 in pancreatic carcinoma: correlation with poor prognosis with possible regulation, *Pancreas*, v. 36: United States, p. e1-9.
- Monteiro, J., and R. Fodde, 2010, Cancer stemness and metastasis: therapeutic consequences and perspectives: *Eur J Cancer*, v. 46, p. 1198-203.
- Moon, H. E., H. Cheon, K. H. Chun, S. K. Lee, Y. S. Kim, B. K. Jung, J. A. Park, S. H. Kim, J. W. Jeong, and M. S. Lee, 2006, Metastasis-associated protein 1 enhances angiogenesis by stabilization of HIF-1alpha: *Oncol Rep*, v. 16, p. 929-35.
- Moon, H. E., H. Cheon, and M. S. Lee, 2007, Metastasis-associated protein 1 inhibits p53-induced apoptosis: *Oncol Rep*, v. 18, p. 1311-4.
- Moon, W. S., K. Chang, and A. S. Tarnawski, 2004, Overexpression of metastatic tumor antigen 1 in hepatocellular carcinoma: Relationship to vascular invasion and estrogen receptor-alpha: *Hum Pathol*, v. 35, p. 424-9.
- Moussalli, M. J., Y. Wu, X. Zuo, X. L. Yang, Wistuba, II, M. G. Raso, J. S. Morris, J. L. Bowser, J. D. Minna, R. Lotan, and I. Shureiqi, 2011, Mechanistic contribution of ubiquitous 15-lipoxygenase-1 expression loss in cancer cells

- to terminal cell differentiation evasion: *Cancer Prev Res (Phila)*, v. 4, p. 1961-72.
- Nagy, L., P. Tontonoz, J. G. Alvarez, H. Chen, and R. M. Evans, 1998, Oxidized LDL regulates macrophage gene expression through ligand activation of PPARgamma: *Cell*, v. 93, p. 229-40.
- Nair, S. S., D. Q. Li, and R. Kumar, 2013, A core chromatin remodeling factor instructs global chromatin signaling through multivalent reading of nucleosome codes: *Mol Cell*, v. 49, p. 704-18.
- Nawa, A., K. Nishimori, P. Lin, Y. Maki, K. Moue, H. Sawada, Y. Toh, K. Fumitaka, and G. L. Nicolson, 2000, Tumor metastasis-associated human MTA1 gene: its deduced protein sequence, localization, and association with breast cancer cell proliferation using antisense phosphorothioate oligonucleotides: *J Cell Biochem*, v. 79, p. 202-12.
- Ngan, C. Y., H. Yamamoto, I. Seshimo, T. Tsujino, M. Man-i, J. I. Ikeda, K. Konishi, I. Takemasa, M. Ikeda, M. Sekimoto, N. Matsuura, and M. Monden, 2007, Quantitative evaluation of vimentin expression in tumour stroma of colorectal cancer: *Br J Cancer*, v. 96, p. 986-92.
- Nicolson, G. L., 1988, Cancer metastasis: tumor cell and host organ properties important in metastasis to specific secondary sites: *Biochim Biophys Acta*, v. 948, p. 175-224.
- Nixon, J. B., K. S. Kim, P. W. Lamb, F. G. Bottone, and T. E. Eling, 2004, 15-Lipoxygenase-1 has anti-tumorigenic effects in colorectal cancer: *Prostaglandins Leukot Essent Fatty Acids*, v. 70, p. 7-15.
- Orlichenko, L. S., and D. C. Radisky, 2008, Matrix metalloproteinases stimulate epithelial-mesenchymal transition during tumor development: *Clin Exp Metastasis*, v. 25, p. 593-600.
- Pakala, S. B., T. M. Bui-Nguyen, S. D. Reddy, D. Q. Li, S. Peng, S. K. Rayala, R. R. Behringer, and R. Kumar, 2010a, Regulation of NF-kappaB circuitry by a

- component of the nucleosome remodeling and deacetylase complex controls inflammatory response homeostasis: *J Biol Chem*, v. 285, p. 23590-7.
- Pakala, S. B., S. D. Reddy, T. M. Bui-Nguyen, S. S. Rangparia, A. Bommana, and R. Kumar, 2010b, MTA1 coregulator regulates LPS response via MyD88-dependent signaling: *J Biol Chem*, v. 285, p. 32787-92.
- Pakala, S. B., K. Singh, S. D. Reddy, K. Ohshiro, D. Q. Li, L. Mishra, and R. Kumar, 2011, TGF-beta1 signaling targets metastasis-associated protein 1, a new effector in epithelial cells: *Oncogene*, v. 30, p. 2230-41.
- Peinado, H., D. Olmeda, and A. Cano, 2007, Snail, Zeb and bHLH factors in tumour progression: an alliance against the epithelial phenotype?: *Nat Rev Cancer*, v. 7, p. 415-28.
- Pfaffl, M. W., 2001, A new mathematical model for relative quantification in real-time RT-PCR: *Nucleic Acids Res*, v. 29, p. e45.
- Philips, B. J., R. Dhir, J. Hutzley, M. Sen, and U. P. Kelavkar, 2008, Polyunsaturated fatty acid metabolizing 15-Lipoxygenase-1 (15-LO-1) expression in normal and tumorigenic human bladder tissues: *Appl Immunohistochem Mol Morphol*, v. 16, p. 159-64.
- Plate, K. H., G. Breier, H. A. Weich, and W. Risau, 1992, Vascular endothelial growth factor is a potential tumour angiogenesis factor in human gliomas in vivo: *Nature*, v. 359, p. 845-8.
- Polyak, K., and R. A. Weinberg, 2009, Transitions between epithelial and mesenchymal states: acquisition of malignant and stem cell traits: *Nat Rev Cancer*, v. 9, p. 265-73.
- Radisky, D. C., 2005, Epithelial-mesenchymal transition: *J Cell Sci*, v. 118, p. 4325-6.
- Raica, M., A. M. Cimpean, and D. Ribatti, 2009, Angiogenesis in pre-malignant conditions: *Eur J Cancer*, v. 45, p. 1924-34.
- Rao, Y., H. Wang, L. Fan, and G. Chen, 2011, Silencing MTA1 by RNAi reverses adhesion, migration and invasiveness of cervical cancer cells (SiHa) via

- altered expression of p53, and E-cadherin/beta-catenin complex: *J Huazhong Univ Sci Technolog Med Sci*, v. 31, p. 1-9.
- Raymond, W. A., and A. S. Leong, 1989, Vimentin--a new prognostic parameter in breast carcinoma?: *J Pathol*, v. 158, p. 107-14.
- Roepman, P., A. de Jager, M. J. Groot Koerkamp, J. A. Kummer, P. J. Slootweg, and F. C. Holstege, 2006, Maintenance of head and neck tumor gene expression profiles upon lymph node metastasis: *Cancer Res*, v. 66, p. 11110-4.
- Sankaran, D., S. B. Pakala, V. S. Nair, D. N. Sirigiri, D. Cyanam, N. H. Ha, D. Q. Li, T. R. Santhoshkumar, M. R. Pillai, and R. Kumar, 2012, Mechanism of MTA1 protein overexpression-linked invasion: MTA1 regulation of hyaluronan-mediated motility receptor (HMMR) expression and function: *J Biol Chem*, v. 287, p. 5483-91.
- Sasaki, H., S. Moriyama, Y. Nakashima, Y. Kobayashi, H. Yukiue, M. Kaji, I. Fukai, M. Kiriyama, Y. Yamakawa, and Y. Fujii, 2002, Expression of the MTA1 mRNA in advanced lung cancer, *Lung Cancer*, v. 35: Ireland, p. 149-54.
- Schmalhofer, O., S. Brabletz, and T. Brabletz, 2009, E-cadherin, beta-catenin, and ZEB1 in malignant progression of cancer: *Cancer Metastasis Rev*, v. 28, p. 151-66.
- Semenza, G. L., 2000, Hypoxia, clonal selection, and the role of HIF-1 in tumor progression: *Crit Rev Biochem Mol Biol*, v. 35, p. 71-103.
- Shay, J. W., and W. E. Wright, 2000, Hayflick, his limit, and cellular ageing: *Nat Rev Mol Cell Biol*, v. 1, p. 72-6.
- Sherr, C. J., and F. McCormick, 2002, The RB and p53 pathways in cancer: *Cancer Cell*, v. 2, p. 103-12.
- Shureiqi, I., and S. M. Lippman, 2001, Lipoxigenase modulation to reverse carcinogenesis: *Cancer Res*, v. 61, p. 6307-12.

- Shureiqi, I., K. J. Wojno, J. A. Poore, R. G. Reddy, M. J. Moussalli, S. A. Spindler, J. K. Greenson, D. Normolle, A. A. Hasan, T. S. Lawrence, and D. E. Brenner, 1999, Decreased 13-S-hydroxyoctadecadienoic acid levels and 15-lipoxygenase-1 expression in human colon cancers: *Carcinogenesis*, v. 20, p. 1985-95.
- Shureiqi, I., X. Xu, D. Chen, R. Lotan, J. S. Morris, S. M. Fischer, and S. M. Lippman, 2001, Nonsteroidal anti-inflammatory drugs induce apoptosis in esophageal cancer cells by restoring 15-lipoxygenase-1 expression: *Cancer Res*, v. 61, p. 4879-84.
- Shureiqi, I., X. Zuo, R. Broaddus, Y. Wu, B. Guan, J. S. Morris, and S. M. Lippman, 2007, The transcription factor GATA-6 is overexpressed in vivo and contributes to silencing 15-LOX-1 in vitro in human colon cancer: *FASEB J*, v. 21, p. 743-53.
- Singh, R. R., and R. Kumar, 2007, MTA family of transcriptional metaregulators in mammary gland morphogenesis and breast cancer: *J Mammary Gland Biol Neoplasia*, v. 12, p. 115-25.
- Solari, F., A. Bateman, and J. Ahringer, 1999, The *Caenorhabditis elegans* genes *egl-27* and *egr-1* are similar to MTA1, a member of a chromatin regulatory complex, and are redundantly required for embryonic patterning: *Development*, v. 126, p. 2483-94.
- Taube, J. H., J. I. Herschkowitz, K. Komurov, A. Y. Zhou, S. Gupta, J. Yang, K. Hartwell, T. T. Onder, P. B. Gupta, K. W. Evans, B. G. Hollier, P. T. Ram, E. S. Lander, J. M. Rosen, R. A. Weinberg, and S. A. Mani, 2010, Core epithelial-to-mesenchymal transition interactome gene-expression signature is associated with claudin-low and metaplastic breast cancer subtypes: *Proc Natl Acad Sci U S A*, v. 107, p. 15449-54.
- Tavolari, S., M. Bonafe, M. Marini, C. Ferreri, G. Bartolini, E. Brighenti, S. Manara, V. Tomasi, S. Laufer, and T. Guarnieri, 2008, Licofelone, a dual COX/5-LOX inhibitor, induces apoptosis in HCA-7 colon cancer cells

- through the mitochondrial pathway independently from its ability to affect the arachidonic acid cascade: *Carcinogenesis*, v. 29, p. 371-80.
- Thiery, J. P., 2002, Epithelial-mesenchymal transitions in tumour progression: *Nat Rev Cancer*, v. 2, p. 442-54.
- Thiery, J. P., H. Acloque, R. Y. Huang, and M. A. Nieto, 2009, Epithelial-mesenchymal transitions in development and disease: *Cell*, v. 139, p. 871-90.
- Toh, Y., H. Kuwano, M. Mori, G. L. Nicolson, and K. Sugimachi, 1999, Overexpression of metastasis-associated MTA1 mRNA in invasive oesophageal carcinomas: *Br J Cancer*, v. 79, p. 1723-6.
- Toh, Y., and G. L. Nicolson, 2009, The role of the MTA family and their encoded proteins in human cancers: molecular functions and clinical implications: *Clin Exp Metastasis*, v. 26, p. 215-27.
- Toh, Y., E. Oki, S. Oda, E. Tokunaga, S. Ohno, Y. Maehara, G. L. Nicolson, and K. Sugimachi, 1997, Overexpression of the MTA1 gene in gastrointestinal carcinomas: correlation with invasion and metastasis: *Int J Cancer*, v. 74, p. 459-63.
- Toh, Y., S. D. Pencil, and G. L. Nicolson, 1994, A novel candidate metastasis-associated gene, *mta1*, differentially expressed in highly metastatic mammary adenocarcinoma cell lines. cDNA cloning, expression, and protein analyses: *J Biol Chem*, v. 269, p. 22958-63.
- Tuncay Cagatay, S., I. Cimen, B. Savas, and S. Banerjee, 2013, MTA-1 expression is associated with metastasis and epithelial to mesenchymal transition in colorectal cancer cells: *Tumour Biol*.
- Tuncay, S., 2009, Functional characterization of 15-Lipoxygenase-1 expression in human colorectal carcinoma cell line HT-29, Middle East Technical University, 106 p.

- van der Horst, G., L. Bos, and G. van der Pluijm, 2012, Epithelial plasticity, cancer stem cells and the tumor supportive stroma in bladder carcinoma: *Mol Cancer Res.*
- Wang, X., K. Zhang, L. Sun, J. Liu, and H. Lu, 2011, Short interfering RNA directed against Slug blocks tumor growth, metastasis formation, and vascular leakage in bladder cancer: *Med Oncol*, v. 28 Suppl 1, p. S413-22.
- Wu, J., H. H. Xia, S. P. Tu, D. M. Fan, M. C. Lin, H. F. Kung, S. K. Lam, and B. C. Wong, 2003, 15-Lipoxygenase-1 mediates cyclooxygenase-2 inhibitor-induced apoptosis in gastric cancer: *Carcinogenesis*, v. 24, p. 243-7.
- Wu, Y., B. Fang, X. Q. Yang, L. Wang, D. Chen, V. Krasnykh, B. Z. Carter, J. S. Morris, and I. Shureiqi, 2008, Therapeutic molecular targeting of 15-lipoxygenase-1 in colon cancer: *Mol Ther*, v. 16, p. 886-92.
- Xia, L., and Y. Zhang, 2001, Sp1 and ETS family transcription factors regulate the mouse Mta2 gene expression: *Gene*, v. 268, p. 77-85.
- Yang, H. W., L. G. Menon, P. M. Black, R. S. Carroll, and M. D. Johnson, 2010, SNAI2/Slug promotes growth and invasion in human gliomas: *BMC Cancer*, v. 10, p. 301.
- Yang, J., and R. A. Weinberg, 2008, Epithelial-mesenchymal transition: at the crossroads of development and tumor metastasis: *Dev Cell*, v. 14, p. 818-29.
- Yi, S., H. Guangqi, and H. Guoli, 2003, The association of the expression of MTA1, nm23H1 with the invasion, metastasis of ovarian carcinoma: *Chin Med Sci J*, v. 18, p. 87-92.
- Yilmaz, M., and G. Christofori, 2009, EMT, the cytoskeleton, and cancer cell invasion: *Cancer Metastasis Rev*, v. 28, p. 15-33.
- Yoo, Y. G., G. Kong, and M. O. Lee, 2006, Metastasis-associated protein 1 enhances stability of hypoxia-inducible factor-1alpha protein by recruiting histone deacetylase 1: *EMBO J*, v. 25, p. 1231-41.
- Yuan, H., M. Y. Li, L. T. Ma, M. K. Hsin, T. S. Mok, M. J. Underwood, and G. G. Chen, 2010, 15-Lipoxygenases and its metabolites 15(S)-HETE and 13(S)-

- HODE in the development of non-small cell lung cancer: *Thorax*, v. 65, p. 321-6.
- Zhang, H., L. C. Stephens, and R. Kumar, 2006, Metastasis tumor antigen family proteins during breast cancer progression and metastasis in a reliable mouse model for human breast cancer: *Clin Cancer Res*, v. 12, p. 1479-86.
- Zhang, X. Y., L. M. DeSalle, J. H. Patel, A. J. Capobianco, D. Yu, A. Thomas-Tikhonenko, and S. B. McMahon, 2005, Metastasis-associated protein 1 (MTA1) is an essential downstream effector of the c-MYC oncoprotein: *Proc Natl Acad Sci U S A*, v. 102, p. 13968-73.
- Zhu, W., M. Y. Cai, Z. T. Tong, S. S. Dong, S. J. Mai, Y. J. Liao, X. W. Bian, M. C. Lin, H. F. Kung, Y. X. Zeng, X. Y. Guan, and D. Xie, 2012, Overexpression of EIF5A2 promotes colorectal carcinoma cell aggressiveness by upregulating MTA1 through C-myc to induce epithelial-mesenchymal transition: *Gut*, v. 61, p. 562-75.
- Zuo, X., J. S. Morris, R. Broaddus, and I. Shureiqi, 2009a, 15-LOX-1 transcription suppression through the NuRD complex in colon cancer cells: *Oncogene*, v. 28, p. 1496-505.
- Zuo, X., J. S. Morris, R. Broaddus, and I. Shureiqi, 2009b, 15-LOX-1 transcription suppression through the NuRD complex in colon cancer cells: *Oncogene*.
- Zuo, X., J. S. Morris, and I. Shureiqi, 2008, Chromatin modification requirements for 15-lipoxygenase-1 transcriptional reactivation in colon cancer cells: *J Biol Chem*, v. 283, p. 31341-7.
- Zuo, X., Z. Peng, Y. Wu, M. J. Moussalli, X. L. Yang, Y. Wang, J. Parker-Thornburg, J. S. Morris, R. R. Broaddus, S. M. Fischer, and I. Shureiqi, 2012, Effects of gut-targeted 15-LOX-1 transgene expression on colonic tumorigenesis in mice: *J Natl Cancer Inst*, v. 104, p. 709-16.
- Zuo, X., Y. Wu, J. S. Morris, J. B. Stimmel, L. M. Leesnitzer, S. M. Fischer, S. M. Lippman, and I. Shureiqi, 2006, Oxidative metabolism of linoleic acid

modulates PPAR-beta/delta suppression of PPAR-gamma activity:
Oncogene, v. 25, p. 1225-41.

APPENDICES

Appendix A: Vector Maps

A.1 pSUPERIOR™.retro.neo+gfp plasmid

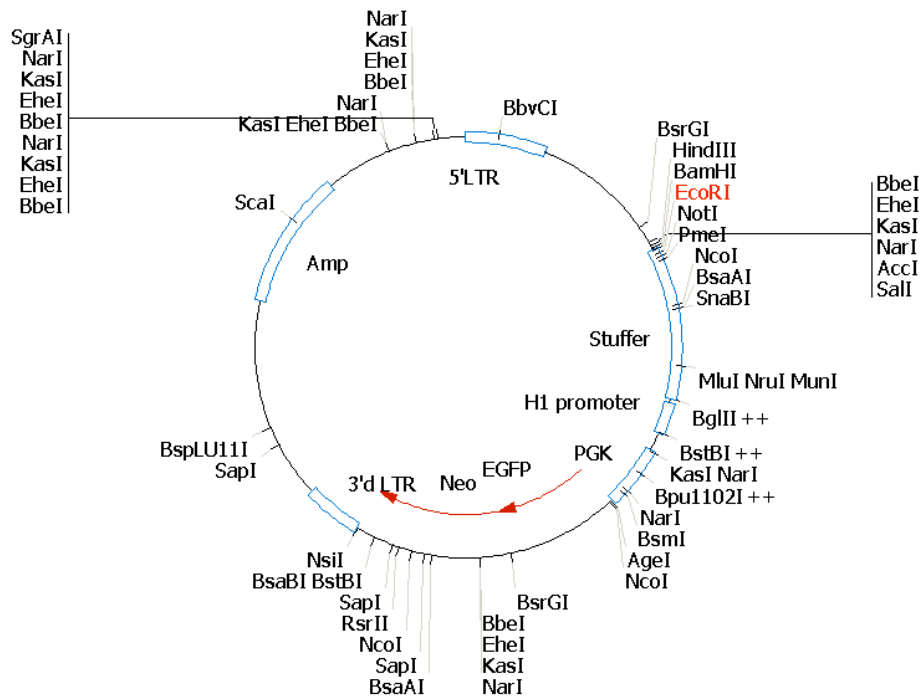


Figure A. 1 pSUPERIOR™.retro.neo+gfp vector map (8368 bp). PGK promoter: 2767-3165, Neo ORF: 3923-4892, EGFP ORF: 3183-3916, H1 promoter: 2651-2444, Stuffer: 1447-2423. Ampicillin resistance ORF: 7440-6574, 3' delta LTR: 4907-5274, 5' delta LTR: 8366-513.

A.2 pcDNATM3.1/V5-His-TOPO plasmid

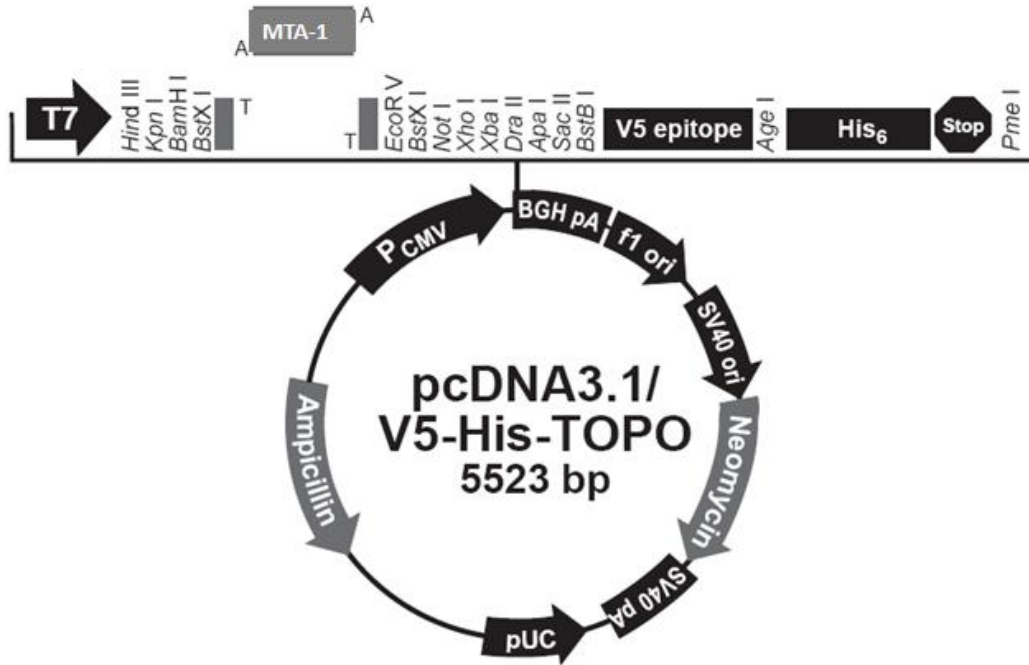


Figure A. 2 pcDNA3.1/V5-His-TOPO vector map (5523 bp). CMV promoter: bases 209-863 T7 promoter/priming site: bases 863-882, Multiple cloning site: bases 902-1019, TOPO® Cloning site: 953-954, V5 epitope: bases 1020-1061, Polyhistidine tag: bases 1071-1088, BGH reverse priming site: bases 1111-1128, BGH polyadenylation signal: bases 1110-1324, f1 origin of replication: bases 1387-1800, SV40 promoter and origin: bases 1865-2190, Neomycin resistance gene: bases 2226-3020, SV40 polyadenylation signal: bases 3039-3277, pUC origin: bases 3709-4382, Ampicillin resistance gene: bases 4527-5387.

A.3 pcDNATM3.1/Zeo (+) plasmid

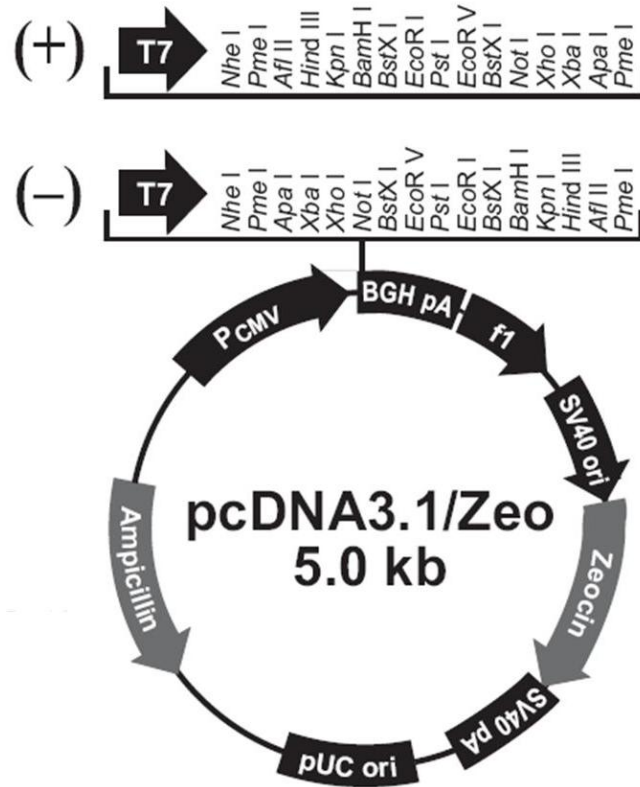
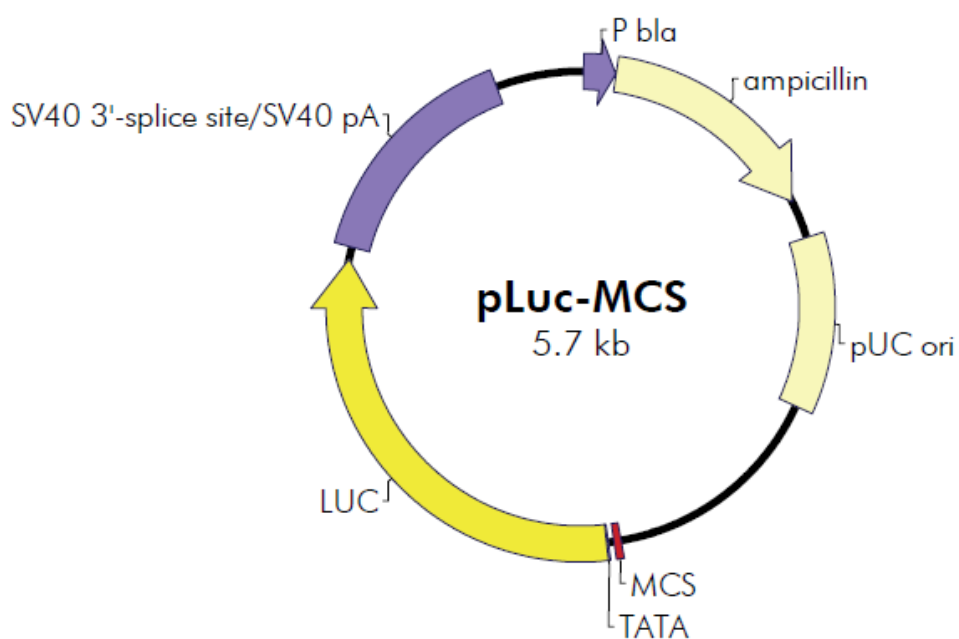


Figure A. 3 pcDNA3.1/ZEO (+) vector map (5015 bp). CMV promoter: bases 209-863 T7 promoter/priming site: bases 863-882, Multiple Cloning site:895-1010, BGH reverse priming site: bases 1022-1039, BGH polyadenylation signal: bases 1021-1235, f1 origin of replication: bases 1298-1711, SV40 promoter and origin: bases 1776-2101, EM7 promoter: bases 2117-2183, ZeocinTM resistance gene: bases 2184-2588, SV40 polyadenylation signal: bases 2688-2817, pUC origin: bases 3709-3874, *bla* pomoter: bases 4880-4978, Ampicillin resistance gene: bases 4019-4879.

A.4 pLuc-MCS™ plasmid



pLuc-MCS Multiple Cloning Site Region (sequence shown 2682-2737)

Hind III Srf I Sma I/Xma I Bgl II Xho I Sal I TATA box
 AAGCTTGCCCGGGCAGATCTCTCGAGGTCGACAGCGGAGACTCTAGAGGGTATATA

Figure A. 4 pLuc-MCS vector map (5.7 kb). *bla* promoter (13-134), Ampicillin resistance (*bla*) ORF (137-994), pUC origin of replication (1145-1810), Multiple cloning site (2682-2713), TATA box (2732-2737), Luciferase ORF (2738-4435), SV40 3'- splice site/SV40 polyA signal (4483-5336).

Appendix B: Generation of vectors

B.1 Generation of shRNA silencing vector:

MTA1 Forward

5'/5Phos/GAT CCC CGA ACA TCT ACG ACA TCT CCT TCA AGA GAG GAG
ATG TCG TAG ATG TTC TTT TTA-3'

Properties:

T_m (50 mM NaCl): 67,3 °C, **GC content:** 43.3 %/, **M_w:** 18,504.0,
nmoles/OD₂₆₀: 1.7, **µg/OD₂₆₀:** 31.8, **Ext. Coefficient:** 582,100 L/(mole.cm)

Amount of oligo:

OD₂₆₀ = 15.6 = 26.7 nMoles = 0.49 mg

MTA1 Reverse

5'/5Phos/AGC TTA AAA AGA ACA TCT ACG ACA TCT CCT CTC TTG
AAG GAG ATG TCG TAG ATG TTC GGG-3'

Properties:

T_m (50 mM NaCl): 67,5 °C, **GC content:** 43.3 %/, **M_w:** 18,602.0,
nmoles/OD₂₆₀: 1.7, **µg/OD₂₆₀:** 31.4, **Ext. Coefficient:** 591,700 L/(mole.cm)

Amount of oligo:

OD₂₆₀ = 5.3 = 9.0 nMoles = 0.17 mg

Oligos were dissolved in sterile, nuclease-free H₂O to a concentration of 3 mg/ml.

The formula below was used for calculations:

ml H₂O required for concentration of Xmg/ml = (µg oligos x 10⁻³) / X

0,49/3 = 0,163.3 ml = 163,3 µl

0,17/3 = 0,0566 ml = 56,7 µl

Annealing reaction:

1 μl of each oligo (forward + reverse) were mixed with 48 μl annealing buffer (Annealing buffer: 100 mM NaCl and 50 mM HEPES pH 7.4).

The mixture was incubated at 90°C for 4 min, and then at 70°C for 10 minutes. Annealed oligos were slowly cooled down to the to 10°C (e.g., step-cool to 37 for 15-20 minutes, then to 10°C or room temperature before using or moving them to refrigerated storage).

Linearization of Psuper (pSUPERIOR.retro.neo+gfp) vector:

Double digestion reaction w/ HindIII and BglII:

BglII	1 μl
HindIII	0,5 μl
(10X) Buffer R	4 μl
pSuper	25,5 μl
Water	9 μl
Total	40 μl

Incubated at 37 °C O/N then at 80 °C for 20 min and 0,6 μl from 0,5 M EDTA was added to inactivate BglII.

The linearized vector was gel purified by using Roche DNA purification kit and used in the ligation reaction.

Ligation into pSUPER vector by using 300 ng/ml vector:

Plasmid concentration after gel purification = 0,5 $\mu\text{g}/\mu\text{l}$

Annealed oligos	2 μ l
T4 buffer	1 μ l
T4 DNA ligase	1 μ l
pSUPER	6 μ l
Total	20 μ l

Incubated O/N at 16°C.

Ligated plasmids were transformed in *E.coli* Top 10 and colonies selected were subjected to plasmid isolation.

Table A. 1 Checking for the positive clones

	Cut w/ EcoRI & HindIII
Positive clone:vector with insert	281 bp
Negative clone:no insert	Approximately 1 kb

Double digestion with EcoRI & HindIII:

EcoRI	1 μ l
HindIII	1 μ l
pSUPER	20 μ l
Nuclease	14 μ l
Free water	14 μ l
Total	50 μ l

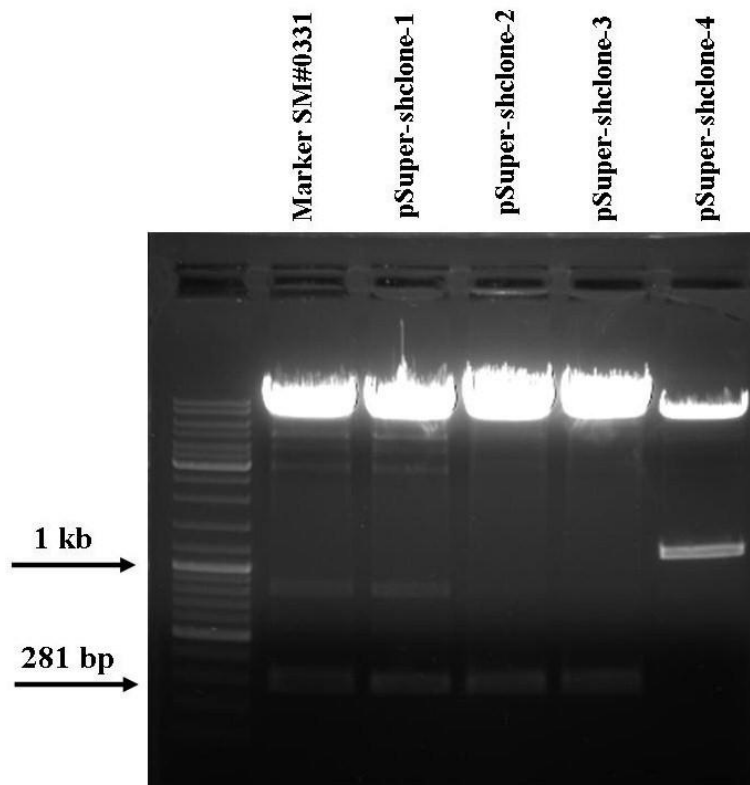


Figure A. 5 Figure EcoRI & HindIII double digested MTA1-shRNA-pSUPER and pSUPER plasmids.

Plasmids from selected clones were isolated and double digested with EcoRI and HindIII restriction enzymes showed that they have the insert while empty plasmid double digestion gave 1 kb band as suggested in the protocol.

CLUSTAL format alignment by MAFFT (v6.847b)		CLUSTAL format alignment by MAFFT (v6.847b)	
Fsuper-MTA1-shR forward	ngnngggggnnctctgctctgcagaatggccaaccttaacgtoggatggccggogaga	Fsuper-MTA1-shR reverse	nnnnnnntnangtgnannctttggatttgggaatcttataaagttctgtatgagaccac ----- * ******
Fsuper-MTA1-shR forward	cggcaccttaacggagacotcatcaccaggttaagatcaaggtctttccactggccc	Fsuper-MTA1-shR reverse	agatcccccgaacatctacgacatctcctcaagaggagatgctgtatgattctttt ----- -gaacatctacgacatctcctctcttgaaggagatgctgtatgattctt ***** ..*****
Fsuper-MTA1-shR forward	gcatggacacccagaccaggtccctacatcgtgacctgggaagccttgctttgacc	Fsuper-MTA1-shR reverse	aagcttatcgatacctgacacctcgagagatgatctaattccggcgctagagaaggag -----
Fsuper-MTA1-shR forward	cctccctgggtcaagcctttgtacacctaagcctccctcctctctccatccgcg	Fsuper-MTA1-shR reverse	tgaggctggataaaggaggatcgaggcgggtcgaacgaggaggtcaagggggagag -----
Fsuper-MTA1-shR forward	ccogtctctcccccctgaaacctctgcttgcaccccgctgatcctccctttatccagc	Fsuper-MTA1-shR reverse	acggggcggatggaggaggaggaggccttagggttacaaggcttgaccacag ----- -gatccc- *****
Fsuper-MTA1-shR forward	cctcaactctctctagggcgggaattagatgatctctcagaggtcgaaggtatcgata	Fsuper-MTA1-shR reverse	gaggggggtcaaaagccaaggtcccaggtcacgatgtagggacactggctgggtctc -----
Fsuper-MTA1-shR forward	agcttaaaaagaacatctacgacatctcctctctgaaggagatgctgtatgattcggg	Fsuper-MTA1-shR reverse	catcgggccaggtgaaaagacctgatcttaacctgggtgatgaggtctcgtttaag ----- -gaacatctacgacatctcctctcaaggaggagatgctgtatgattc ***** ..*****
Fsuper-MTA1-shR forward	gatctgtggtctcaccagaactataagattcccaatccaagacatttcacgtttat	Fsuper-MTA1-shR reverse	tgccgtctcggctatnccagcttaaggttgccattctgcagacagaagtaacc -----
Fsuper-MTA1-shR forward	ggtgattccccagaancacatagcgacatgcaaatattcagggngccactnccccggn	Fsuper-MTA1-shR reverse	aacgtctctcttgacatctaccgactggttgtagcgatccgctcgacatctttccngt -----
Fsuper-MTA1-shR forward	nccctacagccatcttctgcccagggcncacgycgngggngnncgcctannnganc	Fsuper-MTA1-shR reverse	gacctagggtcaaaccttaangngtggtaacagtctgnnctaatttccagacnaatcn -----
Fsuper-MTA1-shR forward	tggccnccnanncttggannggntgatnannccanncnngantctctnccggggngg	Fsuper-MTA1-shR reverse	gannnccngtcagacngagannnnnnnngnatgctgcagcgtcgcagagananacn -----
Fsuper-MTA1-shR forward	-----	Fsuper-MTA1-shR reverse	nnnnntcgggtccnannngaaagcaaaaantnnaocggagngggntnntnggtctc -----

Figure A. 6 Alignment results of MTA1-shRNA-pSUPER sequence to shRNA-MTA1 sequence in MAFFT.

Final confirmation of MTA1-shRNA-pSUPER vectors was done by sequencing. Sequencing results for one of the clones is shown above after blasted to shRNA-MTA1 oligo in MAFFT alignment program.

B.2 Generation of pcDNA3.1/V5-His-TOPO (pcDNA3.1-EV) from MTA1-pcDNA3.1/V5-His-TOPO vector:

Double digetion with HINDIII and XhoI conventional restriction enzymes (fermentas):

Plasmid	15 μ l
HindIII	0,5 μ l
XhoI	0,5 μ l
Tango Buffer	4 μ l
Total	20 μ l

Incubated at 37°C for 4 h, digestion products were gel purified by using Roche gel elution kit.

Digestion with S1 nuclease:

DNA	24 μ l
5X rxn buffer	6 μ l
S1 Nuclease	0,1 μ l
Water	-
Total	30 μ l

Incubate the mixture at RT for 30 minutes and stop the reaction by adding 2 μ l of 0.5 EDTA and heating at 70 °C for 10 minutes.

Ligation with T4 ligase:

DNA	15 ul
10x ligation buffer	4 ul
T4 ligase	1 ul
Total	20 μ l

Incubated at 16°C, overnight.

Generated empty vector was linearized after digestion with XbaI and runned on a gel for confirmation by size. The vector was also double digested with HindIII and XhoI to confirm that there is no MTA1 insert.

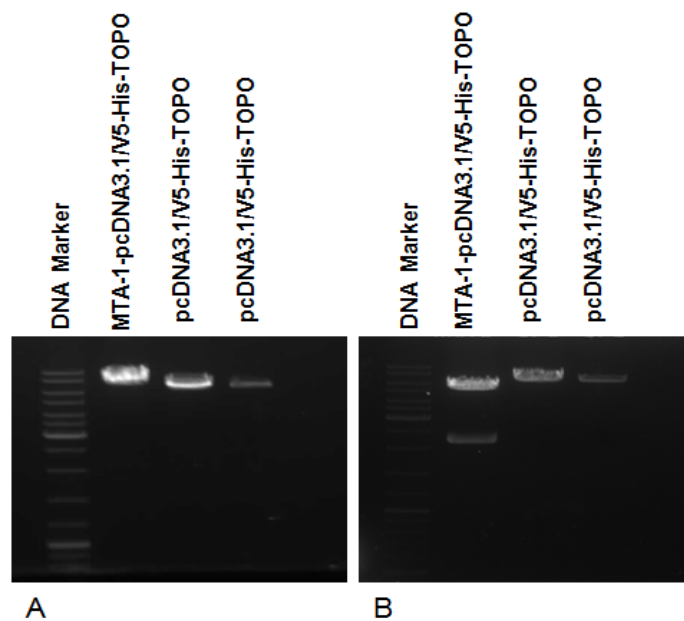


Figure A. 7 Agarose gel images of MTA-1-pcDNA3.1/V5-His-TOPO and pcDNA3.1/V5-His-TOPO vectors after restriction digestion with **A.** XbaI restriction enzyme **B.** HindIII ve XhoI restriction enzymes.

Finally, MTA1 PCR was carried out with MTA1 gene specific primers using the vector as template to confirm that there is no insert. MTA-1-pcDNA3.1/V5-His-TOPO vector was also used for all three experiments as a positive control.

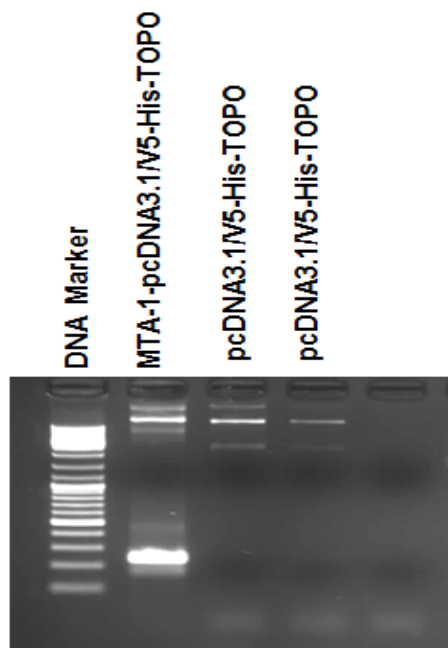


Figure A. 8 RT-PCR analysis of the MTA-1 transcript from MTA-1-pcDNA3.1/V5-His-TOPO and pcDNA3.1/V5-His-TOPO (product size: 244 bp).

B.3 Generation of pLuc-MCS –RI and RII plasmids:

Preparation of RI insert:

Oligos were dissolved in sterile, nuclease-free H₂O to a concentration of 10 mg/ml and 3 mg/ml, according to the formula;

ml H₂O required for concentration of Xmg/ml = (μ g oligos x 10⁻³) / X

$$0,348/3 = 0,116 \text{ ml} = 116 \mu\text{l}$$

$$0,348/10 = 0,0348 \text{ ml} = 34,8 \mu\text{l}$$

$$0,473/3 = 0,158 \text{ ml} = 158 \mu\text{l}$$

$$0,473/10 = 0,0473 \text{ ml} = 47,3 \mu\text{l}$$

Oligos were annealed as explained before.

Preparation of RII insert:

Table A. 2 Region II PCR amplification conditions.

	1X	3X
Template	3 µl	-----
Primer F	3 µl	9 µl
Primer R	3 µl	9 µl
Taq buffer	3 µl	9 µl
Taq polymerase	0,25 µl	0,75 µl
MgCl₂ (25 mM)	1 µl	3 µl
dNTPmix(2 mM)	3 µl	9 µl
ddH₂O	13,75	44,25
V_T	30 µl	90 µl
94 °C	3min	
94 °C	30 sec	36 cycles
59 °C	30 sec	
72 °C	40 sec	
72 °C	10 min	

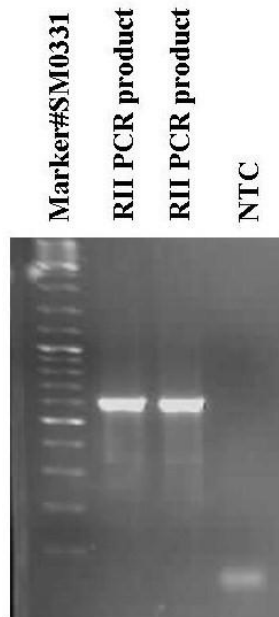


Figure A. 9 Region II PCR products (~600 bp)

Preparation of pLuc-MCS plasmid:

	<u>pLuc-MCS</u>	<u>Insert R1</u>	<u>Insert RII</u>
Nuclease free water	14,5	6 µl	-
10X Buffer R	2 µl	2 µl	2 µl
DNA	1,5 µl	10 µl	16 µl
HindIII	1 µl	1 µl	1 µl
XhoI	1 µl	1 µl	1 µl
Total	20 µl	20 µl	20 µl

Incubated at 37 °C, for 16 h overnight and carried out enzyme inactivation at 80 °C for 20 minutes.

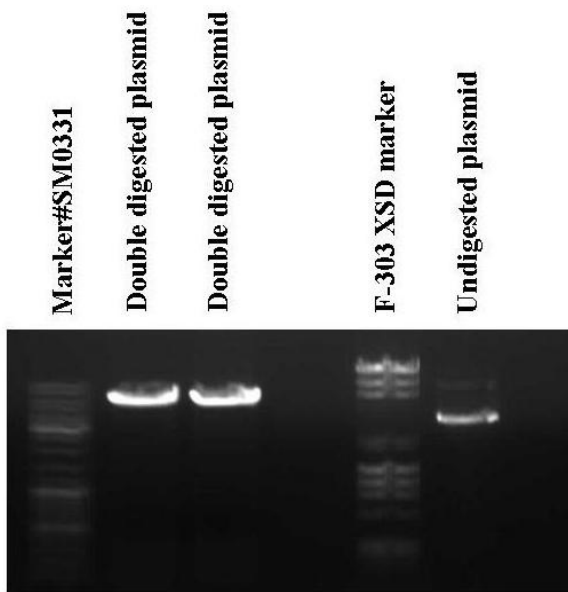


Figure A. 10 Double digested pLuc-MCS plasmid DNA

Digested plasmid DNA and Insert RII was gel purified and used in Ligation reactions.

	RI	RII
Insert DNA	0.5 µg	0.5 µg
T4 buffer	2 µl	2 µl
T4 DNA ligase	1 µl	1 µl
pSUPER	1 µg	1 µg
Total	20 µl	20 µl

The mixture was incubated at 16°C, O/N and 65°C for 10 min for inactivation and transformed into *E.coli* Top 10 competent cells.

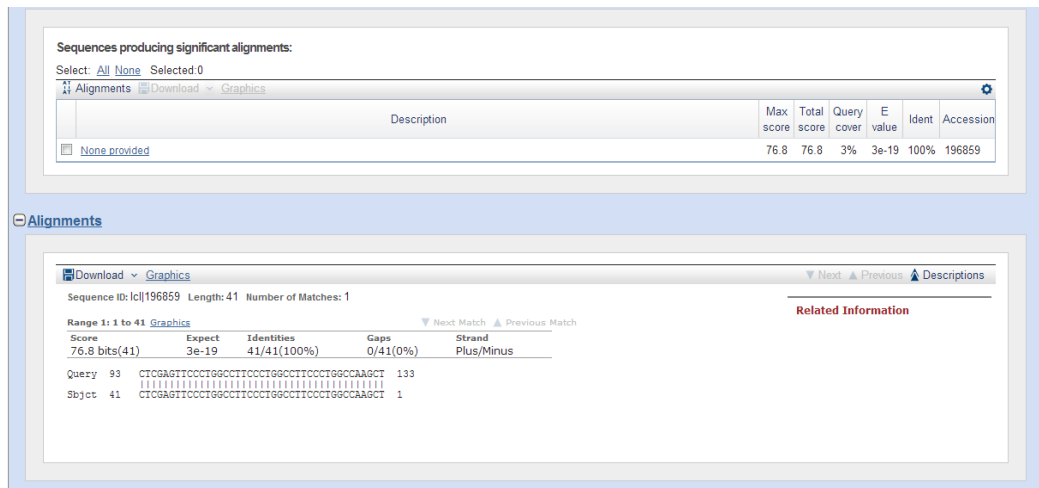


Figure A. 11 pLuc-MCS-RI sequencing results on NCBI Blast

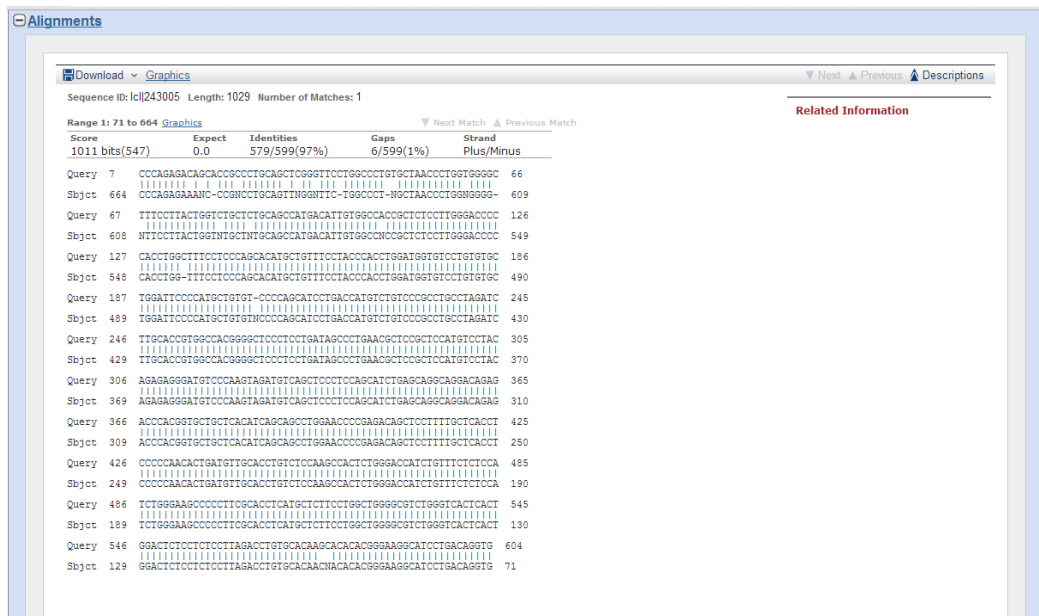


Figure A. 12 pLuc-MCS-RII sequencing results on NCBI blast

Appendix C: Isolation of electrophoretically separated DNA fragments with the Agarose Gel DNA Extraction Kit:

1. Separate the DNA of interest in a 1X agarose gel using 1X TAE buffer and cut out the interested DNA fragment with a sharp scalpel or a razor blade.
2. Transfer DNA in agarose gel into a preweighted reaction tube.
3. Use 300 μ l of the agarose solubilisation buffer per 100 mg of agarose gel. Apply 600 μ l if the agarose concentration used for the gel preparation.
4. Resuspend the silica suspension until a homogeneous suspension is obtained. Add 10 μ l of the silica suspension to the sample (If the sample contains more than 2.5 μ g DNA, increase the amount of silica suspension by 4 μ l for each additional μ g of DNA).
5. Incubate the mixture for 10 min at 56-60° C and vortex every 2-3 min.
6. Centrifuge in a table top centrifuge for 30 s at maximal speed and discard the supernatant.
7. Resuspend the matrix containing the DNA with 500 μ l nucleic acid binding buffer on avortex. Centrifuge and discard the supernatant as before.
8. Wash the pellet with 500 μ l washing buffer. Centrifuge and discard supernatant as before. Repeat this step once.
9. Remove all the liquid with a pipette, then invert the tube on an adsorbent tissue and let dry at room temperature for 15 min.
10. Use 30 μ l of TE buffer (10 mM Tris-HCl, 0.1 mM EDTA, pH 8.0-8.5) for the elution of DNA. Vortex and incubate for 10 min at 15-25 C. Vortex every 2-3 min. After centrifugation at maximum speed for 30 stransfer the DNA containing reaction into a new tube taking care of

Appendix D: High Pure PCR Product Purification:

1. Adjust sample volume to 100 μ l.
2. Add 500 μ l Binding Buffer and mix sample well.
3. Insert one High Pure Filter into the collection tube. Transfer the sample and centrifuge for 30-60 s at maximum speed.
4. Discard the flowthrough solution. Add 500 μ l Washing Buffer and centrifuge for 1 minute at maximum speed.
5. Discard the flowthrough solution. Add 200 μ l Washing Buffer and centrifuge for 1 minute at maximum speed.
6. Discard the flowthrough solution and collection tube.
7. Add 75 μ l Elution Buffer to the upper reservoir of the filter tube, centrifuge for 1 min at maximum speed.

Appendix E: Competent E.coli Preparation

1. *E.coli* Top10 was inoculated into 10 ml LB-broth and left at 37°C with shaking at 240 rpm O/N.
2. Transfer 100 µl of 2,5 ml of culture to each 100 ml LB containing erlenmayer flasks and leave for growing 2-3 h with shaking at 37 °C
3. Take OD measurements at 600 nm till desired growth is obtained (*between 0,4-0,6*).
4. Divide E.coli culture into 8 of 50 ml'lik falcons so 25 ml will be included in each.
5. Keep on ice for 10 min and centrifuge at 4°C at 4000 rpm for 10 min.
6. Resuspend pellet in 5 mL 10 mM CaCl₂ by vortexing.
7. Centrifuge at 3000 rpm for 10 min.
8. Re-suspend pellet in each centrifuge tube with 1 ml 75mM CaCl₂ (*Prepare prior to competent preparation*).
9. Add 20% ice cold glycerol (add 200 µl to each 1ml cells).
10. Divide into eppendorf tubes, freeze in liquid nitrogen and store at -80 C.

Appendix F: Transformation Protocol

1. Thaw competent cells on ice (100 μ l aliquot).
2. Mix with 50 ng plasmid.
3. Incubate on ice for 30 min.
4. Heat shock in water bath at 42°C for 30 sec
5. Leave on ice for 2 min
6. Add 1 ml LB at 42°C (Keep LB medium in water bath at 42°C).
7. Shake at 37°C for 1 h
8. Plate 200 μ l on LB-Amp plates (containing appropriate antibiotic) and left at 37°C for 16 h.

Appendix G: Plasmid isolation protocol

1. Harvest cells by centrifugating 5 mL of the overnight LB-culture. Remove all medium.
2. Resuspend cells in 250 μ L Resuspension Buffer with RNase A until suspension is homogeneous.
3. Add 250 μ L Lysis Buffer to lyse the cells and mix gently by inverting the tube until the mixture is homogeneous.
4. Add 350 μ L Precipitation Buffer and mix immediately by inverting the tube. Do not vortex. Centrifuge the lysate at $>16,000 \times g$ for 10 minutes.
5. Load the supernatant from step 4 onto a spin column in a 2-mL wash tube. Centrifuge the column at $16,000 \times g$ for 1 minute. Discard the flow-through and place the column back into the wash tube.
6. Add 500 μ L Wash Buffer with ethanol to the column. Centrifuge the column at $16,000 \times g$ for 1 minute. Discard the flow-through and place column back into the wash tube.
7. Add 750 μ L Wash Buffer with ethanol to the column. Centrifuge the column at $16,000 \times g$ for 1 minute. Discard the flow-through and place the column into the wash tube. Centrifuge the column at $16,000 \times g$ for 1 minute. Discard the wash tube with the flow-through.
8. Place the Spin Column in a clean 1.5-mL recovery tube. Add 50 μ L of elution buffer to the center of the column. Incubate the column for 1 minute at room temperature.
9. After centrifugation at $16,000 \times g$ for 1 minutes, the *tube contains the purified plasmid DNA*. Discard the column. Store the DNA in aliquots at -20°C .

Appendix H: Protein isolation Protocol with M-PER

1. Carefully remove culture medium from adherent cells.
2. Wash cells once in PBS.
3. Add the appropriate amount of M-PER Reagent to the plate or to each plate well (250 μ l for 6 well plates and 700 μ l for T25 flasks) . Shake gently for 5 minutes.
4. Collect the lysate and transfer to a microcentrifuge tube. Centrifuge samples at $\sim 14,000 \times g$ for 8 minutes to pellet the cell debris.
5. Transfer the supernatant to a new tube for analysis.

Appendix I: RNA isolation protocol with Qiagen Rneasy Kit

1. Harvest monolayer cells from the flask by trypsinization.
2. Disrupt cells with RLT buffer, vortex and mix (Use 350 μ l and 600 μ l of RLT buffer for $<5 \times 10^6$ and $5 \times 10^6 - 1 \times 10^7$, respectively).
3. Add 1 volume of 70% ethanol to the lysate, and mix well by pipetting. Do not centrifuge.
4. Transfer up to 700 μ l of the sample, including any precipitate that may have formed, to and Rneasy spin column placed in a 2 ml collection tube. Close the lid gently, and centrifuge for 15 seconds at $8000 \times g$. Discard the flow-through.
5. Add 700 μ l Buffer RW1 to the Rneasy spin column. Close the lid gently, and centrifuge for 15 seconds at $8000 \times g$ to wash the spin column membrane. Discard the flow-through.
6. Add 500 μ l Buffer RPE to the Rneasy spin column. Close the lid gently, and centrifuge for 15 seconds to wash the spin column membrane. Discard the flow-through.
7. Add 500 μ l Buffer RPE to the RNeasy spin column. Close the lid gently, and centrifuge for 2min at $8000 \times g$ to wash the spin column membrane.
8. Place the RNeasy spin column in a new 2 ml collection tube and discard the old collection tube with the flow-through. Close the lid gently, and centrifuge at full speed for 1 min.
9. Place the RNeasy spin column in a new 1.5 ml collection tube (supplied). Add 30 of μ l RNase-free water directly to the spin column membrane. Close the lid gently, and centrifuge for 1 min at $8000 \times g$ to elute the RNA.

**Appendix J: First strand cDNA synthesis with Revert Aid First strand cDNA
Synthesis kit**

1. Add the following in indicated order:

Template RNA	total RNA	100 ng - 5 μ g
	or poly(A) RNA	10 - 500 ng
	or specific RNA	0.01 pg - 0.5 μ g
Primer	oligo (dT) ₁₈	0.5 μ g (100 pmol)
	or random hexamer	0.2 μ g (100 pmol)
	or gene-specific	15-20 pmol
	DEPC-treated water to	12.5 μ l

2. Add the following components in the indicated order:

5X reaction buffer	4 μ l
RNAse Inhibitor	0.5 μ l (20 u)
dNTP Mix, 10 mM each	2 μ l (1 mM final concentration)
Reverse Transcriptase	1 μ l (200 u)
Total volume:	20 μ l

3. Mix gently and centrifuge briefly.
4. Incubate for 60 minutes at 42°C.
5. Terminate the reaction at 70°C 10 minutes.

Appendix K: Coomassie (Bradford) Protein Assay Standard Test Tube Protocol (Working Range = 100-1500µg/mL) and Standard Curve

1. Pipette 0.03mL (30µL) of each standard or unknown sample into appropriately labeled test tubes.
2. Add 1.5mL of the Coomassie Reagent to each tube and mix well.
3. Incubate samples for 10 minutes at room temperature (RT).
4. With the spectrophotometer set to 595nm, zero the instrument on a cuvette filled only with water. Subsequently, measure the absorbance of all the samples.
5. Subtract the average 595nm measurement for the Blank replicates from the 595nm measurements of all other individual standard and unknown sample replicates.
6. Prepare a standard curve by plotting the average Blank-corrected 595nm measurement for each BSA standard vs. its concentration in µg/mL. Use the standard curve to determine the protein concentration of each unknown sample.

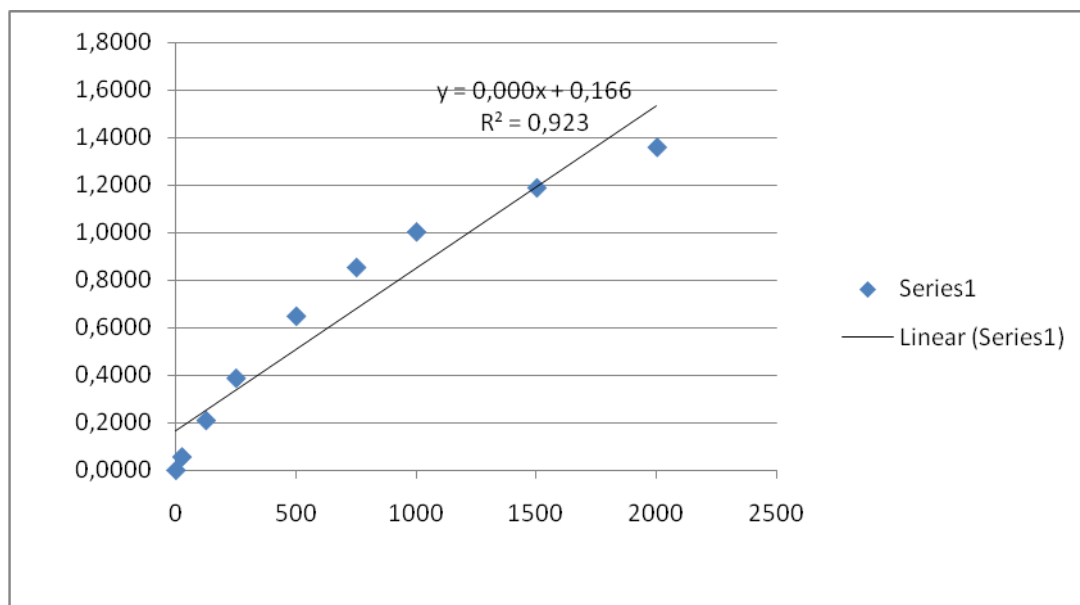


Figure A. 13 Protein standard curve.

Appendix L: VEGF ELISA Assay Standard Preparation protocol and Standard Curve

1. VEGF Standard was reconstituted with 1.0 mL of Calibrator Diluent RD5K which produces a stock solution of 2000 pg/mL.
2. Allow the standard to sit for a minimum of 15 minutes with gentle agitation prior to making dilutions.
3. Pipette 500 µl of Calibrator Diluent RD5K into each tube and use the stock solution to produce a dilution series. Mix each tube thoroughly before the next transfer.

(The 1000 pg/mL dilution serves as the high standard. Calibrator Diluent RD5K serves as the zero standard (0 pg/mL))

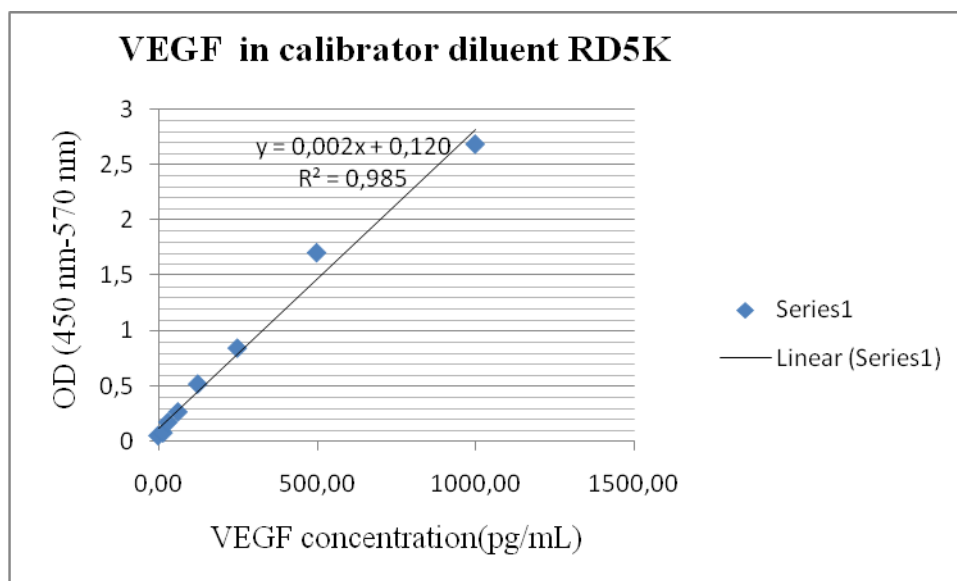


Figure A. 14 VEGF standard curve

Appendix M: Kill curve assay

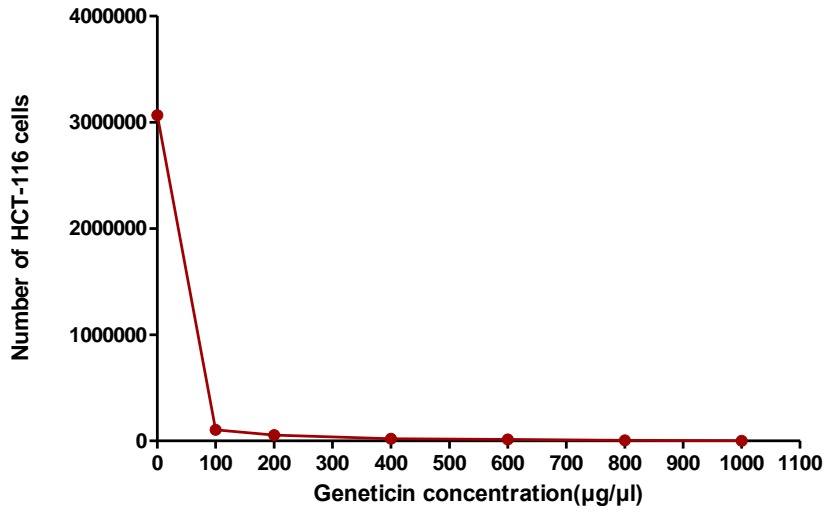


Figure A. 15 Geneticin (G-418) kill curve in HCT-116 cells

Appendix N: ChIP PCR

Table A. 3. Table ChIP PCR conditions for both Region I and II

	Sample or IgG (1X)	Input (1X)
Template	6 µl	3 µl
Primer F	3 µl	3 µl
Primer R	3 µl	3 µl
Taq buffer	3 µl	3 µl
Taq polymerase	0,25 µl	0,25 µl
MgCl₂ (25 mM)	1 µl	1 µl
dNTPmix(2 mM)	3 µl	3 µl
ddH₂O	10,75	13,75 µl
V_T	30 µl	30 µl
94 °C	3min	
94 °C	30 sec	36 cycles
60 °C	30 sec	
72 °C	30 sec	
72 °C	7 min	

Appendix O: Reporter gene assay transfection optimizations

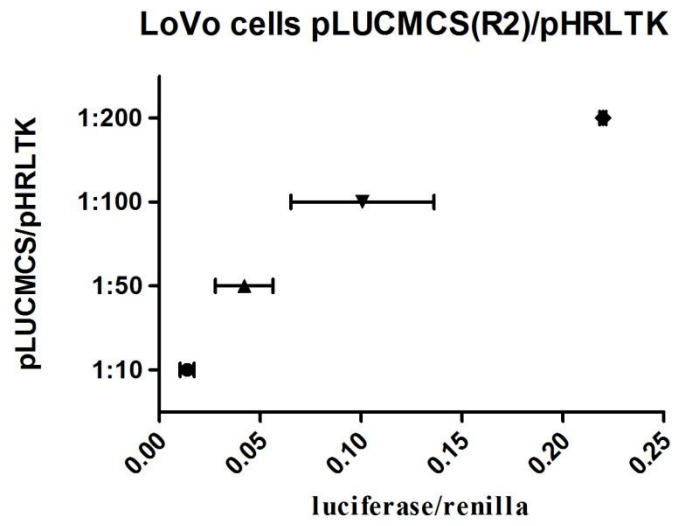


Figure A. 16 Transfection vs luciferase/renilla signal ratios in LoVo cells

Appendix P: BUFFERS

10X TBE Buffer

108 g of Tris Base

55 g boric acid

40 ml of 0.5 M EDTA

Adjust pH ~8.3

Complete to 1L with autoclaved dH₂O.

10 X Blotting buffer (1 L)

30.3 g Trizma Base (0.25M)

144 g Glycine (1.92 M)

pH ~ 8.3

Transfer Buffer (2L)

400 ml Methanol

200 ml 10 X Blotting buffer

1400 ml water

PBS-T Washing Buffer

8 g NaCl

0.27 g KH₂PO₄

3.58 g Na₂HPO₄ 12 H₂O

Add 500 ml dH₂O stir and complete
to 1 L

Adjust pH to 7.4 with HCl

Autoclave

Add 0.1% Tween 20 prior to use

Harsh Stripping Buffer

100 mM β -meOH

2% SDS,

62.5 mM Tris-HCl pH: 6.8

Procedure

1. Pre-warm the stripping buffer at 55-
2. 60°C for 10 minutes
3. Incubate the membranes for 30 minutes at 55-60°C with shaking
4. Wash 3 times with PBS-Tween using large volumes
5. Reblock and probe it

Mild Stripping Buffer

15g glycine

1 g SDS

10 ml Tween 20

Adjust the pH to 2,2

Complete to 1L with distilled water

Procedure

Use a volume that will cover the membrane.

Incubate at room temperature for 5-10 minutes with agitation.

Discard buffer 5-10 minutes fresh stripping buffer.

Appendix R: SDS-PAGE and polyacrylamide gels

Table A. 4 10% SDS-PAGE Gel

	Stacking Gel	Separating Gel
	4%	10%
30% PAA Mix	1.2 ml	5.6 ml
4X Stacking gel mix	2 ml	----
4X Separating gel mix	-----	3.8 ml
ddH₂O	4.7 ml	5.4 ml
10% APS	50 µl	150 µl
TEMED	10 µl	20 µl
Final Volume	8 ml	15 ml

Table A. 5 8% polyacrylamide gel

30 % PAA Mix	8.3 ml
10X TBE Buffer	2.5 ml
ddH₂O	39.1 ml
10% APS	500 µl
TEMED	20 µl
Final Volume	

Appendix S: RT-PCR thermal cycling conditions

Table A. 6 15-LOX-1 RT-PCR thermal cycling conditions

Holding Stage	50.0 °C	2 min
Cycling stage	95.0 °C	10 min
	95.0 °C	15 sec
	59.1 °C	1 min
Holding Stage	4 °C	∞

Table A. 7 MTA1 RT-PCR thermal cycling conditions

Holding Stage	50.0 °C	2 min
Cycling stage	95.0 °C	10 min
	95.0 °C	15 sec
	60.5 °C	1 min
Holding Stage	4 °C	∞

Table A. 8 β -actin RT-PCR thermal cycling conditions

Holding Stage	50.0 °C	2 min
Cycling stage	95.0 °C	10 min
	95.0 °C	15 sec
	60.0 °C	1 min
Holding Stage	4 °C	∞

Appendix T: Appendix Quantitative PCR Standards

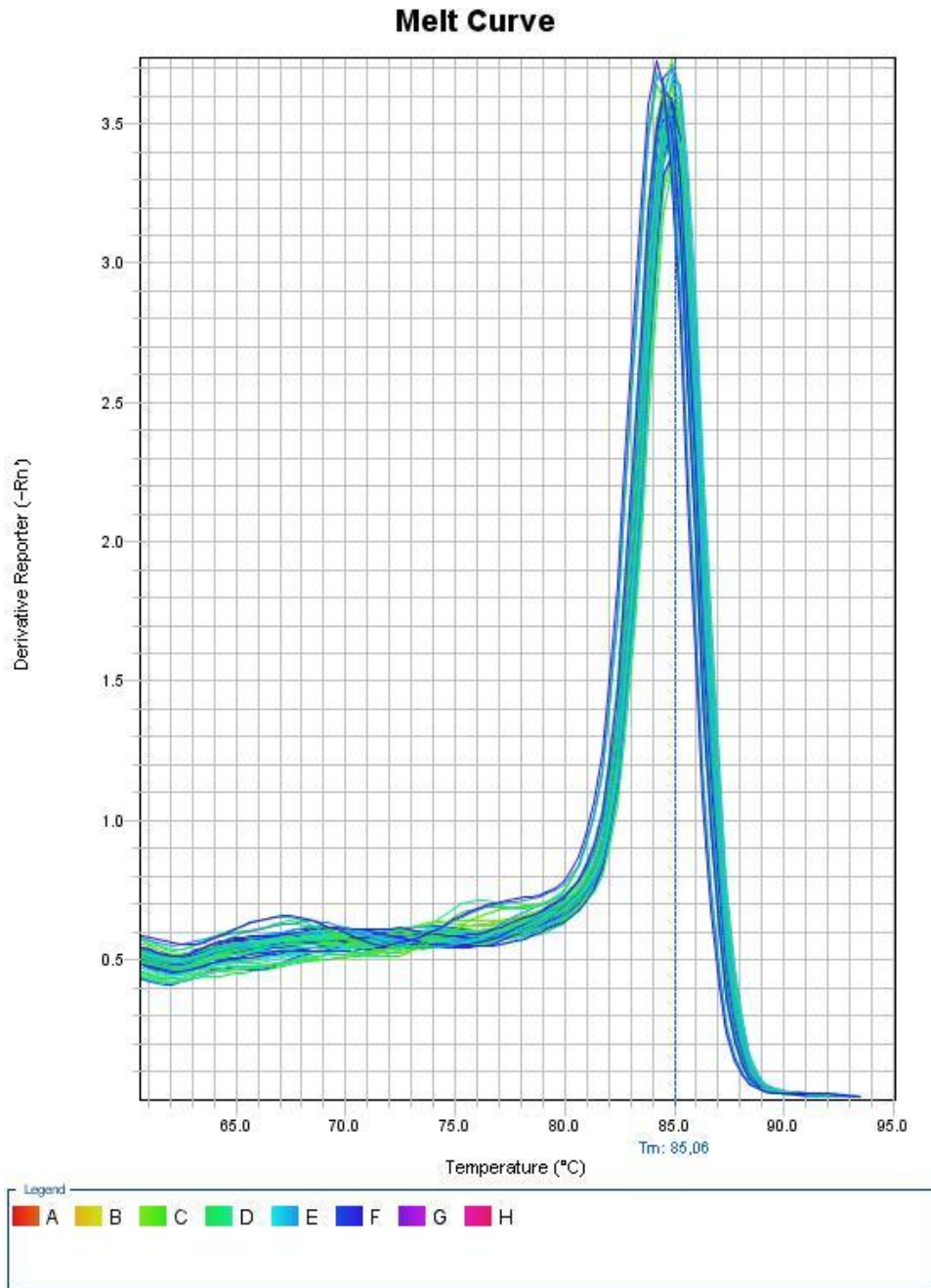


Figure A. 17 MTA1 RT-PCR Melt curve analysis

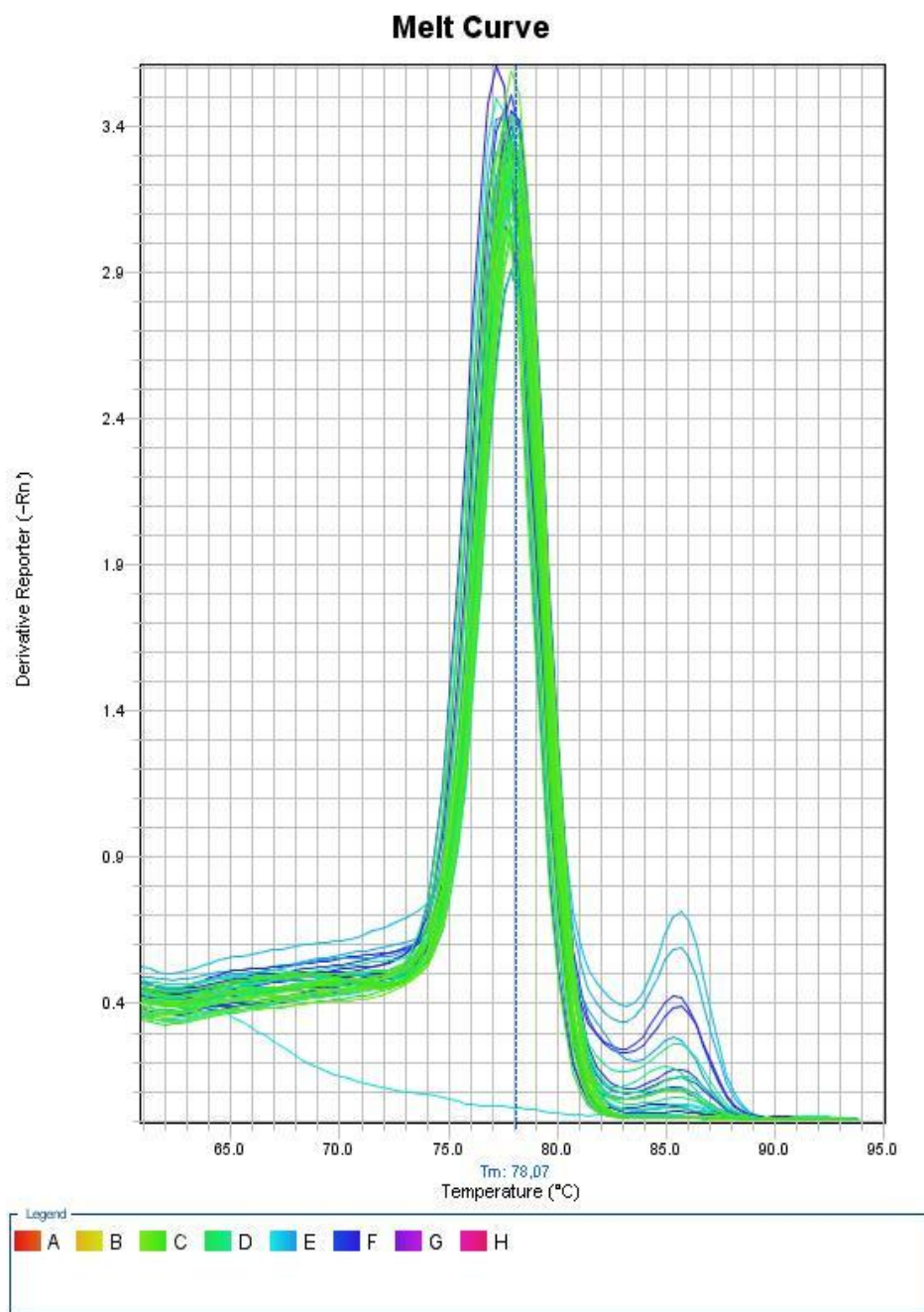


Figure A. 18 15-lox-1 RT-PCR Melt curve analysis

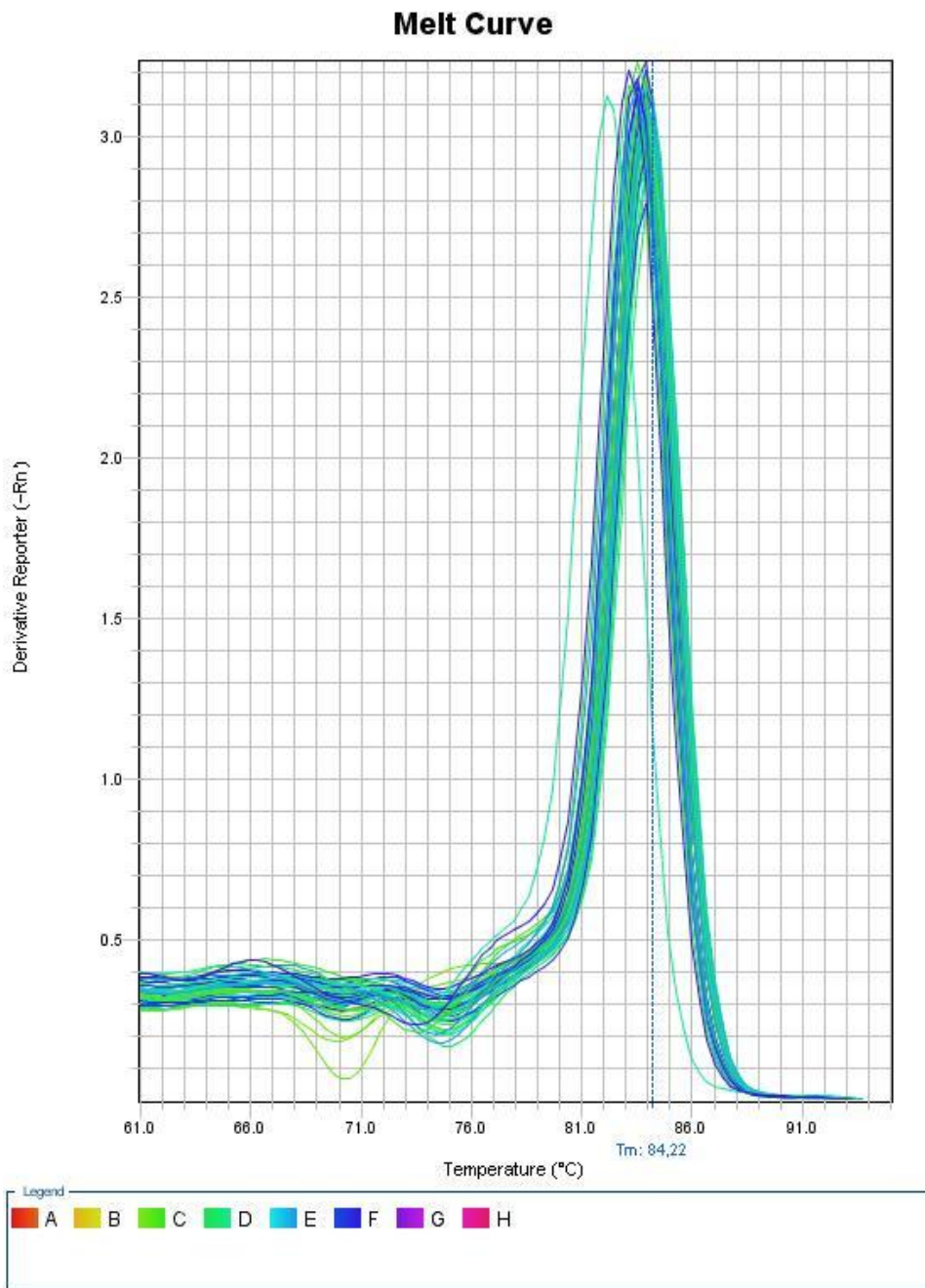


Figure A. 19 β -actin RT-PCR Melt curve analysis.

CURRICULUM VITAE

PERSONAL INFORMATION

Surname, Name: Tunçay Çağatay, Seda

Nationality: Turkish citizen

Date and Place of Birth: 20th January 1984, Aydın/TURKEY

Marital Status: Married

Phone: +90 (312) 286 11 54

Email: sedatuncaycagatay@gmail.com

EDUCATION

Degree	Institution	Year of Graduation
PhD	METU	2014
MS	METU	2009
BS	METU	2007
High School	Aydın Adnan Menderes Anatolian High School	2002

WORK EXPERIENCE

Year	Place	Enrollment
2007-2014	METU	Research/Teaching assistant

FOREIGN LANGUAGES

English (Advanced)

PUBLICATIONS

SCI Papers:

Tunçay Çağatay S, Çimen I, Savaş B, Banerjee S. MTA-1 expression is associated with metastasis and epithelial to mesenchymal transition in colorectal cancer cells. *Tumor Biology* 2013, 34:1189-1204.

Kavas A, Tunçay Çağatay S, Banerjee S, Keskin D, Tezcaner A. Potential of raloxifene on reversing osteoarthritis-like alterations in rat chondrocytes: An in vitro model study. *Journal of Biosciences*, 2013 38, 1–13

Sade A, Tunçay S, Çimen I, Severcan F, Banerjee S . Celecoxib reduces fluidity and decreases metastatic potential of colon cancer cell lines irrespective of COX-2 expression. *Bioscience Reports* 2012, 32, 35-44.

I. Çimen, S. Tunçay and Banerjee, S. (2009) 15-Lipoxygenase-1 expression suppresses the invasive properties of the colorectal carcinoma cell lines HCT-116 and HT-29. *Cancer Sci*, 100,2283-2291.

ISI Current Web Contents papers:

Tuncay S, Banerjee S . MAPK3 (mitogen-activated protein kinase 3). *Atlas Genet Cytogenet Oncol Haematol*. January 2010 .URL : <http://AtlasGeneticsOncology.org/Genes/MAPK3ID425ch16p11.html>

Tuncay S, Banerjee S . MAPK1 (mitogen-activated protein kinase 1). *Atlas Genet Cytogenet Oncol Haematol*. January 2010. URL : <http://AtlasGeneticsOncology.org/Genes/MAPK1ID41288ch22q11.html>

Banerjee S, Tunçay S. ALOX5 (Arachidonate 5-Lipoxygenase). Atlas Genet Cytogenet Oncol Haematol 2006; 10 (4): 562-572. URL : <http://AtlasGeneticsOncology.org/Genes/ALOX5ID42985ch10q11.html>

HONORS and AWARDS

2008-2009 Academic Year METU Best Thesis Award Winner (2010)

Dean's High Honour List: 2007, 2006, 2005 Fall & Spring semesters

Dean's Honour List: 2003, 2004 Fall & Spring semesters